Persoonia 52, 2024: 119–160
www.ingentaconnect.com/content/nhn/pimj

RESEARCH ARTICLE

ISSN (Online) 1878-9080
https://doi.org/10.3767/persoonia.2024.52.05

A comprehensive molecular phylogeny of *Cephalotrichum* and *Microascus* provides novel insights into their systematics and evolutionary history

T.P. Wei[1], Y.M. Wu[2,3], X. Zhang[1,4], H. Zhang[1,5], P.W. Crous[6,7], Y.L. Jiang[1,*]

Key words

divergence times
evolution
multi-gene phylogeny
new taxa
taxonomy

Abstract The genera *Cephalotrichum* and *Microascus* contain ecologically, morphologically and lifestyle diverse fungi in *Microascaceae* (*Microascales*, *Sordariomycetes*) with a world-wide distribution. Despite previous studies having elucidated that *Cephalotrichum* and *Microascus* are highly polyphyletic, the DNA phylogeny of many traditionally morphology-defined species is still poorly resolved, and a comprehensive taxonomic overview of the two genera is lacking. To resolve this issue, we integrate broad taxon sampling strategies and the most comprehensive multi-gene (ITS, LSU, *tef1* and *tub2*) datasets to date, with fossil calibrations to address the phylogenetic relationships and divergence times among major lineages of *Microascaceae*. Two previously recognised main clades, *Cephalotrichum* (24 species) and *Microascus* (49 species), were re-affirmed based on our phylogenetic analyses, as well as the phylogenetic position of 15 genera within *Microascaceae*. In this study, we provide an up-to-date overview on the taxonomy and phylogeny of species belonging to *Cephalotrichum* and *Microascus*, as well as detailed descriptions and illustrations of 21 species of which eight are newly described. Furthermore, the divergence time estimates indicate that the crown age of *Microascaceae* was around 210.37 Mya (95 % HPD: 177.18–246.96 Mya) in the Late Triassic, and that *Cephalotrichum* and *Microascus* began to diversify approximately 27.07 Mya (95 % HPD: 20.47–34.37 Mya) and 70.46 Mya (95 % HPD: 56.96–86.24 Mya), respectively. Our results also demonstrate that multigene sequence data coupled with broad taxon sampling can help elucidate previously unresolved clade relationships.

Citation: Wei TP, Wu YM, Zhang X, et al. 2024. A comprehensive molecular phylogeny of Cephalotrichum and Microascus provides novel insights into their systematics and evolutionary history. Persoonia 52: 119–160. https://doi.org/10.3767/persoonia.2024.52.05.
Effectively published online: 27 June 2024 [Received: 29 December 2023; Accepted: 12 April 2024].

INTRODUCTION

Microascaceae is a highly diverse family in the *Microascales* (*Sordariomycetes*, *Ascomycota*) with a worldwide distribution (Malloch 1970, Abbott 2000, Sandoval-Denis et al. 2016b). Members of this family can colonise diverse niches, and vary in lifestyle from saprobes, endophytes, plant pathogens and animal or human opportunistic taxa (Domsch et al. 2007, Sandoval-Denis et al. 2013, 2016a, b, Lackner et al. 2014, Li et al. 2017, Woudenberg et al. 2017a, b, Mamaghani et al. 2022). Many species of *Microascaceae* are important organisms that affect indoor environments and human health, e.g., species in *Microascus*, *Scedosporium* and *Scopulariopsis*, primarily because several of their species are well-known opportunistic pathogens and show intrinsic resistance to antifungal agents (Mohammedi et al. 2004, Van de Sande et al. 2007, Miossec et al. 2011, Skóra et al. 2015, Álvarez-Uría et al. 2021, Mhmoud et al. 2021). Furthermore, as cellulose-degrading fungi, some species of *Microascaceae* possess the ability to degrade cellulose-based building materials, thereby damaging the building structure (Peterson et al. 2011, Woudenberg et al. 2017a, b). On the other hand, several species of *Microascaceae* can also produce various enzymes and antioxidants with anticancer and anti-inflammatory activities, as well as antifungal, antibacterial and nematicidal metabolites, which are widely used in the medicinal, industrial and agricultural fields (Shao et al. 2015, Zutz et al. 2016, Zhu et al. 2018).

Cephalotrichum was established by Link (1809) for two asexual species, *C. rigescens* and *C. stemonitis*, with *C. stemonitis* designated as the generic type, which was previously included in genera such as *Doratomyces, Periconia* and *Stysanus* (Corda 1837, Hughes 1958, Abbott 2000). The diagnostic characteristics of species in this genus includes formation of dry conidia in basipetal chains from percurrently proliferating conidiogenous cells, and indeterminate synnemata (Abbott 2000, Sandoval-Denis et al. 2016b, Woudenberg et al. 2017b). The morphological simplicity of the *Cephalotrichum* morphotype has historically led to the amalgamation of numerous unrelated species, thereby creating a heterogeneous genus. Previous taxonomy studies of *Cephalotrichum*, *Doratomyces* and *Trichurus* were based mainly on morphological characters and have been the subject of discussion in various treatments (Jiang et al.

[1] Department of Plant Pathology, College of Agriculture, Guizhou University, Guiyang, 550025, Guizhou Province, China; corresponding author e-mail: yljchsd@163.com.
[2] Department of Plant Pathology, College of Plant Protection, Shandong Agricultural University, Taian, 271018, China.
[3] Shandong Key Laboratory of Agricultural Microbiology, Taian, 271018, China.
[4] Institute of Biotechnology, Guizhou Academy of Agricultural Sciences, Guiyang, 550009, Guizhou Province, China.
[5] Guizhou Academy of Testing and Analysis, Guiyang, 550014, Guizhou Province, China.
[6] Westerdijk Fungal Biodiversity Institute, Uppsalalaan 8, 3584 CT Utrecht, The Netherlands.
[7] Department of Biochemistry, Genetics and Microbiology, Forestry and Agricultural Biotechnology Institute (FABI), University of Pretoria, Pretoria, South Africa.

2011, Seifert et al. 2011, De Beer et al. 2013). *Doratomyces* was introduced by Corda (1829) based on *D. neesii*, and currently comprises 22 species. Later, *D. neesii* was treated as a synonym of the older name *C. stemonitis* (Hughes 1958). Since *Cephalotrichum* shares morphological characteristics with *Doratomyces*, the former was considered a synonym of *Doratomyces* (Morton & Smith 1963). Another genus, *Trichurus*, which is typified by *T. cylindricus*, was introduced by Clements & Pound (1896). Morphologically, the genus is very similar to *Cephalotrichum* and *Doratomyces*, except that it produces setae in the upper part of its synnemata (Morton & Smith 1963). However, the sole presence of setae was not considered to support their distinction at generic level (Hasselbring 1896, Swart 1964, Hammill 1977). Although molecular phylogenetic studies recognised the polyphyly of many morphologically-defined taxa within these genera, multi-locus DNA sequence data confirmed support for *Doratomyces* and *Trichurus* to be treated as synonyms of *Cephalotrichum* (Sandoval-Denis et al. 2016b, Jiang et al. 2017). In a systematic revision of the *Cephalotrichum*, Woudenberg et al. (2017b) re-evaluated all taxa for which molecular data were available at the time, and accepted 16 phylogenetic species. Over the past several years, the taxonomy of *Cephalotrichum* has been well studied and dramatically changed, and many species have been synonymized with known names after comparing morphological characteristics and related DNA sequence data, but some taxa remain to be corrected and typified.

Microascus, typified by *M. longirostris*, is the largest genus of the family *Microascaceae* and was introduced by Zukal (1885) for a group of saprobic ascomycetes. It is characterised by solitary annellidic conidiogenous cells with a long and narrow annellated zone, smooth to roughened conidia, mostly ostiolate ascomata with papillate or long cylindrical necks, and coloured ascospores with a single, mostly inconspicuous germ pore (Barron et al. 1961, Abbott et al. 2002, Guarro et al. 2012, Sandoval-Denis et al. 2016a). A further asexual genus, *Scopulariopsis*, was introduced by Bainier (1907) to accommodate *S. brevicaulis* (type species), *S. rubellus* and *S. rufulus*. It is characterised by the production of long chains of dry conidia from annellidic conidiogenous cells on branched (simple to penicillate) conidiophores (Morton & Smith 1963, Samson et al. 2010, Jagielski et al. 2013, 2016). Following the description of the genus, more than 114 species have been introduced with many of them now considered to be synonyms. Historically, the sexual morphs of *Scopulariopsis* were for a long time accommodated in the ascomycete genus *Microascus*, while *Scopulariopsis* commonly includes fungi that only exhibited asexual reproduction (Von Arx 1975, Abbott et al. 1998, Abbott & Sigler 2001, Lumbsch & Huhndorf 2007). However, except for a few species, the sexual morphs of most scopulariopsis-like species are unknown, and have had a confused taxonomic history. Additionally, many species of this group can only reproduce asexually, and even among fungi that reproduce sexually, often some strains/species easily lose their ability to sporulate sexually (Jagielski et al. 2016, Sandoval-Denis et al. 2016a, Sun et al. 2020, Zhang et al. 2021). Considering the limitations related to morpho-taxonomy, many molecular phylogenetic studies based on DNA sequences suggest that these scopulariopsis-like fungi should be redefined (Issakainen et al. 2003, Ropars et al. 2012, Sandoval-Denis et al. 2013, Lackner et al. 2014). Subsequently, many of these morphology-based genera in *Microascaceae*, such as *Cephalotrichum*, *Microascus* and *Scopulariopsis*, have been re-described using multigene phylogenetic analysis combined with morphology (Sandoval-Denis et al. 2016b, Woudenberg et al. 2017a). Phylogenetically, *Microascus* and *Scopulariopsis* were separated into two distinct lineages within *Microascaceae*, which are two distinct genera that both contained asexually and sexually reproducing species (Jagielski et al. 2016, Sandoval-Denis et al. 2016a). Following these studies, Woudenberg et al. (2017b) analysed a large set of scopulariopsis-like isolates, including the available ex-type strains of numerous species, recognising 33 and 12 species in the genera *Microascus* and *Scopulariopsis*, respectively. These advancements provide a stable taxonomic framework for *Microascaceae*, but the phylogenetic relationships of some poorly documented taxa remain unresolved due to its complex taxonomic history, which poses a handicap to defining generic boundaries.

Fossils are direct evidence of biological evolution and studies have shown that using molecular clocks calibrated with fossil information to estimate divergence times can more accurately infer the ages of different lineages, providing additional evidence for classification arrangements at different taxonomic levels (Berbee & Taylor 2010, Dos Reis et al. 2015, Píchová et al. 2018, Wang et al. 2018, Ho 2020). Until now most molecular dating studies in the fungal tree of life have focused on higher taxonomic levels, with only a few divergence events involving smaller groups of fungi (Taylor et al. 2014, Liu et al. 2017, Zhu et al. 2019). Despite increasing interest in dating the origin and diversification of different groups of fungi, it has been difficult to choose a reliable calibration point for the divergence time estimation due to the lack of satisfactory fossil data (Hedman 2010, Zhao et al. 2017, Steenwyk et al. 2019, Wang et al. 2022). This is largely attributed to the microscopic nature and the difficulty in recognizing them in the fossil record (Beimforde et al. 2014, Garnica et al. 2016). Moreover, fungi are delicate organisms that cannot be well preserved, leading to scarcity in the availability of fossil resources (Prieto & Wedin 2013, Taylor et al. 2015). Many studies on molecular evolution have highlighted the importance of precisely assigning fossils to particular nodes to constrain the molecular clock, and these analyses have provided a better understanding of fungal evolution (Sung et al. 2008, Benton et al. 2009, Lukoschek et al. 2012, Tischer et al. 2019). In recent years, as more and more fungal fossils with geological information are continuously discovered, molecular clock analyses and divergence time estimates have been widely applied in various taxonomic studies. To infer the origin and subsequent evolution of the main fungal lineages, Tedersoo et al. (2018) proposed an updated phylum- and class-level fungal classification accounting for monophyly and divergence times to provide a more natural classification, and improve the taxonomic and phylogenetic precision in evolutionary and biodiversity analyses. Thus, given the rich species diversity of *Microascaceae* and its adverse effects on human health, it is necessary to infer the timing of their origin in the fungal tree of life, and to reveal the evolutionary history of this family and related lineages.

In this study, we updated the species diversity of *Cephalotrichum* and *Microascus* using phylogenetic analyses of combined datasets of ITS, LSU, *tef1* and *tub2* gene sequences from 47 strains representing 21 species. Subsequently, divergence time estimations were performed utilizing fossils representing the four major *Hypocreomycetidae* subclasses as calibration points to evaluate the phylogenetically-delimited genera in *Microascaceae*. Our main purpose was to: 1) determine the placement of newly collected taxa with evidence from morphological characters and phylogenetic analyses; 2) resolve species boundaries within *Cephalotrichum* and allied genera by using morphology, molecular markers and evolutionary analyses; and 3) use molecular clock analysis to infer the origins of this group of microascaceous saprobic fungi.

MATERIALS AND METHODS

Isolates and specimens

Isolates used in this study were obtained from various types of soil and dust samples in China by dilution plate isolation methods. The samples were stored in zip-lock bags or envelopes and taken to the laboratory for examination. Single-conidial cultures were established on water agar (WA; agar 20 g, deionized water 1 000 mL). All fungal colonies were isolated and purified prior to identification. For subculture, pure cultures were transferred to potato dextrose agar (PDA; potato 200 g, dextrose 20 g, agar 20 g, deionized water 1 000 mL) and cultivated under cool white light at 26 °C for 4 wk. Additional strains were obtained from the Culture Collection of the Department of Plant Pathology, Shandong Agricultural University. In total 47 isolates were collected in this study, comprising 31 *Cephalotrichum* isolates (14 species) and 16 *Microascus* isolates (seven species). These strains were subsequently deposited in the Culture Collection of the Department of Plant Pathology, Agriculture College, Guizhou University, China (GUCC). An overview of the strains collected in this study and other strains used in the phylogenetic analyses is listed in Table 1 and 2.

Morphological analysis

Oatmeal agar (OA; oatmeal extract 30 g, agar 20 g, deionized water 1 000 mL) favours synnematal development of microascaceous fungi and morphological descriptions are mainly based on cultures grown on this medium. Inoculated medium plates were incubated upside down at 25 °C under continuous near-ultraviolet light to promote sporulation. The macroscopic characters (colony diameter, obverse and reverse colours, texture of aerial mycelium, soluble pigments and exudates) of the colony were observed using a super depth of field 3D microscope (VHX-7000, Keyence, Japan) and digital images were captured. To examine the asexual structures of the isolates, a slide culture method was used for microscopic observation (Crous et al. 2019). Lactic acid (60 %) was used as mounting fluid, and slides were gently heated over a flame of an alcohol lamp to remove air bubbles. Microscopic micrographs were captured using a Zeiss Axioscope 5 compound microscope with a Axiocam 208 colour digital camera (Zeiss, Germany). For certain images of micromorphological structures, the stacking software Zerene Stacker v. 1.04 (Zerene Systems, USA) was used. The ZEN v. 3.0 software was used to measure at least 30 randomly selected representative reproductive structures, and calculate the average value, standard deviation, minimum–maximum values and extreme measurements.

DNA extraction, amplification and sequencing

Total genomic DNA was extracted from fresh mycelium grown on PDA using the BIOMIGA Fungus Genomic DNA Extraction Kit GD2416 (Biomiga, USA) following the protocols provided by the manufacturer. The isolated DNA was stored at -20 °C for PCR amplification and subsequent sequencing. The PCR amplification and sequencing of the ITS region (ITS1, 5.8S rDNA and ITS2) using the primer pair ITS5/ITS4 (White et al. 1990), and the 28S rRNA gene (LSU) was amplified using primer pair LR5/LR0R (Vilgalys & Hester 1990, Vilgalys & Sun 1994). Partial β-tubulin fragments (*tub*2) were generated using the primer combination BT2a/BT2b (Glass & Donaldson 1995), for translation elongation factor 1-alpha (*tef1*-α) the primers 983F/2218R (Rehner & Buckley 2005) were used. The amplification cycles were performed following Sandoval-Denis et al. (2016a, b) and Woudenberg et al. (2017a, b). PCR products were purified at the Sangon Biotech, China, and the amplicons were sequenced in both directions using the same primers used for amplification to ensure accuracy. All newly generated sequences in this study were deposited in GenBank and are listed in Table 1.

Phylogenetic analyses

Phylogenetic analysis was based on concatenated DNA sequence datasets (ITS, LSU, *tef1* and *tub2*) to determine the generic boundaries and species relationships. The forward and reverse sequences for each locus were assembled into a consensus sequence using ContigExpress component from the Vector NTI Advance v. 11.5 software package (Invitrogen, Carlsbad, CA, USA) (Lu & Moriyama 2004), and then BLAST searches were performed in the NCBI database to compare homology with representative sequences. Multiple sequence alignments were generated with MAFFT v. 7.5.2 (Rozewicki et al. 2019) and the alignment was manually optimized using BioEdit v. 7.1.9 (Hall 1999) and MEGA v. 11 (Tamura et al. 2021). Individual alignments were concatenated using Sequence Matrix v. 1.9 (Vaidya et al. 2011), and the final alignments were exported as Phylip or Nexus files. Phylogenetic re-construction was conducted using Maximum Likelihood (ML) and Bayesian Inference (BI). The best-fit nucleotide substitution models for the four gene partitions were tested under the output strategy of Akaike information criterion (AIC) (Nylander 2004) using jModelTest v. 2.1.7 (Darriba et al. 2012) and incorporated into the analyses.

The BI analyses were performed in MrBayes v. 3.2.1 (Ronquist et al. 2012) based on the best-fit models of evolution for the four loci. The Markov Chain Monte Carlo (MCMC) algorithm of four chains were run for two runs from random trees for 2 M generations. The analyses lasted until the average standard deviation of the split frequencies dropped below 0.01; trees were sampled every 100th generation. The first 25 % was discarded as burn-in to ensure that stationarity in log-likelihood had been reached, and the remaining trees were used to calculate the posterior probabilities. The ML analyses were preformed using RAxML v. 8.2.12 (Stamatakis 2014) through the CIPRES website (http://www.phylo.org) to obtain another measure of branch support. The GTR+GAMMA model was chosen and ML bootstrap analyses were estimated with 1 000 rapid bootstrap replications. The clade is supported when its RAxML Bootstrap support value is ≥ 50 %, and the Bayesian PP value is ≥ 0.90. The phylogenetic trees were viewed using FigTree v. 1.4.4 (Rambaut 2018) and edited in Adobe Illustrator CC 2022 (Adobe Systems, USA). The final alignments and the phylogenetic trees obtained from this study were deposited in TreeBASE (http://www.treebase.org) under submission number No. S31029.

Fossil calibrations and divergence time estimates

A time-calibrated phylogeny for the *Microascaceae* was constructed from four gene datasets (ITS, LSU, *tub2* and *tef1*) of 184 species (Table 1, 2). This dataset includes 15 genera and representative species of *Microascaceae*, as well as reference taxa corresponding to fossil calibration. For the evolutionary model, we calibrated the phylogeny with the divergence time and fossil information of the subclass *Hypocreomycetidae* provided by previous studies (Dayarathne et al. 2019, Tischer et al. 2019, Chuaseeharonnachai et al. 2020, Wang et al. 2022). The following four calibration points were selected, including three fossil data and an additional secondary calibration: a uniform distribution for *Scopulariopsis* (lower = 34.2, upper = 38.7), an exponential distribution for *Ophiocordyceps* (offset = 100, mean = 27.5), a uniform distribution for *Colletotrichum* (lower = 61.6, upper = 72.3), and a truncated normal distribution with an upper hard bound (truncation) of 186 Mya and a standard deviation (SD) of 25 Mya was applied to calibrate *Hypocreomycetidae*.

Table 1 Strains used in the phylogenetic analysis of *Cephalotrichum* and *Microascus* and GenBank accession numbers.

Species	Strain[1]	Host/Substrate	Locality	GenBank accession number[2]			
				ITS	LSU	*tef1*	*tub2*
Cephalotrichum asperulum	CBS 582.71 T	Soil	Argentina	LN850960	MH872033	LN851061	LN851114
	UTHSC DI14-65	Bronchoalveolar lavage fluid	USA	LN850962	LN851009	LN851063	LN851116
	GUCC 18600	Isolated from farmland soil	China	**OR713130**	**OR722738**	**OR727363**	**OR727410**
	GUCC 18601	Isolated from vegetable soil	China	**OR713131**	**OR722739**	**OR727364**	**OR727411**
C. brevistipitatum	CBS 157.57 T	Tuber	Netherlands	LN850984	LN851031	LN851084	LN851138
C. brunneisporum	GUCC 18602 T	Isolated from forest soil	China	**OR713132**	**OR722740**	**OR727365**	**OR727412**
	GUCC 18603	Isolated from farmland soil	China	**OR713133**	**OR722741**	**OR727366**	**OR727413**
	GUCC 18604	Isolated from cotton soil	China	**OR713134**	**OR722742**	**OR727367**	**OR727414**
C. cylindricum	UAMH 1348 T	Seed of sorghum	USA	LN850965	LN851012	LN851066	LN851119
	CBS 646.70	Soil	France	KY249251	–	KY249330	KY249292
	GUCC 18605	Isolated from steppe soil	China	**OR713135**	**OR722743**	**OR727368**	**OR727415**
	GUCC 18606	Isolated from shrub soil	China	**OR713136**	**OR722744**	**OR727369**	**OR727416**
C. dendrocephalum	CBS 528.85 T	Cultivated soil	Iraq	LN850966	MH873591	LN851067	LN851120
C. domesticum	CBS 142035 T	Indoor air, house	Netherlands	KY249280	–	KY249360	KY249318
	CBS 255.50	Mushroom compost	Netherlands	KY249278	MH868115	KY249358	KY249316
	GUCC 18607	Isolated from bamboo forest soil	China	**OR713137**	**OR722745**	**OR727370**	**OR727417**
	GUCC 18608	Isolated from botanical garden grass soil	China	**OR713138**	**OR722746**	**OR727371**	**OR727418**
C. gorgonifer	UTHSCSA DI14-64	Bronchoalveolar lavage fluid	USA	LN850980	LN851027	LN851080	LN851134
	UT29CE	*Solanum tuberosum* tuber	Iran	MW718111	MW721025	MW732211	MW732191
	GUCC 18609	Isolated from forest soil	China	**OR713139**	**OR722747**	**OR727372**	**OR727419**
	GUCC 18610	Isolated from farmland soil	China	**OR713140**	**OR722748**	**OR727373**	**OR727420**
	GUCC 18611	Isolated from forest soil	China	**OR713141**	**OR722749**	**OR727374**	**OR727421**
C. guizhouense	CGMCC 3.18330 T	Air from cave	China	MF419788	MF419758	MF419728	MF434549
	LC 7457	Limestone from cave	China	MF419791	MF419761	MF419731	MF434552
	LC 7458	Limestone from cave	China	MF419792	MF419762	MF419732	MF434553
C. hinnuleum	UD CT 1-3-3	Soil	South Korea	LC509451	LC509453	LC509454	LC519561
	KNU-19GWF1	Soil	South Korea	LC519564	LC519565	LC519562	LC519563
C. inflatum	HHAUF160201	Soil	China	MF002125	MF041796	MF039904	MF511702
C. laeve	CGMCC 3.18329 T	Cave	China	MF419808	MF419778	MF419748	MF434569
	LC 7476	Limestone from cave	China	MF419810	MF419780	MF419750	MF434571
C. lageniforme	GUCC 18612 T	Isolated from coniferous forest soil	China	**OR713142**	**OR722750**	**OR727375**	**OR727422**
	GUCC 18613	Isolated from forest soil	China	**OR713143**	**OR722751**	**OR727376**	**OR727423**
C. lignatile	CBS 209.63 T	Timber in cave	Belgium	KY249269	MH869874	KY249349	KY249309
C. microsporum	CBS 523.63 T	Wheat field soil	Germany	LN850967	LN851014	LN851068	LN851121
	CBS 132.68	*Ligustrum vulgare*, dead twig	Netherlands	KY249270	–	KY249350	KY249310
	GUCC 18614	Isolated from forest soil	China	**OR713144**	**OR722752**	**OR727377**	**OR727424**
	GUCC 18615	Isolated from lawn soil	China	**OR713145**	**OR722753**	**OR727378**	**OR727425**
C. multisynnematum	GUCC 18616 T	Isolated from farmland soil	China	**OR713146**	**OR722754**	**OR727379**	**OR727426**
	GUCC 18617	Isolated from vegetable soil	China	**OR713147**	**OR722755**	**OR727380**	**OR727427**
C. nanum	CBS 191.61 T	Dung of deer	England	LN850969	MH869582	LN851070	LN851123
	CBS 188.60	Unknown	Italy	KY249274	MH869498	KY249354	KY249313
	UAMH 9126	Dung of bison	Canada	LN850970	LN851017	LN851071	LN851124
	GUCC 18618	Isolated from meadow soil	China	**OR713148**	**OR722756**	**OR727381**	**OR727428**
	GUCC 18619	Isolated from forest soil	China	**OR713149**	**OR722757**	**OR727382**	**OR727429**
C. oligotrophicum	CGMCC 3.18328 T	Cave	China	MF419801	MF419771	MF419741	MF434562
	LC 7462	Limestone from cave	China	MF419796	MF419766	MF419736	MF434557
C. purpureofuscum	CBS 174.68	Zea mays, grain	Unknown	KY249281	MH870812	KY249361	KY249319
	UAMH 9209	Indoor air	Canada	LN850971	LN851018	LN851072	LN851125
	GUCC 18620	Isolated from broad-leaved forest soil	China	**OR713150**	**OR722758**	**OR727383**	**OR727430**

Table 1 (cont.)

Species	Strain[1]	Host/Substrate	Locality	GenBank accession number[2]			
				ITS	LSU	*tef1*	*tub2*
C. purpureofuscum (cont.)	GUCC 18621	Isolated from farmland soil	China	**OR713151**	**OR722759**	**OR727384**	**OR727431**
C. silvanum	GUCC 18622 T	Isolated from farmland soil	China	**OR713152**	**OR722760**	**OR727385**	**OR727432**
	GUCC 18623	Isolated from forest soil	China	**OR713153**	**OR722761**	**OR727386**	**OR727433**
C. stemonitis	CBS 103.19 T	Seed	Netherlands	LN850951	LN850952	LN850953	LN850954
	CBS 180.35	Unknown	Unknown	LN850972	LN851019	LN851073	LN851126
	GUCC 18624	Isolated from grassland soil	China	**OR713154**	**OR722762**	**OR727387**	**OR727434**
	GUCC 18625	Isolated from grassland soil	China	**OR713155**	**OR722763**	**OR727388**	**OR727435**
	GUCC 18626	Isolated from lawn soil	China	**OR713156**	**OR722764**	**OR727389**	**OR727436**
C. telluricum	CBS 336.32 T	Soil	Cyprus	KY249287	–	KY249367	KY249325
	CBS 568.50	Soil	Canada	KY249288	–	KY249368	KY249326
C. tenuissimum	CBS 127792 T	Soil	USA	KY249286	MH876141	KY249366	KY249324
	UT36CE	*Solanum tuberosum* tuber	Iran	MW718245	MW721039	MW732223	MW732204
	GUCC 18627	Isolated from forest soil	China	**OR713157**	**OR722765**	**OR727390**	**OR727437**
	GUCC 18628	Isolated from farmland soil	China	**OR713158**	**OR722766**	**OR727391**	**OR727438**
C. transvaalense	CBS 448.51 T	Timber	South Africa	LN850964	LN851011	LN851065	LN851118
C. verrucisporum	CBS 187.78	Sand dune soil	Netherlands	LN850986	LN851033	LN851086	LN851140
	HHAUF160178	Soil	China	MF448346	MF041793	MF039900	MF511699
	GUCC 18629	Isolated from willow forest soil	China	**OR713159**	**OR722767**	**OR727392**	**OR727439**
	GUCC 18630	Isolated from lawn soil	China	**OR713160**	**OR722768**	**OR727393**	**OR727440**
Microascus aculeatus	CGMCC 3.15292 T	Pig farm soil	China	–	MK357842	MK361126	MK361129
M. alveolaris	UTHSC 07-3491 T	Human BAL fluid	USA	LM652385	HG380484	HG380407	LM652601
M. ampulliformis	GUCC 18631 T	Isolated from farmland soil	China	**OR713161**	**OR722769**	**OR727394**	**OR727441**
	GUCC 18632	Isolated from forest litter	China	**OR713162**	**OR722770**	**OR727395**	**OR727442**
M. anfractus	CGMCC 3.17950 T	Plant debris	China	KU746686	KU746732	KX855231	KU746777
M. appendiculatus	CBS 594.78 T	Human, skin	Algeria	LN850781	LN850830	KX924055	LN850878
M. atrogriseus	CBS 295.52 T	Culture contaminant	UK	LM652433	KX924030	KX924056	KX924265
	CBS 897.68	Wheat field soil	Germany	LM652436	LM652520	LM652571	LM652649
	GUCC 18633	Isolated from meadow soil	China	**OR713163**	**OR722771**	**OR727396**	**OR727443**
	GUCC 18634	Isolated from shrub soil	China	**OR713164**	**OR722772**	**OR727397**	**OR727444**
M. brunneosporus	CBS 138276 T	Human, BAL fluid	USA	KX923834	HG380497	HG380420	KX924269
M. campaniformis	CBS 138126 T	Human BAL fluid	USA	LM652391	HG380495	HG380418	LM652606
M. chartarum	CBS 294.52 T	Wall paper	England	LM652393	HG380463	HG380386	LM652607
M. chinensis	CBS 139628 T	Human, nail	China	LN850760	LN850809	LN850906	LN850858
	BMU01895	Human, nail	China	LN850761	LN850810	LN850907	LN850859
	GUCC 18635	Isolated from vegetable soil	China	**OR713165**	**OR722773**	**OR727398**	**OR727445**
	GUCC 18636	On decaying *Camellia sinensis* leaf litter	China	**OR713166**	**OR722774**	**OR727399**	**OR727446**
M. cinereus	CBS 138709 T	Human, BAL fluid	USA	KX923837	KX924031	KX924063	KX924272
M. cirrosus	CBS 217.31	Leaf of *Prunus* sp.	Italy	KX923838	KX924032	KX924064	KX924273
M. cleistocarpus	CBS 134638 T	Discarded cloth	China	KX923851	KX924033	KX924076	KX924286
M. collaris	CGMCC 3.19321 T	Sanshan cave, plant debris	China	MK329109	MK329012	MK336042	MK336120
M. croci	CBS 158.44 T	*Crocus* sp.	Netherlands	KX923852	LM652508	KX924077	KX924287
	MUCL 9002	*Crocus* sp.	Netherlands	LM652407	–	LM652560	LM652621
M. echinulatus	GUCC 18637 T	Isolated from vegetable soil	China	**OR713167**	**OR722775**	**OR727400**	**OR727447**
	GUCC 18638	Isolated from vegetable soil	China	**OR713168**	**OR722776**	**OR727401**	**OR727448**
M. ennothomasiorum	CBS 144074 T	Human skin	Germany	LS447483	LS444242	LS444241	LS444240
M. expansus	CBS 138127 T	Human sputum	USA	LM652410	HG380492	HG380415	LM652624
M. fusisporus	CBS 896.68 T	Wheat-field soil	Germany	LM652432	LN850825	HG380372	LM652645
M. globulosus	CGMCC :3.17927 T	Bat guano	China	KU746688	KU746734	KX855233	KU746779

Table 1 (cont.)

Species	Strain[1]	Host/Substrate	Locality	GenBank accession number[2]			
				ITS	LSU	*tef1*	*tub2*
M. gracilis	CBS 369.70 T	Food	Japan	LM652412	HG380467	HG380390	LM652625
M. hollandicus	CBS 141582 T	Indoor horse arena	Netherlands	KX923869	KX924034	KX924094	KX924304
M. hyalinus	CBS 766.70 T	Cow dung	USA	KX923870	LM652513	LM652564	KX924305
	CBS 134639	Goat dung	China	KX923871	–	KX924095	KX924306
M. intricatus	CBS 138128 T	Human sputum	USA	KX923872	HG380496	HG380419	KX924307
M. levis	CGMCC 3.19308 T	Luotian cave, soil	China	MK329108	MK329015	MK336045	MK336123
M. longicollis	CBS 752.97	Nut of *Anacardium occidentale*	Brazil	KX923874	KX924035	KX924097	KX924309
M. longirostris	CBS 196.61 T	Wasp's nest	USA	LM652421	LM652515	LM652566	LM652634
	CBS 415.64	Soil	Japan	LM652422	–	LM652567	LM652635
M. macrosporus	CBS 662.71	Soil	USA	LM652423	LM652517	LM652568	LM652636
M. melanosporus	CBS 272.60 T	Grains of *Oryza sativa*	USA	KX923876	KX924036	LM652572	KX924311
	CBS 102829	Cheese warehouse	Netherlands	KX923878	–	KX924100	KX924313
	GUCC 18639	Isolated from orchard soil	China	**OR713169**	**OR722777**	**OR727402**	**OR727449**
	GUCC 18640	Isolated from farmland soil	China	**OR713170**	**OR722778**	**OR727403**	**OR727450**
	GUCC 18641	Isolated from flower bed soil	China	**OR713171**	**OR722779**	**OR727404**	**OR727451**
	GUCC 18642	Isolated from farmland soil	China	**OR713172**	**OR722780**	**OR727405**	**OR727452**
M. micronesiensis	CBS 141523 T	Indoor dust	Micronesia	KX923905	KX924037	KX924128	KX924340
	DTO 223-A5	Indoor	Micronesia	KX923906	–	KX924129	KX924341
M. murinus	CBS 830.70 T	Composted municipal	Germany	KX923908	HG380481	KX924131	KX924342
	CBS 864.71	Municipal waste	Germany	LN850770	LN850819	LN850916	LN850867
M. onychoides	CBS 139629 T	Human nail	China	LN850774	LN850823	LN850920	LN850871
M. paisii	CBS 213.27 T	Man	Italy	LM652434	LM652518	LM652569	LM652647
M. pseudolongirostris	CBS 462.97 T	Human nail	Netherlands	LN850782	LN850831	KX924147	LN850879
M. pseudopaisii	CBS 141581 T	Air of a basement	Netherlands	KX923923	KX924038	KX924148	KX924358
M. pyramidus	CBS 212.65 T	Desert soil	USA	LM652439	HG380435	HG380358	LM652652
M. qinghaiensis	GUCC 18643 T	Isolated from flower bed soil	China	**OR713173**	**OR722781**	**OR727406**	**OR727453**
	GUCC 18644	Isolated from flower bed soil	China	**OR713174**	**OR722782**	**OR727407**	**OR727454**
M. restrictus	CBS 138277 T	Human left hallux	USA	LM652440	HG380494	HG380417	LM652653
M. rothbergiorum	CBS 148579 T	From *Stylophora pistillata* (*Pocilloporidae*)	Israel	OM509733	OM509736	OM470475	OM470474
M. senegalensis	CBS 277.74 T	Mangrove soil	Senegal	KX923929	LM652523	KX924153	KX924363
M. sparsimycelialis	CGMCC 3.19307 T	Sanshan cave, soil	China	MK329111	MK329016	MK336046	MK336124
	LC12480	Sanshan cave, soil	China	MK329112	MK329017	MK336047	MK336125
M. spinosporus	CGMCC 3.15286 T	Pig farm soil	China	MK357851	MK357843	MK361127	MK361130
M. superficialis	CGMCC 3.19638 T	Sanshan cave, animal faeces	China	MK329113	MK329018	MK336048	MK336126
	LC12600	Sanshan cave, animal faeces	China	MK329114	MK329019	MK336049	MK336127
M. terreus	CBS 601.67 T	Soil	Ukraine	LN850783	LN850832	LN850928	LN850880
M. trautmannii	CBS 141583 T	Oriented strand board	Germany	KX923942	KX924039	KX924166	KX924376
M. trigonosporus	CBS 218.31 T	Unknown	Puerto Rico	KX923943	HG380436	HG380359	KX924377
M. trigonus	CGMCC 3.19636 T	Luotian cave, soil	China	MK329117	MK329022	MK336052	MK336130
M. truncatus	GUCC 18645 T	Isolated from farmland soil	China	**OR713175**	**OR722783**	**OR727408**	**OR727455**
	GUCC 18646	Isolated from forest soil	China	**OR713176**	**OR722784**	**OR727409**	**OR727456**
M. verrucosus	CBS 138278 T	Human BAL fluid	USA	LM652446	HG380493	HG380416	LM652658
	CGMCC 3.15285	Pig farm soil	China	MK357852	MK357844	MK361128	MK361131

[1] T: Ex-holotype or ex-type strains.

[2] ITS: internal transcribed spacers and intervening 5.8S nrDNA; LSU: partial large subunit (28S) nrRNA gene; *tef1:* partial translation elongation factor 1-alpha gene; *tub2*: partial β-tubulin gene. Accession numbers of sequences generated in this study are in **bold**; – indicates unavailable sequences or unknown collection data.

Table 2 Overview species and strains used in phylogenetic analysis.

Order/Family	Species	Strain[1]	Host/Substrate	Locality	GenBank accession numbers[2]			
					ITS	LSU	*tef1*	*tub2*
Coronophorales/*Scortechiniaceae*	*Neocryptosphaerella celata*	GKM1231 T	On decorticated fallen branch	Kenya	–	FJ968975	FJ969035	–
	Pseudocryptosphaerella elliptica	SMH4722 T	On decorticated fallen branch	Ecuador	–	FJ968974	FJ969029	–
	Pseudocatenomycopsis rothmanniae	CPC 22733 T	Stem of *Rothmannia engleriana*	Zambia	KF777185	KF777237	–	–
	Yuxiensis granularis	HKAS 109580 T	Undetermined deciduous host	China	MZ713183	MZ713198	MZ712577	–
Falcocladiales/*Falcocladiaceae*	*Falcocladium africanum*	CBS 145045 T	Leaves of *Eucalyptus brassiana*	Ghana	MK047418	MK047469	–	–
	F. eucalypti	CBS 146052 T	Leaves of *Eucalyptus* sp.	South Africa	MN562106	MN567614	–	–
	F. multivesiculatum	CBS 120386	Leaf litter of *Eucalyptus grandis*	Brazil	JF831936	JF831932	–	–
	F. sphaeropedunculatum	CBS 111292	Living leaves of *Eucalyptus pellita*	Brazil	JF831938	JF831933	–	–
Glomerellales/*Glomerellaceae*	*Colletotrichum arboricola*	CBS 144795 T	*Fuchsia magellanica*	Chile	MH817944	MK014743	–	MH817962
	C. feijoicola	CBS 144633 T	*Acca sellowiana*	Portugal	MK876413	MK876420	–	MK876507
/*Reticulascaceae*	*Kylindria peruamazonensis*	CBS 838.91	Rotten petiole	Peru	GU180628	GU180638	–	–
Hypocreales/*Bionectriaceae*	*Emericellopsis alkalina*	CBS 127350 T	Alkaline soil	Russia	KC987171	KC987247	KC998993	KC987133
/*Clavicipitaceae*	*Metapochonia variabilis*	CGMCC 3.17925 T	Soil	China	KU746684	KU746730	KX855229	KU746775
/*Cordycipitaceae*	*Amphichorda guana*	CGMCC 3.17908 T	Soil	China	KU746665	KU746711	KX855211	KU746757
/*Nectriaceae*	*Nectria cinnabarina*	CBS 125165	*Aesculus* sp.	France	HM484548	HM484562	HM484527	HM484606
	Paracremonium variiforme	CGMCC 3.17931 T	Water	China	KU746691	KU746737	KX855237	KU746783
	Thyronectria concentrica	CBS 121121 T	Decaying leaves of *Agave americana*	Italy	HM484547	HM484572	HM484524	HM484609
/*Ophiocordycipitaceae*	*Ophiocordyceps brunneirubra*	BCC 14478 T	Termite	Thailand	MH754734	MH753688	GU797122	–
	O. sinensis	ARSEF 6282 T	*Hepialidae* sp.	China	KM652173	KM652126	KM652009	–
/*Stachybotryaceae*	*Melanopsamma pomiformis*	CBS 325.90	*Fagus sylvatica*, decaying bark	Italy	KU846048	KU846067	KU846094	KU846111
	Xenomyrothecium tongaense	CBS 598.80 T	*Halimeda* sp.	Tonga	KU847246	KU847272	KU847314	KU847336
/*Tilachlidiaceae*	*Tilachlidium brachiatum*	CBS 505.67	*Hypholoma fasciculare*	Poland	KM231839	KM231720	KM231976	KM232110
Melanosporales/*Ceratostomataceae*	*Echinusitheca citrispora*	CBS 137837 T	Soil	USA	KP981477	KP981453	KP981581	–
	Harzia cameroonensis	CBS 136420	Unidentified creeper plant	Cameroon	MH866096	MH877635	–	–
	Melanospora verrucispora	NBRC 31375 T	Soil	PNG	KP981480	KP981456	KP981584	–
	Microthecium quadrangulatum	CBS 112763 T	Soil	Spain	KP981492	KP981471	KP981599	–
	Paramicrothecium sambuci	CBS 148306 T	On dead stem base of *Sambucus nigra*	Germany	OK664749	OK663788	–	OK651217
Microascales/*Ceratocystidaceae*	*Ceratocystis fimbriata*	C1099	*Ipomoea batatas*	USA	KC493160	MG980927	MG980731	MG980827
	Meredithiella fracta	CBS 142645	Mycangium of *Corthylus papulans*	USA	KY744578	KY744590	KY773179	MG269945
	Thielaviopsis thielavioides	CBS 130.39	Ulmus, root	USA	AF275486	AF222480	HM569627	MG269958
	Toshionella nipponensis	CBS 141492 T	Culture from female	Japan	KX342064	MG269978	KX354420	MG269942
	Wolfgangiella madagascarensis	M286	Ambrosia growth in unidentified tree	Madagascar	KX342062	MG269975	KX354417	MG269950
/*Gondwanamycetaceae*	*Custingophora blanchettei*	CBS 134693	Bark of *Phytolacca* sp.	Uruguay	MH866081	MH877569	–	–
	Gondwanamyces proteae	CBS 486.88	On flower of *Protea repens*	South Africa	AY372072	AF221011	–	–
	Knoxdaviesia cecropiae	CBS 124460	On sapwood of *Cecropia angustifolia*	Costa Rica	MH863372	MH874894	–	–
	K. dimorphospora	FMR 15026 T	Human	Spain	LT671628	LT671629	–	–
/*Graphiaceae*	*Graphium euwallaceae*	UCR2980 T	*Persea americana*	USA	KF540224	MT252037	KF534805	MK108970
	G. laricis	CMW5601 T	*Larix decidua*	Austria	AY148183	KM495389	HM630588	–
	G. penicillioides	CBS 102632	*Populus nigra*	Czech	KY852474	KY852485	HM630600	MG269968
/*Halosphaeriaceae*	*Ascosacculus fusiformis*	MFLUCC 14-0036	Submerged wood	Thailand	MK878373	MK835842	–	–
	Cirrenalia iberica	CBS 142289 T	Soil	Spain	KY853436	KY853496	–	–
	Cucurbitinus constrictus	CGMCC 3.19606	On submerged decaying twig	China	MN431306	MN431419	–	–
	Natantispora unipolaris	NTOU3741	Phragmites on the shore	China	KM624523	KM624522	–	–
	Pileomyces formosanus	BBH30192 T	Unidentified trapped bamboo culm	China	JX003862	KX686804	–	–
	Tinhaudeus formosanus	NTOU3805 T	Mangrove wood	China	KT159895	KT159899	–	–

Table 2 (cont.)

Order/Family	Species	Strain[1]	Host/Substrate	Locality	GenBank accession numbers[2]			
					ITS	LSU	*tef1*	*tub2*
/*Microascaceae*	*Acaulium acremonium*	CBS 104.65 T	Wheat field soil	Germany	KY852468	KY852479	LN851056	LN851109
	A. albonigrescens	CBS 109.69 T	Litter, treated	Japan	KY852469	KY852480	LN851058	LN851111
	A. album	CBS 539.85 T	Hair in dung in pole cat	Netherlands	MN991960	MN991968	MN982411	MN982419
	A. caviariforme	CBS 536.87 T	Decaying meat	Belgium	LM652392	LN851005	LN851059	LN851112
	A. retardatum	CBS 707.82 T	From paddy soil	Japan	MN991961	MN991969	MN982412	–
	A. stercorarius	CGMCC 3.20206 T	Dung of marmot	China	MZ157171	MZ198011	MZ220697	MZ231120
	Enterocarpus grenotii	CBS 380.78 T	Dung of *Vulpes ruppeli*	Sahara	MH861153	MH872914	–	–
	Fairmania singularis	CBS 505.66 T	Barrel bottom	USA	LN850988	LN851036	LN851089	LN851143
	Gamsia aggregata	CBS 251.69 T	Dung of carnivore	USA	LM652378	LN851037	LN851090	LN851144
	G. dimerus	CBS 235.66 T	Wheat field soil	Germany	LN850991	LN851040	LN851093	LN851147
	G. kooimaniorum	CBS 143185 T	from garden soil	Netherlands	LT904719	LT904720	–	LT904701
	G. simplex	CBS 546.69 T	Milled *Oryza sativa*	Japan	LM652379	LM652501	LN851094	LN851148
	Kernia anthracina	CGMCC 3.19001 T	Dung of marmot	China	MK773539	MK773542	MK773568	MK773545
	K. geniculotricha	CBS 599.68 T	On dung of *Oryctolagus cuniculus*	Germany	MN991956	MN991964	MN982408	MN982414
	K. hippocrepida	CBS 774.70 T	On dung of *Erethizon dorsatus*	Canada	MN991954	–	MN982406	MN982413
	K. pachypleura	CBS 776.70 T	On dung of *Loxodonta africana*	Uganda	MN991958	MN991965	MN982410	MN982417
	Lophotrichus macrosporus	CBS 379.78	Dung of goat	Sahara	MH861152	MH872913	–	–
	L. martinii	CBS 292.52	On dung	USA	MH857042	MH868575	–	–
	Pithoascus ater	CBS 400.34 T	Human nail	Unknown	LM652447	LM652526	LM652576	LM652659
	Pit. exsertus	CBS 819.70 T	From *Megachile willoughbiella*	Denmark	LM652449	LM652528	LM652578	LM652661
	Pit. intermedius	CBS 217.32 T	Root of *Fragaria vesca*	USA	LM652450	LM652529	LM652579	LM652662
	Pit. lunatus	CBS 103.85 T	Skin showing *Tinea plantaris*	Germany	LN850784	LN850833	LN850929	LN850881
	Pit. nidicola	CBS 197.61 T	From *Dipodomys merriami*	USA	LM652451	LM652530	LM652580	LM652663
	Pit. stoveri	CBS 176.71 T	Root of *Beta vulgaris*	USA	LM652453	LM652532	LM652581	LM652664
	Pseudoscopulariopsis asperispora	CGMCC 3.19302 T	Luotian cave, soil	China	MK329129	MK329034	MK336064	MK336142
	Pse. hibernica	UAMH 2643	From soil	Ireland	LM652454	LM652533	LM652582	LM652665
	Pse. schumacheri	CBS 435.86 T	From soil	Spain	LM652455	LM652534	LM652583	LM652666
	Scedosporium americanum	CBS 218.35 T	Human mycetoma pedis	Paraguay	AM712309	–	–	MT813192
	Sce. aurantiacum	FMR 8630 T	Ulcer of ankle	Spain	AJ888440	–	–	AJ889597
	Sce. boydii	CBS 101.22 T	Mycetoma Texas	USA	AJ888435	–	–	AJ889590
	Sce. dehoogii	CBS 117406 T	Garden soil	Spain	KT163400	–	–	KT163401
	Sce. multisporum	CGMCC 3.20470 T	Isolated from green belt soil	China	MZ469286	–	–	MZ488560
	Scopulariopsis africana	CBS 118736 T	Mud, salt pan	South Africa	KX923954	KX924040	KX924176	KX924388
	Sco. alboflavescens	CBS 399.34 T	Human, skin	Austria	KX923956	LM652539	KX924179	JQ434537
	Sco. asperula	CBS 298.67	*Triticum aestivum*	Turkey	LN850789	LN850837	LN850934	LN850886
	Sco. brevicaulis	CBS 127812	Indoor air	Canada	LM652465	HG380440	HG380363	KX924423
	Sco. caseicola	CBS 480.62 T	Cheese-coating	Netherlands	KX924020	KX924041	KX924247	KX924454
	Sco. cordiae	CBS 138129 T	Human, finger	USA	KX924022	HG380499	KX924249	KX924456
	Sco. crassa	CGMCC 3.17941 T	Soil	China	KU746704	KU746750	KX855249	KU746795
	Sco. flava	CBS 207.61 T	Cheese	UK	LM652493	HG380464	HG380387	LM652697
	Sco. macurae	CBS 506.66 T	Chicken litter	Canada	LN850805	LN850854	KX924250	LN850902
	Sco. sexualis	CBS 250.64 T	*Oryza sativa*, milled	Burma	KX924024	KX924042	KX924251	KX924458
	Wardomyces anomalus	CBS 299.61 T	Air cell of egg	Canada	LN850992	LN851044	LN851095	LN851149
	Wes. giganteus	CBS 746.69 T	Insect frass in dead log	Canada	LM652411	LM652510	LN851096	LN851150
	Wes. inflatus	CBS 367.62 T	Greenhouse soil	Belgium	LN850994	LN851048	LN851099	LN851153
	Wes. ovalis	CBS 234.66 T	Wheat field soil	Germany	LN850996	LN851050	LN851101	LN851155
	Wes. pulvinatus	CBS 112.65 T	Salt-marsh	England	LN850997	LN851051	LN851102	LN851156
	Wardomycopsis ellipsoconidiophora	CGMCC 3.19322 T	Sanshan cave, animal faeces	China	MK329141	MK329046	MK336076	MK336147
	Wis. humicola	CBS 487.66 T	Soil	Canada	LM652497	LM652554	LN851103	LN851157
	Wis. inopinata	FMR 10305	Soil	Myanmar	LM652498	LM652555	LN851106	LN851160
	Wis. litoralis	CBS 119740 T	Beach soil	Spain	LN851000	LN851055	LN851107	LN851161

Table 2 Overview species and strains used in phylogenetic analysis.

Order/Family	Species	Strain[1]	Host/Substrate	Locality	GenBank accession numbers[2]			
					ITS	LSU	*tef1*	*tub2*
/*Microascaceae* (cont.)	*Wis. longicatenata*	CGMCC 3.17947 T	Air	China	KU746710	KU746756	KX855255	KU746801
	Yunnania carbonaria	CBS 205.61 T	Soil	Panama	KX923820	HG380462	KX924044	KX924254
	Y. penicillata	CBS 130296 T	Molded pork sample	China	JN831359	KY659809	KY659808	KY659807
	Y. smithii	CBS 855.68 T	Garden soil	Germany	KX923822	KX924028	KX924046	KX924256
/*Synnematotriadelphiaceae*	*Synnematotriadelphia stilboidea*	CBS 221.85 T	On dead leaves of *Roystonea regia*	Cuba	MF434781	MF434792	–	–
/*Triadelphiaceae*	*Triadelphia disseminata*	CBS 138592 T	From a human patient	Saudi Arabia	MF434784	MF434788	–	–
	T. hexaformispora	TBRC 9288 T	On unidentified submerged twig	Thailand	MK588842	MK588850	–	–
	T. loudetiae	CBS 589.77 T	In rhizosphere of *Loudetia simplex*	Ivory Coast	MF434776	MF434785	–	–
Sordariales/*Bombardiaceae*	*Ramophialophora globispora*	CGMCC 3.17939 T	Plant debris	China	KU746700	KU746746	KX855245	KU746791
/*Chaetomiaceae*	*Chaetomium contagiosum*	CBS 128494 T	Cornea of Homo sapiens, North East	USA	KT214555	KT214589	KT214694	KT214732
Torpedosporales/*Juncigenaceae*	*Elbamycella rosea*	MUT 4937 T	*Padina pavonica*	Italy	MK775496	MK775499	–	–
/*Torpedosporaceae*	*Torpedospora ambispinosa*	CBS 294.60	Driftwood	USA	MH857988	MH869542	–	–
Trichosphaeriales/*Trichosphaeriaceae*	*Gibellulopsis simonii*	CBS 144923 T	Soil	Netherlands	MK047467	MK047517	–	–
	Lectera nordwiniana	CBS 144921 T	Soil	Netherlands	MK047461	MK047511	MK047570	–
	Plectosphaerella plurivora	CBS 131742 T	Apex turion of *Asparagus officinalis*	Italy	KY399826	KY662248	KY421324	KY421298

[1] T: Ex-holotype or ex-type strains.
[2] ITS: internal transcribed spacers and intervening 5.8S nrDNA; LSU: partial large subunit (28S) nrRNA gene; *tef1*: partial translation elongation factor 1-alpha gene; *tub2*: partial β-tubulin gene.
Accession numbers of sequences generated in this study are in **bold**; – indicates unavailable sequences or unknown collection data.

Divergence time estimates were performed using the BEAST v. 2.7.6 (Bouckaert et al. 2019) software package. The dataset partition scheme and setting priors were implemented in BEAUti v. 2.7.6 according to the best-fit substitution model for each gene. To accommodate for rate heterogeneity across the branches of the tree, we used an uncorrelated relaxed clock model with lognormal distribution in the fossil analysis. A Yule process speciation rate was used for the tree prior. Two independent Markov chain Monte Carlo (MCMC) runs of 100 M generations were performed, with sampling at every 1 000th generation. Tracer v. 1.7.2 (Rambaut et al. 2018) was used to evaluate convergence and ensure that adequate ESS values for all parameters were > 200. After discarding the first 25 % representing the burn-in phase, the remaining trees were combined using LogCombiner v. 2.7.6, and then the time-calibrated species tree was summarised as a Maximum Clade Credibility (MCC) tree in TreeAnnotator v. 2.7.6. The MCC tree was viewed and modified in the Interactive Tree of Life (iTOL) (https://itol.embl.de) online tool (Letunic & Bork 2021).

RESULTS

Phylogenetic analyses

Phylogenetic tree reconstructions were carried out using two different datasets (Sequence data of 68 *Cephalotrichum* and 72 *Microascus* strains) and two different approaches (ML and BI). For each dataset, the two tree-building approaches obtained almost identical topologies, and the ML tree was selected to represent and discuss the phylogenetic relationships among taxa (Fig. 1, 2). In *Cephalotrichum* (Fig. 1), the combined dataset of 24 taxa and four genes consisted of 3 083 characters (630 for ITS, 904 for LSU, 981 for *tef1* and 568 for *tub2*), 2 575 of which are constant, 147 are variable and parsimony-uninformative, while 361 are parsimony-informative. Sequences of *Wardomyces inflatus* and *W. pulvinatus* were used as the outgroups. The jModelTest selected the best-fit model for four gene regions (ITS GTR+I+G, LSU GTR+I+G, *tef1* GTR+G, *tub2* HKY+I+G) based on the results under the output strategy of AIC. For *Microascus* (Fig. 2), the sequence data comprised 49 taxa with *Pseudoscopulariopsis schumacheri* and *Scopulariopsis soppii* as the outgroup taxa. The alignment consisted of 2 933 characters (654 for ITS, 852 for LSU, 901 for *tef1* and 526 for *tub2*), including 2 138 constant, 623 parsimony-informative and 172 parsimony-uninformative. The optimal nucleotide substitution model of the four gene regions (ITS GTR+G, LSU GTR+I+G, *tef1* TrN+I+G, *tub2* HKY+G) was used for the phylogenetic analyses.

Within *Cephalotrichum*, the phylogenetic analyses recognized 24 species with strong support, which chiefly clustered in 11 subclades (Fig. 1), including four newly described species, *C. brunneisporum*, *C. lageniforme*, *C. multisynnematum* and *C. silvanum*. As the tree shows, almost all the relationships between the major clades are highly supported by three independent algorithms. Among these clades, *C. nanum* diverged first, and then a monophyletic group formed by the type species *C. stemonitis* and its sister species *C. hinnuleum*. Subsequently, its sister subclade branched into two lineages, one which was comprised of *C. lignatile* and *C. silvanum*, and the other of four strains of *C. microsporum*. Species within the *C. brunneisporum*, *C. multisynnematum* and *C. tenuissimum* subclades share a broad range of morphological and ecological traits, which reflects in their phylogenetic placement as a monophyletic group. In particular, the *C. brevistipitatum*, *C. dendrocephalum*, *C. inflatum* and *C. purpureofuscum* clades are strongly supported monophyletic lineages, with an emergent internal structure. Additionally, there is a strongly supported subclade consisting mainly of *C. domesticum*, a species with a worldwide

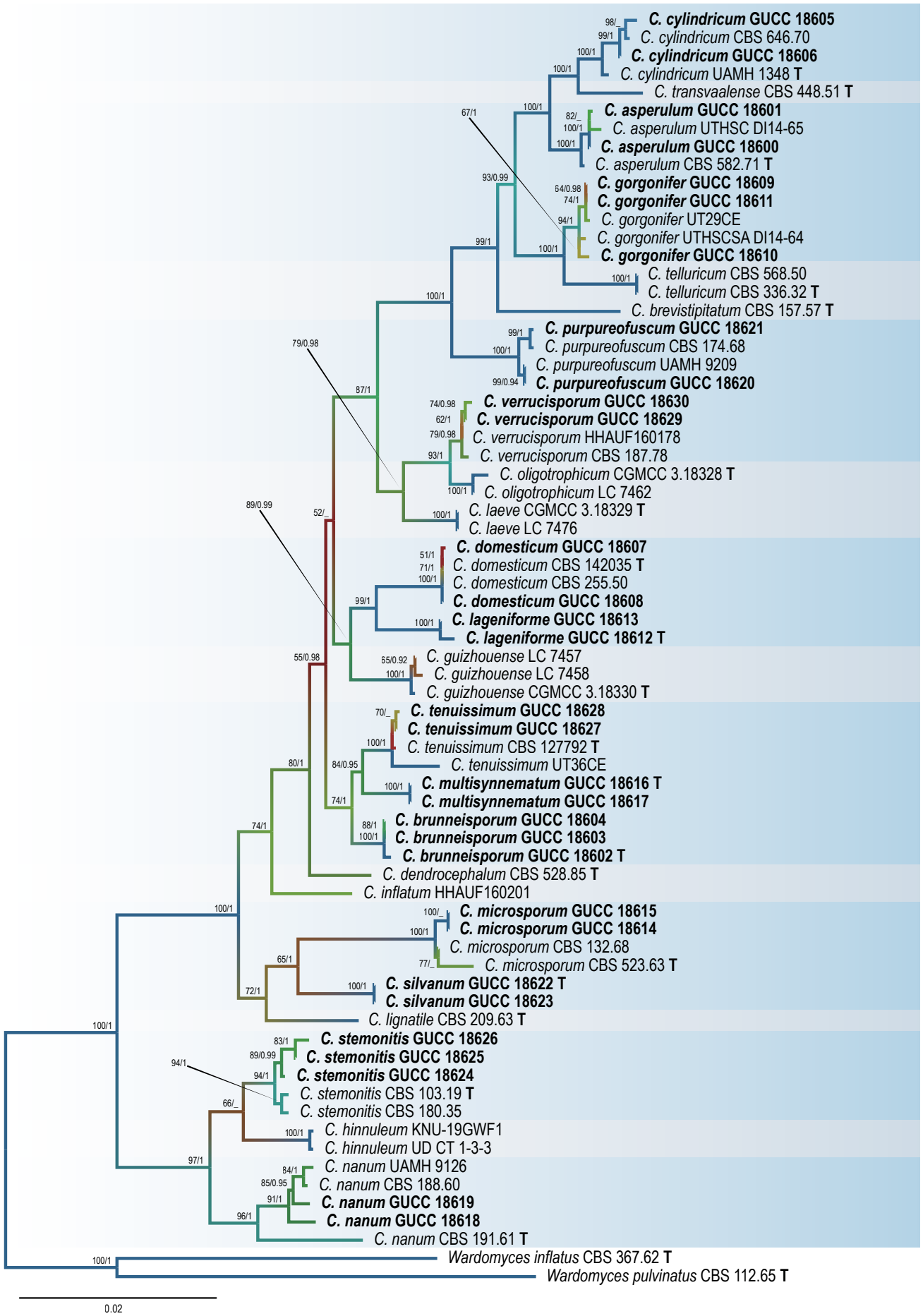

Fig. 1 Phylogenetic tree of *Cephalotrichum* inferred with a Maximum Likelihood (RAxML) analysis of the combined ITS, LSU, *tef1*, and *tub2* gene sequences. The statistical support of the branches is represented by different colours, with RAxML Bootstrap support values ≥ 50 % (MLBS) and Bayesian posterior probabilities ≥ 0.90 (BIPP) shown at the nodes (MLBS/BIPP). *Wardomyces inflatus* (CBS 367.62 T) and *W. pulvinatus* (CBS 112.65 T) were used as outgroups. Those in **bold** are new taxa proposed in the current study and the strains obtained. Ex-type strains are indicated with (**T**) at the end of the taxa labels.

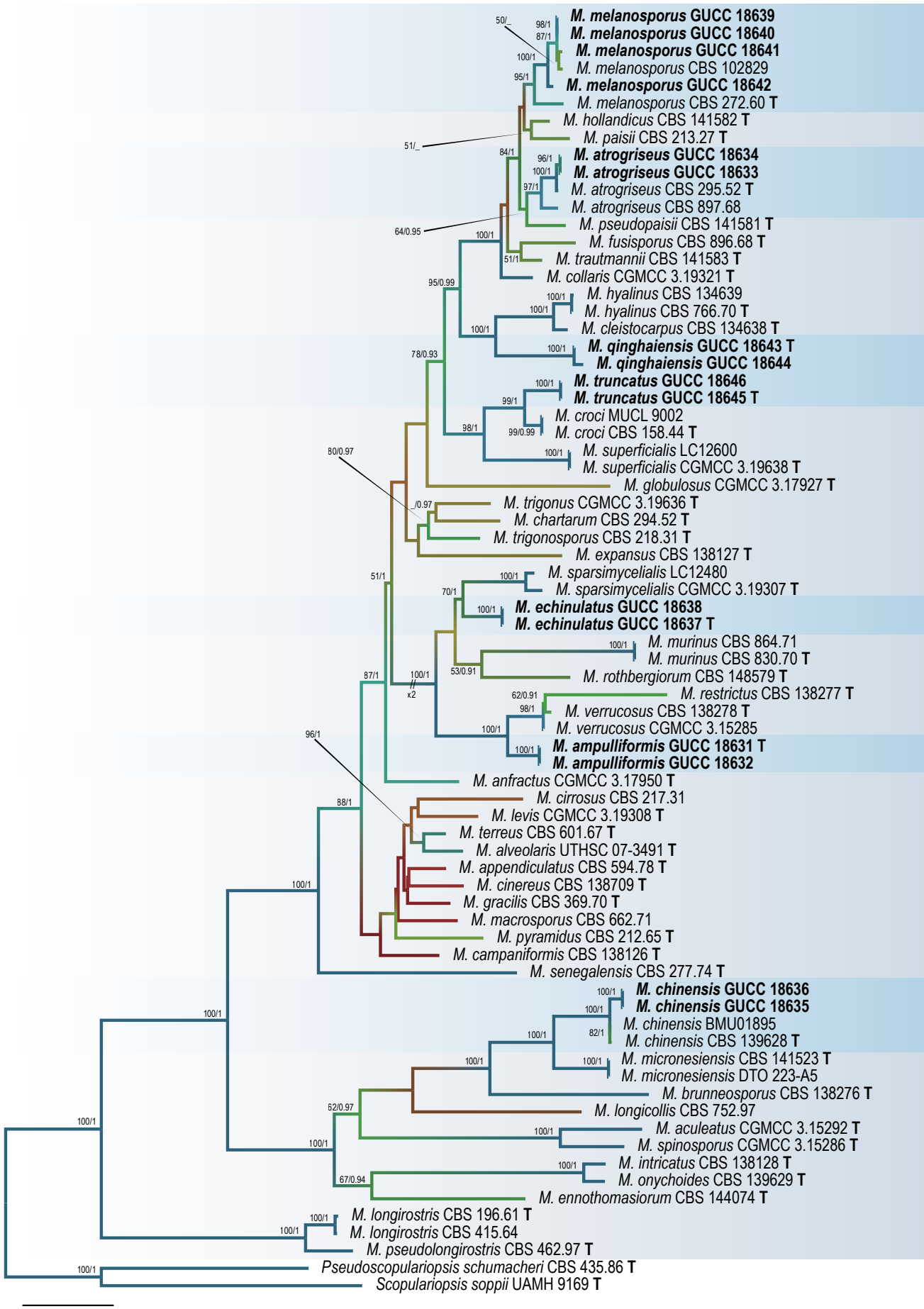

Fig. 2 Phylogenetic tree of *Microascus* inferred with a Maximum Likelihood (RAxML) analysis of the combined ITS, LSU, *tef1*, and *tub2* gene sequences. The statistical support of the branches is represented by different colours, with RAxML Bootstrap support values ≥ 50 % (MLBS) and Bayesian posterior probabilities ≥ 0.90 (BIPP) shown at the nodes (MLBS/BIPP). *Pseudoscopulariopsis schumacheri* (CBS 435.86 T) and *Scopulariopsis soppii* (UAMH 9169 T) were used as outgroups. Those in **bold** are new taxa proposed in the current study and the strains obtained. Ex-type strains are indicated with (**T**) at the end of the taxa labels.

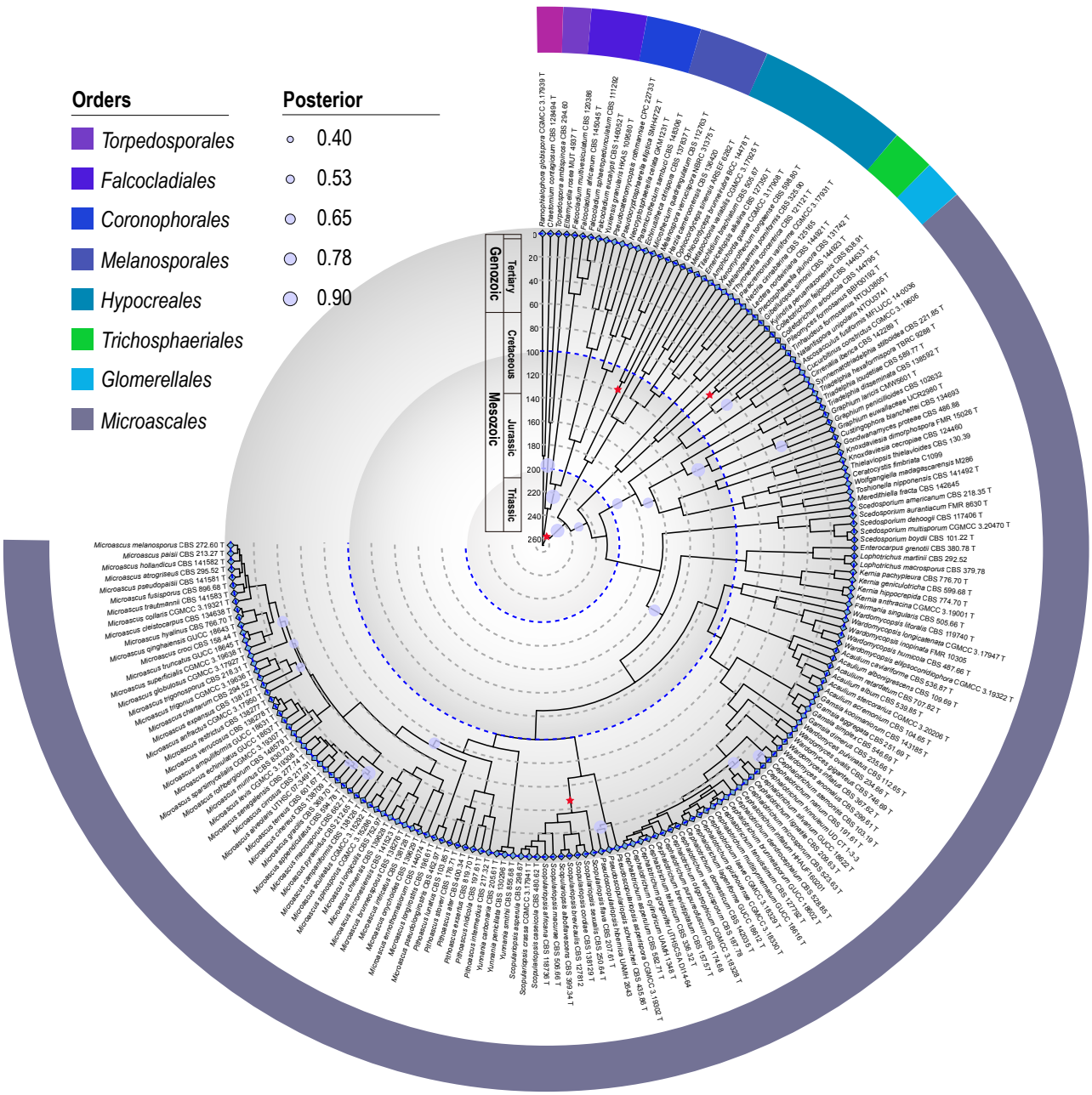

Fig. 3 Maximum clade credibility (MCC) tree with divergence times estimates for main groups of the subclass *Hypocreomycetidae* obtained from a Bayesian approach (BEAST) using four fossil constraints. Different orders of the subclass *Hypocreomycetidae* are depicted using different-coloured blocks. Assignments of the fossil constraints are marked with red stars. Nodes with posterior probabilities (PP) lesser than 0.90 are marked with blue circles in proportion to their PP values. For reference, the time scale is shown right above the phylogenetic tree.

distribution, as well as a new species, *C. lageniforme*, but also including *C. guizhouense*, a species known only from caves in China. *Cephalotrichum oligotrophicum* was placed as sister to *C. verrucisporum*, and this clade served as sister to *C. laeve*. All analyses suggested that the *C. asperulum*, *C. cylindricum* and *C. transvaalense* were located at the terminal end of the phylogenetic tree, and together they constituted a sister subclade with *C. gorgonifer* as well as *C. telluricum*.

The phylogenetic tree of *Microascus* distinguished 49 species, which chiefly clustered in 14 subclades (Fig. 2), of which four correspond to the novel species proposed here, namely *M. ampulliformis*, *M. echinulatus*, *M. qinghaiensis* and *M. truncatus*. Within the ingroup, *M. longirostris* and *M. pseudolongirostris* were placed as the basal lineage with strong support, which is the earliest diverging clade of the genus. Importantly, the *Microascus* core clade is represented by the following species: *M. aculeatus*, *M. brunneosporus*, *M. chinensis*, *M. ennothomasiorum*, *M. intricatus*, *M. longicollis*, *M. micronesiensis*, *M. onychoides* and *M. spinosporus*. In contrast, the *M. alveolaris*, *M. cirrosus*, *M. levis* and *M. terreus* clades were resolved as monophyletic groups of four species, and showed close relationships with *M. appendiculatus*, *M. cinereus* and *M. gracilis*, while *M. campaniformis*, along with *M. macrosporus* and *M. pyramidus* were placed as basal branches of this lineage, although their branching order was less resolved. However, relationships among these species were less resolved. *Microascus anfractus*, *M. globulosus* and *M. senegalensis* subclades formed several well-circumscribed monophyletic lineages with strong support. Moreover, the analysis showed that strains from *M. ampulliformis*, *M. echinulatus, M. murinus*, *M. restrictus*, *M. rothbergiorum*, *M. sparsimycelialis* and *M. verrucosus* formed a subclade, in which *M. ampulliformis* and *M. echinulatus* were inferred as two well-supported monophyletic new species. On the other hand, *M. chartarum*, *M. expansus*, *M. trigonosporus* and *M. trigonus* belong to a monophyletic subclade, but each species is weakly supported. It should be pointed out that all isolates of the new species *M. truncatus*

were more closely related to *M. croci* than to *M. superficialis*. Similarly, *M. cleistocarpus* was inferred as a sister group of *M. hyalinus*, which shares the most recent common ancestor with *M. qinghaiensis*, while *M. qinghaiensis* was identified as a divergent lineage. In particular, *M. fusisporus* and *M. trautmannii* are resolved as the closest phylogenetic relative to *M. collaris*, which serves as the basal taxon of this lineage. *Microascus atrogriseus* and *M. pseudopaisii* clustered in the same subclade and received moderate to strong support. *Microascus hollandicus* and *M. paisii* formed a branch sister to the clade comprising all strains of *M. melanosporus*.

Divergence time estimation

One hundred and eighty-four taxa were selected for molecular dating to estimate the divergence time of the *Microascaceae*, including 15 genera representing this family, and four calibrating points (Table 2, Fig. 3). *Chaetomium contagiosum* and *Ramophialophora globispora* were selected as outgroups. Based on the clear divergence age estimates, the divergence time of the *Microascales* crown group is 223.06 Mya (95 % HPD: 189.89–259.68 Mya), which is also within the period that major fungal orders diverged, similar to those described in previous reports (Liu et al. 2017). Dating analyses supported the supposition that the *Microascaceae* originated as an independent group in the Late Triassic (210.37 Mya, 95 % HPD: 177.18–246.96 Mya) and diversified in the Middle Jurassic (162.99 Mya, 95 % HPD: 129.75–198.48 Mya) (Fig. 3). At the genus level, the crown age of *Microascus* was estimated to be approximately the Late Cretaceous, at 76.21 Mya (95 % HPD: 61.03–92.38 Mya), while the two genera *Yunnania* and *Pithoascus* evolved 6.59–48.85 Mya. For *Cephalotrichum*, the ßdivergence times of the species range from 3.18 Mya to 39.79 Mya, while for *Wardomyces* it is 8.25 Mya to 74.28 Mya. Moreover, *Pseudoscopulariopsis* and *Scopulariopsis* share the most common ancestor at 65.84 Mya (95 % HPD: 49.59–85.90 Mya) in the Late Cretaceous. *Acaulium* originated earlier as an independent group in the Middle Cretaceous (94.07 Mya, 95 % HPD: 74.58–115.70 Mya), while *Gamsia* originated later as an independent group in the Late Cretaceous (74.28 Mya, 95 % HPD: 57.50–92.90 Mya).

TAXONOMY

Cephalotrichum Link, Mag. Ges. Naturf. Freunde Berlin 3: 20. 1809

Synonyms. *Doratomyces* Corda, Deutschl. Fl., Abt. 3, Pilze Deutschl. 2: 65. 1829.
Echinobotryum Corda, Deutschl. Fl., Abt. 3, Pilze Deutschl. 3: 51. 1831.
Stysanus Corda, Icon. Fungorum (Prague) 1: 21. 1837.
Synpenicillium Costantin, Bull. Soc. Mycol. France 4: 62. 1888.
Trichurus Clem., Bot. Surv. Nebraska 4: 7. 1896.
Berkeleyna Kuntze, Revis. Gen. Pl. (Leipzig) 3: 447. 1898.
Pycnostysanus Lindau, Verh. Bot. Vereins Prov. Brandenburg 45: 160. 1904.
Stysanopsis Ferraris, Ann. Mycol. 7: 281. 1909.
Capnostysanus Speg., Physis (Buenos Aires) 4: 295. 1918.

Type species. *Cephalotrichum stemonitis* Link

Notes — *Cephalotrichum*, typified by *C. stemonitis*, is characterised by the formation of dry-spored, indeterminate synnemata and enteroblastic percurrent conidiogenesis (Link 1809, Abbott 2000, Sandoval-Denis et al. 2016b, Woudenberg et al. 2017b). Other genera of *Microascaceae*, such as *Microascus*, *Scopulariopsis* and *Wardomycopsis*, except that they never form synnemata, have very similar asexual morphs to *Cephalotrichum*, especially when isolates grow on a rich culture medium like PDA. The 33 strains (14 species) of *Cephalotrichum* collected in China in the present study indicate that the genus has a wide geographical distribution range.

Cephalotrichum asperulum (J.E. Wright & S. Marchand) Sand.-Den. et al., Stud. Mycol. 83: 201. 2016 — Fig. 4

Basionym. *Doratomyces asperulus* J.E. Wright & S. Marchand, Bol. Soc. Argent. Bot. 14: 308. 1972.

Description — Wright & Marchand (1972).

Materials examined. China, Hubei Province, Shiyan City, isolated from farmland soil, 2006, *Y.L. Jiang* (HGUP 18600), living culture GUCC 18600; Shaanxi Province, Hanzhong City, Yangxian County, isolated from vegetable soil, 2005, *T.Y. Zhang* (HGUP 18601), living culture GUCC 18601.

Notes — This species was originally introduced as *Doratomyces asperulus* from the humus-rich soil of grassland in Argentina (Wright & Marchand 1972), and subsequently transferred to *Cephalotrichum* as a synonym of *C. purpureofuscus* (Abbott 2000). Later, Sandoval-Denis et al. (2016b) confirmed the taxonomic position of this species within *Cephalotrichum* and introduced a new name *C. asperulum* based on a multigene phylogenetic analysis and detailed morphological studies. In this study, phylogenetic inference revealed that our two newly collected isolates clustered together with the ex-type culture of *C. asperulum* with high statistical support (Fig. 1). Furthermore, despite that *C. asperulum* shares a sister relationship with *C. transvaalense*, the high number of variable positions in the ITS (4 bp, 1 %), LSU (6 bp, 1 %), *tef1* (11 bp, 1 %) and *tub2* (24 bp, 4 %) alignments supports the split into two distinct taxa. Morphologically, the most remarkable features of *C. asperulum* are the presence of apically pointed and coarsely roughened conidia with a spiral-sculpted appearance (Fig. 4). Therefore, we identified our isolates as *C. asperulum* based on morphology and their identical sequences.

Cephalotrichum brunneisporum T.P. Wei & Y.L. Jiang, *sp. nov.* — MycoBank MB 850570; Fig. 5

Etymology. Referring to the dark brown conidia produced by this fungus.

Typus. China, Qinghai Province, Tongren City, isolated from forest soil, 2006, *Y.L. Jiang* (holotype HGUP 18602, culture ex-type GUCC 18602).

Hyphae septate, subhyaline to pale brown, branched, smooth and thin-walled, 1.5–3 µm wide. *Synnemata* (355–)401–1042.5 (–1102) µm high, scattered or caespitose, stipes dark brown to black, composed of rather compact attached hyphae, with some anastomoses between adjacent hyphae, unbranched or with 1–2 side branches, somewhat interwoven and rough-walled towards the base, (247.5–)262–636(–713) × (13.5–)14–36 (–40) µm, conidial heads brown to olive grey, obclavate to cylindrical, (108.5–)113–405(–546) × (91–)98.5–199(–226) µm. Setae absent. *Conidiophores* in synnemata arising directly from vegetative hyphae, branched or unbranched, septate, pale brown to brown, irregularly mono- or biverticillate, with all elements tightly appressed, metulae (5.5–)6–19(–25) × 2.5–3(–4) µm. *Conidiogenous cells* percurrent, commonly penicillately arranged, (3.5–)4–6.5(–7.5) × (2–)2.5–3 µm, ampulliform to cylindrical, subhyaline to pale brown, smooth and thin-walled, tapering gradually to a cylindrical annellate zone, (1–)1.5(–2) µm wide. *Conidia* obovoid to cylindrical, with truncate base and rounded apex, single or in short chains, smooth or finely verruculose, olive brown to dark brown, (4.5–)5–6 × 3–4(–4.5) µm (av. ± SD = 5.5 ± 0.5 × 3.5 ± 0.3 µm, n = 30). Sexual morph not observed.

Culture characteristics — Colonies on OA reaching up to 67–75 mm diam after 21 d at 25 °C, flat, with sparse aerial mycelium, white with iron grey synnemata, margin entire to undulate. On PDA reaching 40–56 mm diam, compact, finely felty, slightly raised, with abundant aerial mycelium, white or cream-coloured to olivaceous grey from margin to centre, margin regular. On SNA attaining 55–72 mm diam, flat, with

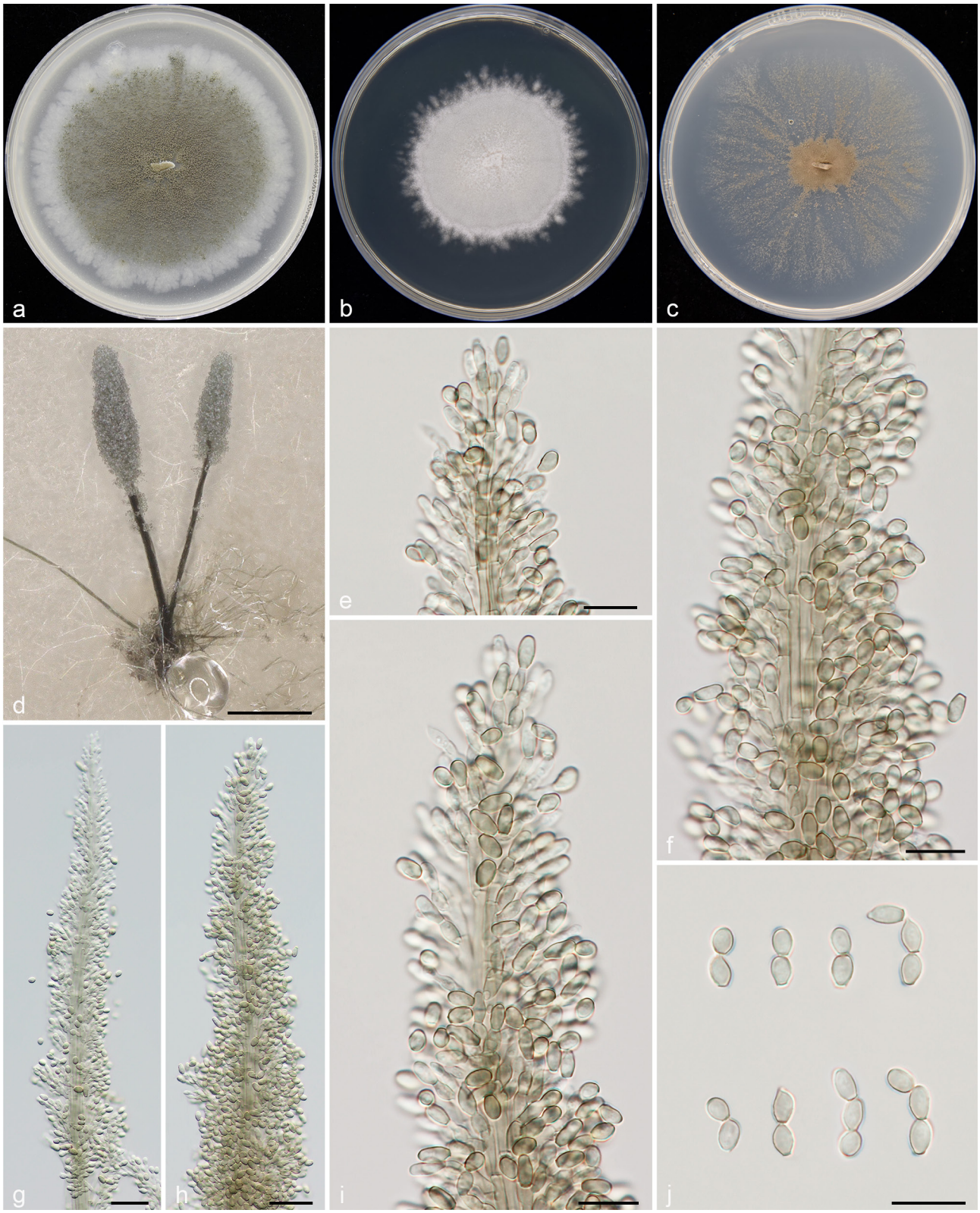

Fig. 4 *Cephalotrichum asperulum* (GUCC 18600). a–c. Colony on OA, PDA and SNA; d. synnemata; e–h. detail of the apical portion of a synnema; i. conidiophores, conidiogenous cells and conidia; j. ovoid to ellipsoidal conidia in chains. — Scale bars: d = 200 µm, g, h = 20 µm, all others = 10 µm.

dense dark brown synnemata at the centre, cream-coloured or pale grey in outer region, aerial mycelium scanty, with fimbriate margin.

Additional materials examined. China, Qinghai Province, Xinghai County, isolated from farmland soil, 2006, *Y.L. Jiang* (HGUP 18603), living culture GUCC 18603; Shandong Province, Dongying City, isolated from cotton soil, 2008, *H.M. Liu* (HGUP 18604), living culture GUCC 18604.

Notes — In the present study *C. brunneisporum* is introduced as a new species based on morphological and phylogenetic differences to other *Cephalotrichum* species. According to our phylogenetic inference, the three newly collected isolates representing *C. brunneisporum* were resolved as a strongly supported genealogically exclusive lineage in the phylogeny inferred from the combined dataset (Fig. 2). Although *C. brunneisporum* shares a sister relationship with *C. multisynnematum*, it differs from the latter by 32 bp in the four loci dataset. Furthermore, they can also be distinguished based on their morphological characteristics as *C. brunneisporum* is characterised by obovoid

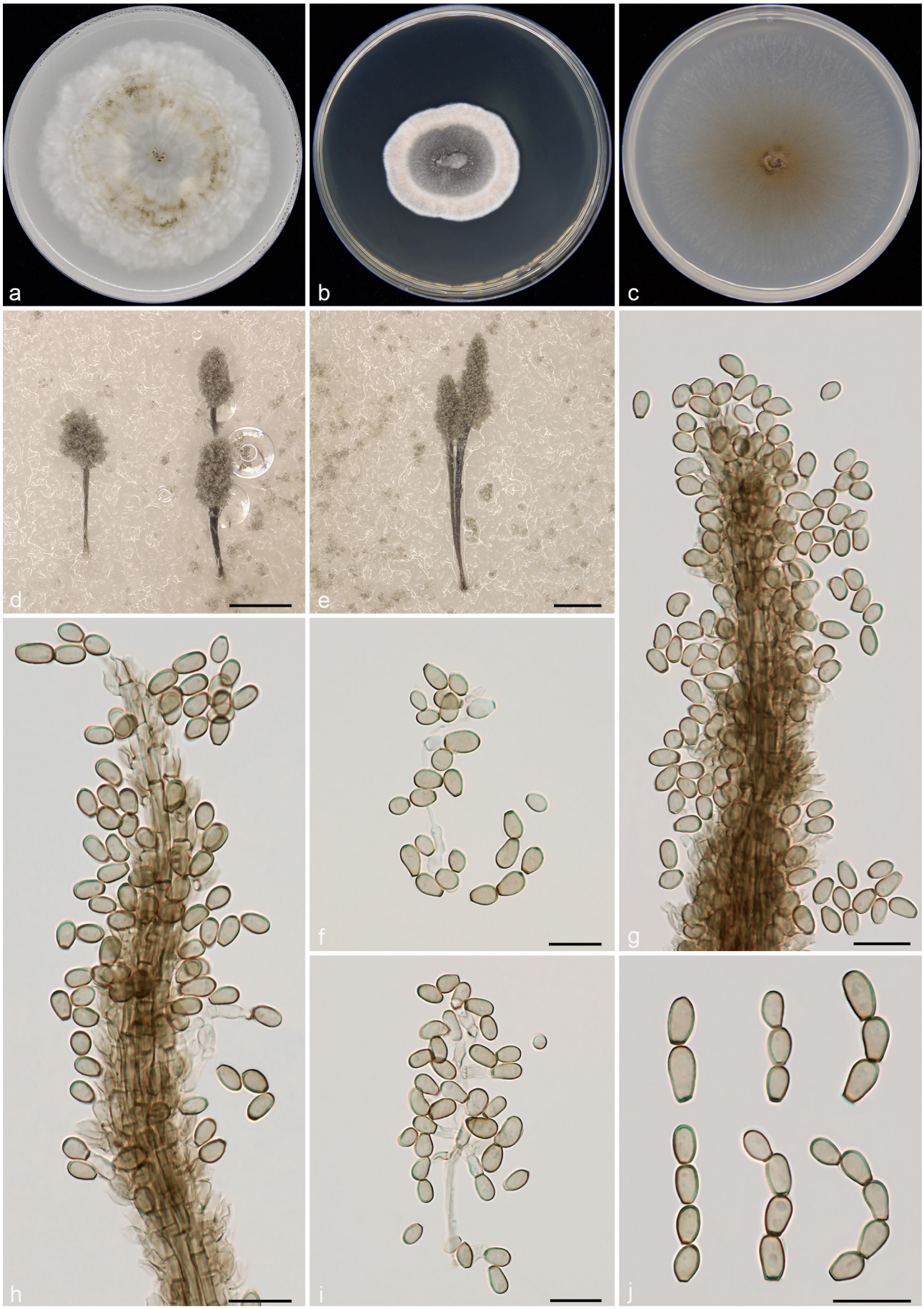

Fig. 5 *Cephalotrichum brunneisporum* (culture ex-type GUCC 18602). a–c. Colony on OA, PDA and SNA; d, e. synnemata; f, i. conidiophores, polyblastic conidiogenous cells bearing conidia; g, h. detail of the apical portion of a synnema; j. obovoid to cylindrical conidia in chains. — Scale bars: d, e = 200 µm, all others = 10 µm.

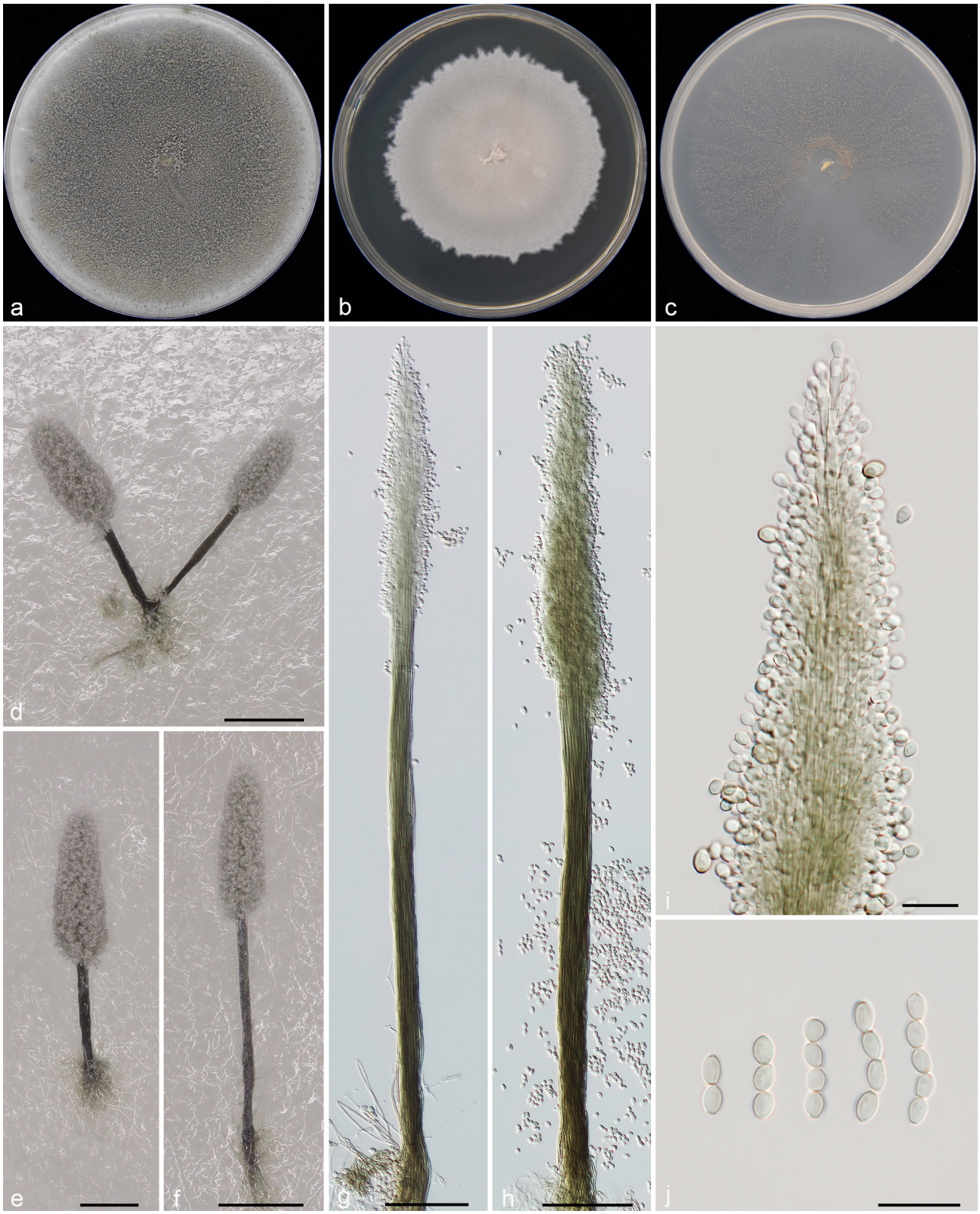

Fig. 6 *Cephalotrichum cylindricum* (GUCC 18605). a–c. Colony on OA, PDA and SNA; d–f. synnemata; g, h. detail of the apical portion of synnema; i. tip of synnema with annellidic conidiogenous cells and conidia; j. ovoid to ellipsoidal conidia in chains. — Scale bars: d–f = 200 µm, g, h = 50 µm, all others = 10 µm.

to cylindrical, olive brown to dark brown, smooth or finely verruculose conidia (4.5–6 × 3–4.5 µm), and 355–1102 µm high synnemata. In contrast, the conidia of *C. multisynnematum* are subglobose or pyriform, with thickened and darkened secession scars, brown to olive green and smaller (3.5–4.5 × 3–4 µm), as well as longer synnemata (541.5–1252 µm) (Fig. 11).

Cephalotrichum cylindricum (Clem. & Shear) S.P. Abbott, Stud. Mycol. 83: 207. 2016 — Fig. 6

Basionym. *Trichurus cylindricus* Clem. & Shear, Bot. Surv. Nebraska 4: 7. 1896.
Synonym. *Trichurus terrophilus* Swift & Povah, Mycologia 21: 214. 1929.

Descriptions — Swift (1929), Abbott (2000).

Materials examined. China, Qinghai Province, Dari County, isolated from steppe soil, 2007, H.Q. Pan (HGUP 18605), living culture GUCC 18605; Sichuan Province, Leshan City, Mount Emei, isolated from shrub soil, 2005, *Y.L. Jiang* (HGUP 18606), living culture GUCC 18606.

Fig. 7 *Cephalotrichum domesticum* (GUCC 18607). a–c. Colony on OA, PDA and SNA; d. synnemata; e. synnema with stipes and conidial head; f. young synnema; g. apical portion of synnema; h. ellipsoidal to cylindrical conidia in chains. — Scale bars: d = 200 µm, e, f = 20 µm, all others = 10 µm.

Notes — Molecular analyses in this study showed that our isolates (GUCC 18605 and GUCC 18606) clustered together with *C. cylindricum* (culture ex-epitype UAMH 1348) with full statistical support (Fig. 1), and the nucleotide homology between GUCC 18605 and UAMH 1348 for ITS, LSU, *tef1* and *tub2* is high at 99 % (567/568 bp), 100 % (882/882 bp), 99 % (927/931 bp) and 99 % (533/539 bp), respectively. Additionally, the morphological characters of our studied specimens fit well with *C. cylindricum* (Sandoval-Denis et al. 2016b; Fig. 6). *Cephalotrichum cylindricum* was originally reported from the decaying seeds of *Cucurbita maxima*, and subsequently from the seed of *Sorghum* and the timber of *Eucalyptus saligna* (Swift 1929, Abbott 2000, Sandoval-Denis et al. 2016b). This study expands its habitat range from the United States and South Africa to China, further confirming its lifestyle as saprophytic.

Cephalotrichum domesticum Woudenb. & Seifert, Stud. Mycol. 88: 146. 2017 — Fig. 7

Description — Woudenberg et al. (2017b).

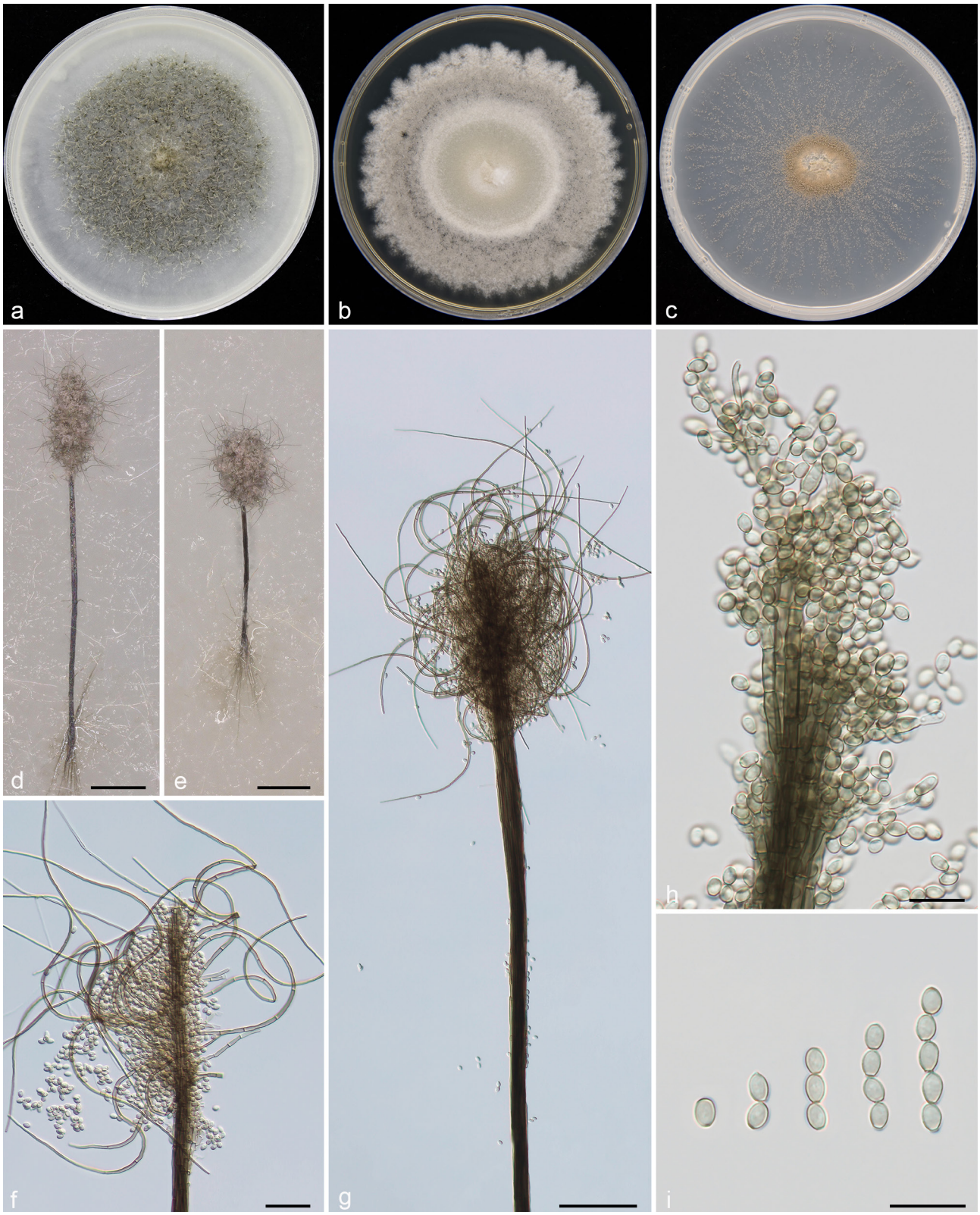

Fig. 8 *Cephalotrichum gorgonifer* (GUCC 18609). a–c. Colony on OA, PDA and SNA; d, e. synnemata; f, g. detail of synnemal setae; h. top of synnema showing divergent conidiophores; i. ovoid to ellipsoidal conidia in chains. — Scale bars: d, e = 200 µm, f = 20 µm, g = 50 µm, all others = 10 µm.

Materials examined. China, Chongqing City, Beibei District, isolated from bamboo forest soil, 2005, *Y.L. Jiang* (HGUP 18607), living culture GUCC 18607; Guangxi Province, Guilin City, isolated from botanical garden grass soil, 2005, *Y.L. Jiang* (HGUP 18608), living culture GUCC 18608.

Notes — In the present study, the phylogenetic result shows that our new collections (GUCC 18607 and GUCC 18608) cluster together with *C. domesticum* with high statistical support (Fig. 2). *Cephalotrichum domesticum* always clustered outside the sections *C. lageniforme* and *C. guizhouense*, being resolved as a sister to the latter two species. Furthermore, this taxon (CBS 255.50) has lower nucleotide homology with the latter two species in ITS (3 and 3 bp), LSU (2 and 2 bp), *tef1* (16 and 7 bp) and *tub2* (17 and 29 bp). Its distinguishing features include pale brown to brown, smooth-walled and ellipsoidal to cylindrical conidia with truncate base and rounded or pointed apex (Fig. 7). These distinctive characteristics serve to differentiate *C. domesticum* from other closely related taxa. This is the second report of *C. domesticum*, representing a

Fig. 9 *Cephalotrichum lageniforme* (culture ex-type GUCC 18612). a–c. Colony on OA, PDA and SNA; d, e. synnemata; f–k. conidiophores, polyblastic conidiogenous cells and conidia; l. synnema with stipes and conidial head; m. apical portion of a synnema. — Scale bars: d, e = 250 µm, all others = 10 µm.

new record from China, having previously been isolated in the Netherlands from manure, plaster and indoor air (Woudenberg et al. 2017b).

Cephalotrichum gorgonifer (Bainier) Sand.-Den. et al., Stud. Mycol. 83: 207. 2016 — Fig. 8

Basionym. *Trichurus gorgonifer* Bainier, Bull. Soc. Mycol. France 23: 230. 1907.
Synonyms. *Trichurus spiralis* Hasselbr., Bot. Gaz. 29: 321. 1900.
Cephalotrichum heliciforme T.Y. Zhang, Mycosystema 33: 948. 2014.

Descriptions — Ellis (1971), Domsch et al. (2007).

Materials examined. China, Guangdong Province, Huizhou City, Huidong County, isolated from forest soil, 2004, *Y.L. Jiang* (HGUP 18609), living culture GUCC 18609; Dongguan City, isolated from farmland soil, 2004, *Y.L. Jiang* (HGUP 18610), living culture GUCC 18610; Qinghai Province, Jainca County, isolated from forest soil, 2006, *H.M. Liu* (HGUP 18611), living culture GUCC 18611.

Notes — *Cephalotrichum gorgonifer* was initially described as *Trichurus gorgonifer* because of the presence of its spirally coiled setae, and later transferred to *Cephalotrichum* (Ellis 1971, Domsch et al. 2007, Zhang et al. 2014). This species has a widespread distribution and has been recorded from compost, domestic waste, soil, wood, house, human hair and foot, bronchoalveolar lavage fluid, and maxillary sinus fluid in Canada, Italy, South Africa, the Netherlands, Germany and the USA (Sandoval-Denis et al. 2016b, Woudenberg et al. 2017b). Some strains of *C. gorgonifer* were isolated from human clinical samples, mainly hair and respiratory specimens (Sandoval-Denis et al. 2016b). However, the three strains obtained in the present study and the majority of isolates that have been reported for this species thus far originate from soil and decaying vegetable materials, indicating that this species can also be saprophytic, corroborating the supposition that it can be saprophytic or an opportunistic pathogen.

Cephalotrichum lageniforme T.P. Wei & Y.L. Jiang, *sp. nov.* — MycoBank MB 850571; Fig. 9

Etymology. Referring to the shape of conidiogenous cells produced by this species.

Typus. China, Sichuan Province, Jiuzhaigou County, Jiuzhaigou Valley Scenic and Historic Interest Area, isolated from coniferous forest soil, 2005, *Y.L. Jiang* (holotype HGUP 18612, culture ex-type GUCC 18612).

Hyphae pale brown to brown, septate, branched, smooth and thin-walled, 1.5–2 µm diam. *Synnemata* solitary, up to (1409–)1647–2473.5(–2508.5) µm tall, stipes dark brown to black, composed of rather compact attached hyphae, unbranched, (736–)887–1581(–1597) × (24.5–)30–50(–52) µm, upper portion forming an ellipsoidal to broad fusiform sporulating head, brown to olive grey, (429–)560–892.5(–918) × (263–)369–545(–627) µm; sessile conidiomata lacking a stipe present in some transfers, forming brown to olive green, subglobose conidial tufts. *Conidiophores* arising from synnemata or vegetative hyphae, unbranched or sparingly branched, septate, pale brown to brown, monoverticillate to irregularly bi- or terverticillate, commonly aggregated in dense synnemata or reduced to single conidiogenous cells, (7.5–)10.5–82(–98) × (1.5–)2–3 µm. *Conidiogenous cells* terminal or intercalary, lageniform to cylindrical or irregularly fusiform, smooth and thin-walled, subhyaline to pale brown, tapering gradually to a cylindrical annellate zone 1.5–2 µm wide, usually in groups of 1–9 on short metulae, (3–)3.5–6.5(–7) × 2.5–3 µm. *Conidia* ovoid to subcylindrical, base truncate to short obconically truncate with visible secession scars, apex obtuse, single or in short chains, brown to olive green, smooth or finely verruculose, (4–)4.5–6 × 2.5–3.5 µm (av. ± SD = 5.2 ± 0.5 × 3 ± 0.3 µm, n = 30). Sexual morph not observed.

Culture characteristics — Colonies on OA reaching 68–79 mm diam after 21 d in darkness at 25 °C, flat, with entire margin, aerial mycelium moderately dense, whitish or pale grey to olivaceous brown from margin to centre. On PDA reaching 43–54 mm diam, compact, finely felty, with abundant aerial mycelium, cream-coloured or pale grey to dark grey from margin to centre, with entire to undulate margin, spreading and lacking synnemata. On SNA attaining 67–69 mm diam, planar, spreading, pale grey to dark brown with conspicuous concentric rings, margin entire, with sparse aerial mycelium.

Additional material examined. China, Guizhou Province, Anshun City, Puding County, isolated from forest soil, 15 Nov. 2022, *T.P. Wei* (HGUP 18613), living culture GUCC 18613.

Notes — Based on the analysis of DNA sequences of four markers, *C. lageniforme* forms a strongly supported subclade in *Cephalotrichum*, which is resolved with *C. domesticum* as two phylogenetically distinct sister lineages (Fig. 1). Although *C. lageniforme* is phylogenetically allied to *C. domesticum*, it is genetically distinct by 38 bp (GUCC 18612 vs CBS 255.50: ITS, 3 bp, LSU, 2 bp, *tef1*, 16 bp and *tub2*, 17 bp) in the four loci dataset. Morphologically, *C. domesticum* differs from *C. lageniforme* in having ellipsoidal to cylindrical, pale brown to brown, smooth and larger conidia (5.5–6.5 × 3–4 µm vs 4–6 × 2.5–3.5 µm) with rounded or pointed apices, as well as shorter synnemata (130–245 µm vs 1409–2508.5 µm) (Woudenberg et al. 2017b; Fig. 7). The ovoid to subcylindrical, brown to olive green, and smooth or finely verruculose conidia of *C. lageniforme* differ from other reported members of *Cephalotrichum* (Fig. 9).

Cephalotrichum microsporum (Sacc.) P.M. Kirk, Kew Bull. 38: 578. 1984 — Fig. 10

Basionym. *Stysanus microsporus* Sacc., Michelia 1: 274. 1878.
Synonyms. *Doratomyces microsporus* (Sacc.) F.J. Morton & G. Sm., Mycol. Pap. 86: 77. 1963.
Graphium graminum Cooke & Massee, Grevillea 16: 11. 1887.
Graphium pistillarioides Speg., Revista Fac. Agron. Univ. Nac. La Plata 2: 254. 1896.

Descriptions — Morton & Smith (1963), Ellis (1971), Domsch et al. (2007).

Materials examined. China, Anhui Province, Bengbu City, isolated from forest soil, 2007, *Y.L. Jiang* (HGUP 18614), living culture GUCC 18614; Guizhou Province, Guiyang City, Huaxi Wetland Park, isolated from lawn soil, 6 Aug. 2018, *X. Zhang* (HGUP18615), living culture GUCC 18615.

Notes — *Cephalotrichum microsporum* is a saprophytic fungus isolated from rotted trunks of *Robinia pseudacacia*, dead twigs of *Ligustrum vulgare*, indoor air, and wheat-field soil in Italy, the Netherlands, Canada and Germany (Sandoval-Denis et al. 2016b). This species was previously reported *Stysanus microsporus* and later transferred to the genus *Doratomyces* (as *D. microsporus*) and *Cephalotrichum* (Saccardo 1878, Morton & Smith 1963, Kirk & Spooner 1984). In this study, the phylogenetic results agreed with the previous results of Sandoval-Denis et al. (2016b). The two strains we collected and the two cultures representing *C. microsporum* clustered in a separate lineage, clearly distant from the branch bearing their sister species (*C. lignatile* and *C. silvanum*) (Fig. 1), which also shows low sequence similarity. Morphologically, the ovoid to ellipsoidal, 3.5–5 × 2–3 µm, green brown and smooth conidia, as well as 500–1000 µm tall synnemata of *C. microsporum* easily distinguish it from allied species (Fig. 10).

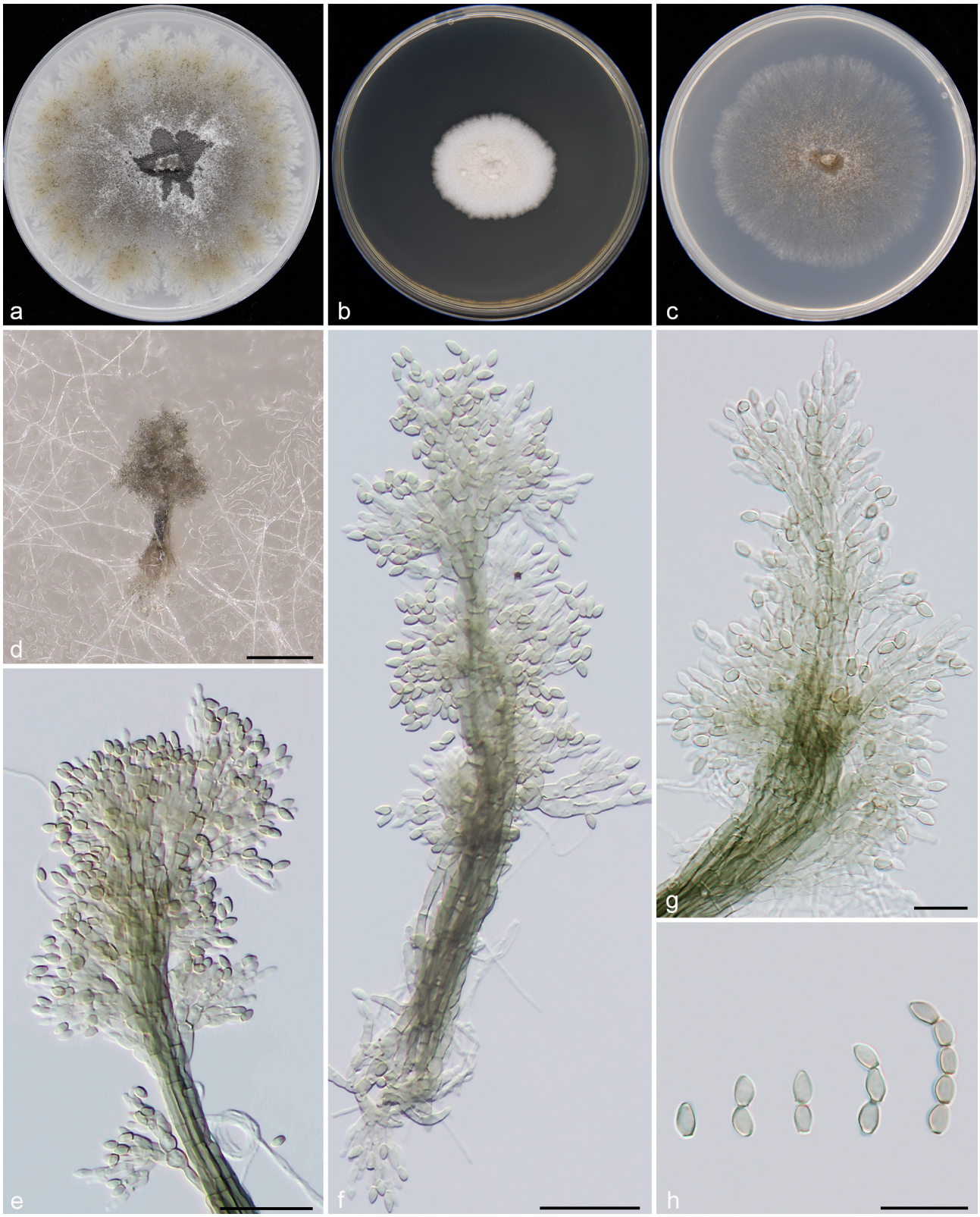

Fig. 10 *Cephalotrichum microsporum* (GUCC 18614). a–c. Colony on OA, PDA and SNA; d. synnemata; e, f. apical portion of synnema; g. top of synnema showing divergent conidiophores; h. ovoid to ellipsoidal conidia in chains. — Scale bars: d = 100 µm, e, f = 20 µm, all others = 10 µm.

Cephalotrichum multisynnematum T.P. Wei & Y.L. Jiang, *sp. nov.* — MycoBank MB 850572; Fig. 11

Etymology. Referring to the multiple branched synnemata produced by this fungus.

Typus. China, Qinghai Province, Haixi Mongolian and Tibetan Autonomous Prefecture, Ulan County, isolated from farmland soil, 2007, *Y.L. Jiang* (holotype HGUP 18616, culture ex-type GUCC 18616).

Mycelium superficial or immersed, hyphae branched, septate, subhyaline to brown, thin-walled, 1.5–2 µm wide. *Synnemata* scattered, up to (541.5–)668.5–943(–1252) µm tall, stipes dark brown to black, composed of rather compact attached hyphae, with some anastomoses between adjacent hyphae, unbranched or with 1–3 side branches, (319.5–)321–839.5(–936) × 22–36.5(–47) µm, upper portion forming a cylindrical sporulating head, brown to olive grey, (199–)210–415.5(–426.5) × (91–)94–170(–171) µm. *Setae* absent. *Conidiophores* irregularly mono- to bi- or terverticillate, septate, unbranched or sparingly branched, pale brown to brown, smooth, usually aggregated

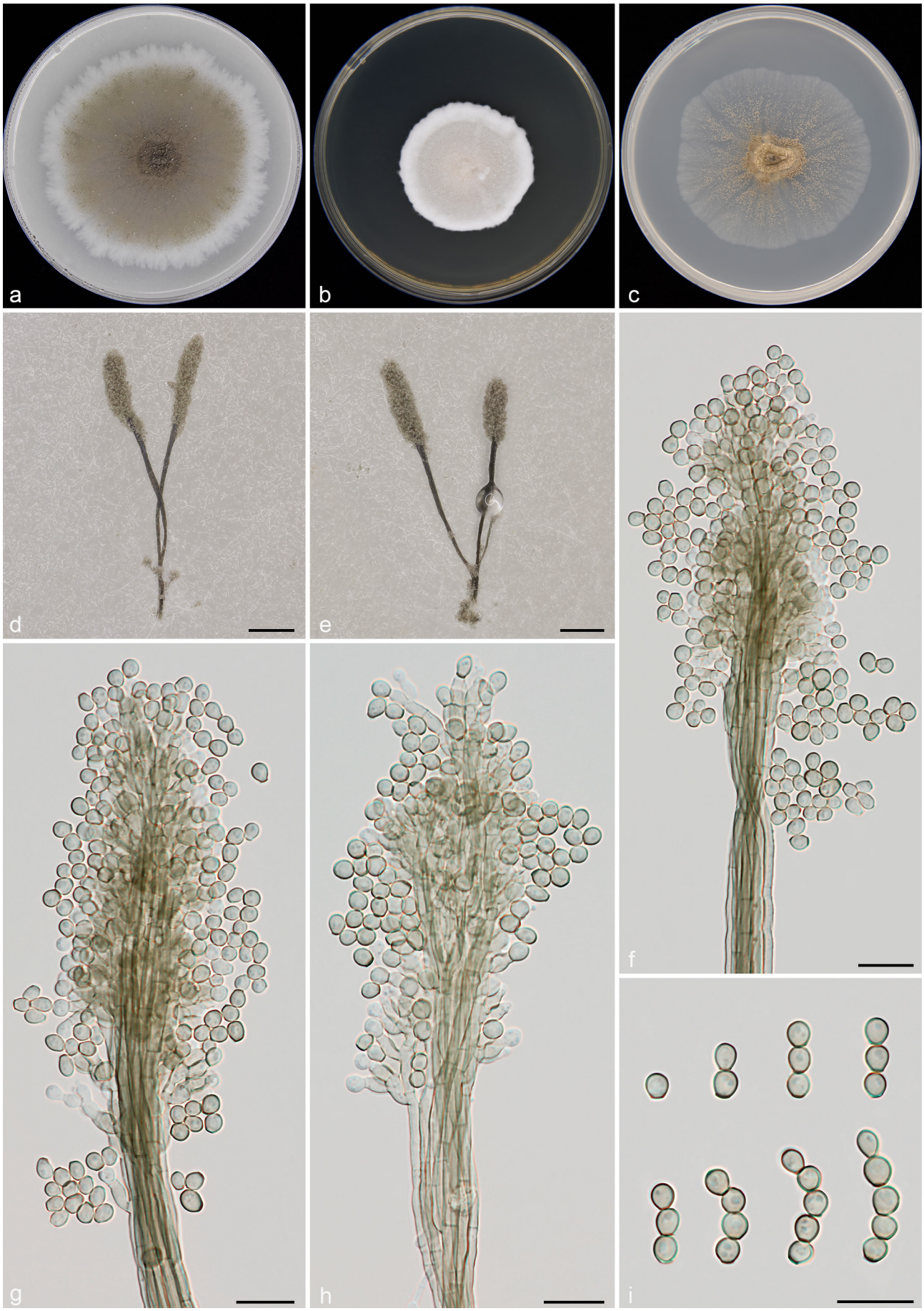

Fig. 11 *Cephalotrichum multisynnematum* (culture ex-type GUCC 18616). a–c. Colony on OA, PDA and SNA; d, e. branched synnemata; f, g. detail of the apical portion of synnema; h. top of synnema showing divergent conidiophores; i. subglobose or pyriform conidia in chains. — Scale bars: d, e = 200 µm, all others = 10 µm.

in synnemata, with all elements tightly appressed, occasionally reduced to conidiogenous cells, (16–)16.5–57.5(–58.5) × 2–3(–3.5) µm. *Conidiogenous cells* cylindrical or elongate ampulliform, terminal or intercalary, subhyaline to pale brown, smooth and thin-walled, with a distinct shoulder tapering to a cylindrical annellated zone 1.5–2.5 µm wide, annellations inconspicuous or slightly prominent, 3.5–5.5(–6) × 2–3 µm. *Conidia* subglobose or pyriform, apex rounded, base truncate to short obconically truncate, with thickened and darkened secession scars, smooth or finely verruculose, brown to olive green, single or in short chains, 3.5–4(–4.5) × 3–4 µm (av. ± SD = 3.7 ± 0.2 × 3.5 ± 0.2 µm, n = 30). Sexual morph not observed.

Culture characteristics — Colonies on OA reaching up to 66–71 mm diam after 21 d at 25 °C, olivaceous brown centre with white to cream-coloured outer ring, colony centre with conspicuous synnemata, margin discrete or dentate. On PDA reaching 38–45 mm diam, cottony, finely felty, abundant aerial mycelium, white to cream or beige, raised in the periphery, synnemata not produced, with an entire edge. On SNA attaining 56–58 mm diam, flat, spreading, with dense dark brown synnemata at the centre and grey loose synnemata near the edge.

Additional material examined. China, Shaanxi Province, Hanzhong City, Yangxian County, isolated from vegetable soil, 2005, *T.Y. Zhang* (HGUP 18617), living culture GUCC 18617.

Notes — *Cephalotrichum multisynnematum* is phylogenetically related to *C. brunneisporum* and *C. tenuissimum*, but *C. multisynnematum* forms a distinct branch as the sister clade to the latter two species, and is genetically distant from all species of *Cephalotrichum* (Fig. 1). Moreover, this new species differs by 32 bp and 26 bp from *C. brunneisporum* and *C. tenuissimum*, respectively, in the combined dataset. Morphologically, *C. brunneisporum* differs from *C. multisynnematum* by its obovoid to cylindrical, olive brown to dark brown and larger conidia (4.5–6 × 3–4.5 µm vs 3.5–4.5 × 3–4 µm), as well as shorter synnemata (355–1102 µm vs 541.5–1252 µm) (Fig. 5); *C. tenuissimum* differs by its ellipsoidal, hyaline to pale green brown, smooth and larger conidia (4.5–6.5 × 3–4 µm), as well as shorter synnemata (495–900 µm) (Woudenberg et al. 2017b; Fig. 16). In this study, multi-locus phylogenetic analyses and morphological features strongly support the recognition of *C. multisynnematum* as one phenotypically and phylogenetically distinct species.

Cephalotrichum nanum (Ehrenb.) S. Hughes, Canad. J. Bot. 36: 744. 1958 — Fig. 12

Basionym. *Periconia nana* Ehrenb., Sylv. Mycol. Berol. (Berlin) 13: 24. 1818.
Synonyms. *Stilbum nanum* (Ehrenb.) Spreng., Syst. Veg., ed. 16. 4: 547. 1827.
Graphium nanum (Ehrenb.) Sacc., Syll. Fung. (Abellini) 4: 616. 1886.
Doratomyces nanus (Ehrenb.) F.J. Morton & G. Sm., Mycol. Pap. 86: 80. 1963.
Stysanus verrucosus Oudem., Ned. Kruidk. Arch., 3 sér. 2: 923. 1903.

Descriptions — Morton & Smith (1963), Ellis (1971), Domsch et al. (2007).

Materials examined. China, Qinghai Province, Yushu Tibetan Autonomous Prefecture, Yushu City, isolated from meadow soil, 2007, *Y.L. Jiang* (HGUP 18618), living culture GUCC 18618; Shaanxi Province, Baoji City, Meixian County, isolated from forest soil, 2005, *T.Y. Zhang* (HGUP 18619), living culture GUCC 18619.

Notes — *Cephalotrichum nanum* was originally described as *Periconia nana* (Ehrenberg 1818) before Sprengel (1827) placed it in *Stilbum* as *S. nanum*. After this, the species was successively transferred to *Graphium* (as *G. nanum*, Saccardo 1886) and *Doratomyces* (as *D. nanus*, Morton & Smith 1963), with a complex taxonomic history. Based on our multi-locus phylogenetic analyses, *C. nanum*, *C. hinnuleum* and *C. stemonitis* formed a fully supported subclade at the most basal position within *Cephalotrichum* (Fig. 1). Although *C. nanum* is most closely related to *C. hinnuleum*, it differs by 45 bp in the four loci dataset. Morphologically, this species differs from its sister species in the production of globose to subglobose or ovoid, coarsely warted, green brown and smaller conidia (6–8.5 × 4.5–7.5 µm) (Domsch et al. 2007; Fig. 12), while *C. hinnuleum* has an echinobotrym-like morph with ovoid to navicular, warted, slightly pointed and larger conidia (8.5–10 × 5.5–7 µm) (Sandoval-Denis et al. 2016b). This species has a widespread distribution and has been recorded on indoor air, deer dung, bison dung, and soil in Canada, England, the USA, and Germany (Domsch et al. 2007, Sandoval-Denis et al. 2016b, Woudenberg et al. 2017b). This study expands its habitat range to China and confirms it to be saprophytic.

Cephalotrichum purpureofuscum (Schwein.) S. Hughes, Canad. J. Bot. 36: 744. 1958 — Fig. 13

Basionym. *Aspergillus purpureofuscus* Schwein., Trans. Amer. Philos. Soc. 4: 282. 1832.
Synonyms. *Doratomyces purpureofuscus* (Schwein.) F.J. Morton & G. Sm., Mycol. Pap. 86: 74. 1963.
Stilbum brevipes Wallr., Fl. Crypt. Germ. (Norimbergae) 2: 326. 1833.
Sporocybe brevipes (Wallr.) Sacc., Syll. Fung. (Abellini) 4: 607. 1886.
Cephalotrichum brevipes (Wallr.) Kuntze, Revis. Gen. Pl. (Leipzig) 3: 453. 1898.
Cephalotrichum leucocephalum Wallr., Fl. Crypt. Germ. (Norimbergae) 2: 330. 1833.
Graphium leucocephalum (Wallr.) Sacc., Syll. Fung. (Abellini) 4: 615. 1886.
Pachnocybe grisea Berk., Engl. Fl., Fungi (Edn 2) (London) 5: 334. 1836.
Graphium griseum (Berk.) Sacc., Syll. Fung. (Abellini) 4: 616. 1886.
Sporocybe grisea (Berk.) Goid., Ann. Bot., Roma 21: 49. 1935.
Periconia fusca Corda, Icon. Fungorum (Prague) 1: 19. 1837.
Stysanus fuscus (Corda) E.W. Mason & M.B. Ellis, Mycol. Pap. 56: 31. 1953.
Periconia discolor Corda, Icon. Fungorum (Prague) 3: 13. 1839.
Stysanus mandlii Mont., Ann. Sci. Nat., Bot. 4: 365. 1845.
Periconia brassicicola Berk. & Broome, Ann. Mag. Nat. Hist. 15: 33. 1875.
Sporocybe brassicicola (Berk. & Broome) Sacc., Syll. Fung. (Abellini) 4: 606. 1886.
Cephalotrichum brassicicola (Berk. & Broome) Kuntze, Revis. Gen. Pl. (Leipzig) 3: 453. 1898.
Stysanus medius Sacc., Michelia 2: 300. 1881.
Stysanopsis media (Sacc.) Ferraris, Ann. Mycol. 7: 281. 1909.
Cephalotrichum medium (Sacc.) S. Hughes, Canad. J. Bot. 36: 744. 1958.
Pycnostysanus medius (Sacc.) Bat. & Peres, Nova Hedwigia 2: 469. 1960.
Doratomyces medius (Sacc.) Matsush., Matsush. Mycol. Mem. 1: 33. 1980.
Sporocybe sacchari Speg., Revista Fac. Agron. Univ. Nac. La Plata 2: 253. 1896.

Descriptions — Morton & Smith (1963), Ellis (1971), Domsch et al. (2007).

Materials examined. China, Sichuan Province, Dujiangyan City, isolated from broad-leaved forest soil, 2005, *Y.L. Jiang* (HGUP 18620), living culture GUCC 18620; Fujian Province, Fuqing City, isolated from farmland soil, 2004, *Y.L. Jiang* (HGUP 18621), living culture GUCC 18621.

Notes — *Cephalotrichum purpureofuscum* is a widespread saprophytic fungus and has been recorded on tunnel walls containing cellulose, indoor air and grain in the Netherlands, Germany and Canada (Sandoval-Denis et al. 2016b, Woudenberg et al. 2017b). In the present study, it was also confirmed from Fujian and Sichuan Provinces of China. Multi-locus phylogenetic analyses indicated that our two newly collected strains clustered together with *C. purpureofuscum*, forming a fully supported monophyletic lineage, which was genetically distant from all species of *Cephalotrichum* (Fig. 1). Morphologically, the distinguishing features of *C. purpureofuscum* include ovoid to ellipsoidal, 5–8 × 3–4.5 µm, smooth or slightly roughened and green brown conidia. Furthermore, it lacks setae, and has 800–1600 µm tall synnemata (Sandoval-Denis et al. 2016b; Fig. 13).

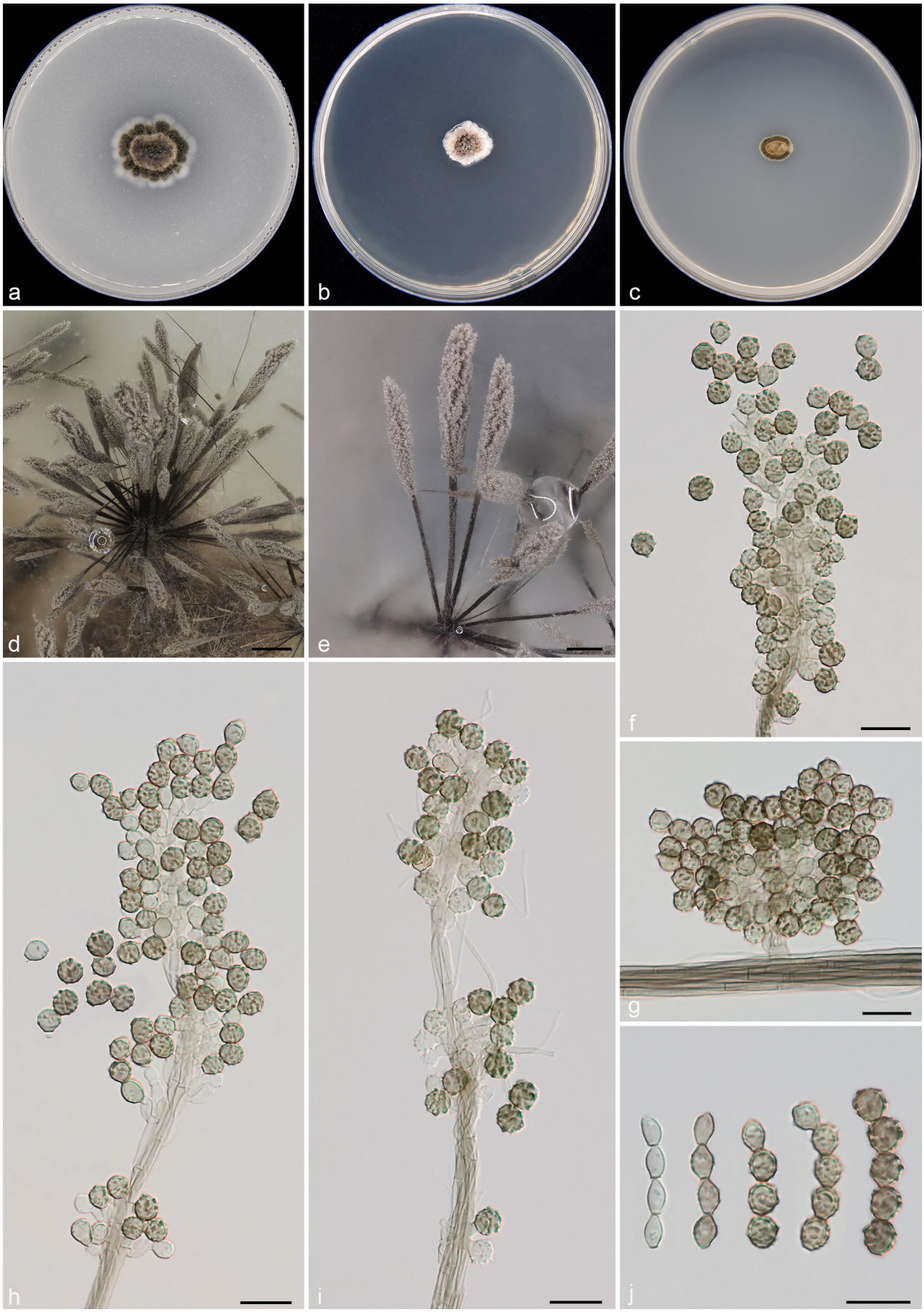

Fig. 12 *Cephalotrichum nanum* (GUCC 18618). a–c. Colony on OA, PDA and SNA; d, e. synnemata; f, h, i. detail of the apical portion of synnema; g. conidiophores, polyblastic conidiogenous cells bearing conidia; j. maturation process of the subspherical to ovoid conidia. — Scale bars: d = 500 µm, e = 250 µm, all others = 10 µm.

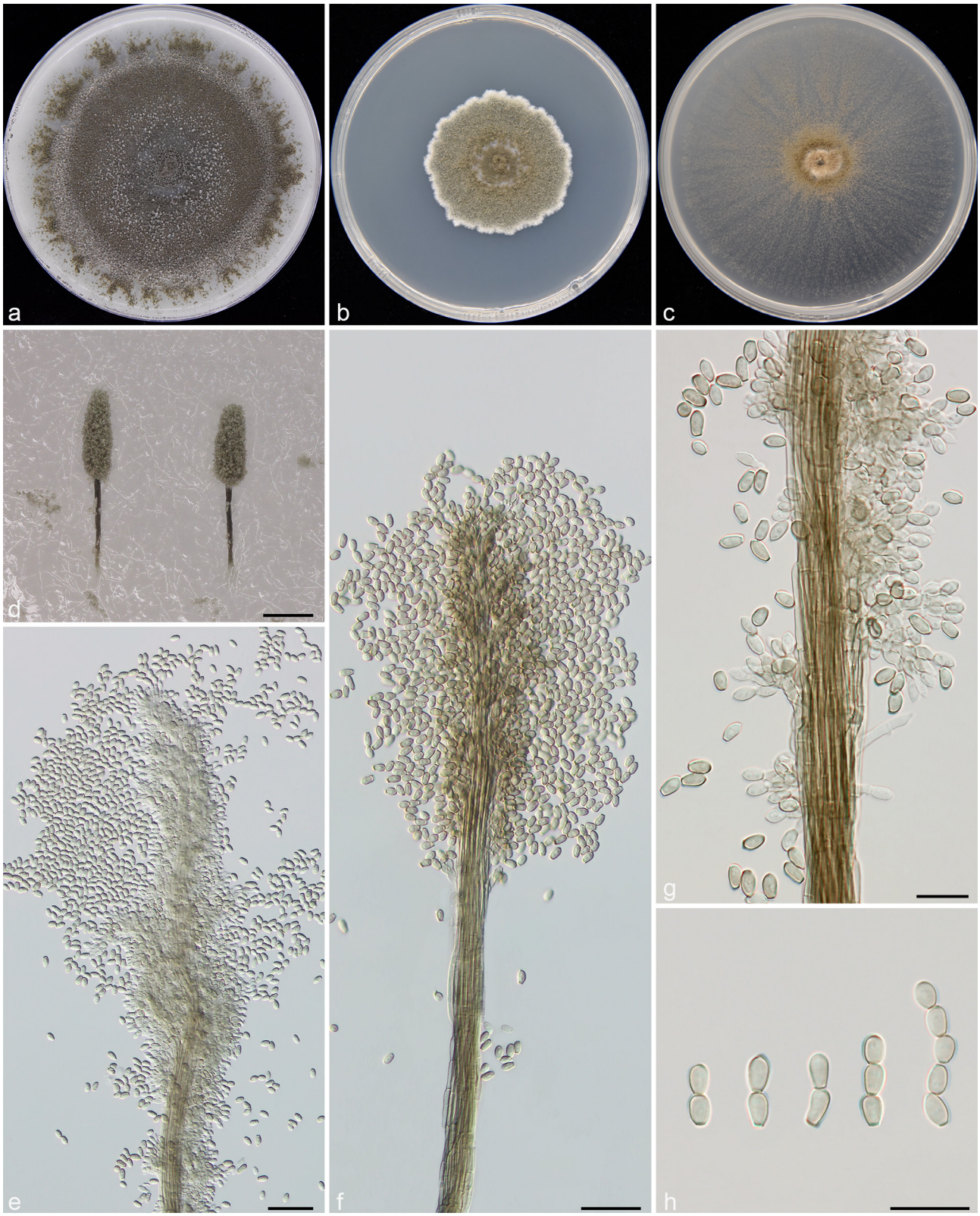

Fig. 13 *Cephalotrichum purpureofuscum* (GUCC 18620). a–c. Colony on OA, PDA and SNA; d. synnemata; e, f. apical portion of synnema; g. conidiophores, conidiogenous cells bearing conidia; h. ovoid to ellipsoidal conidia in chains. — Scale bars: d = 200 µm, e, f = 20 µm, all others = 10 µm.

Cephalotrichum silvanum T.P. Wei & Y.L. Jiang, *sp. nov.* — MycoBank MB 850573; Fig. 14

Etymology. From Latin *silva*, forest, wood, referring to the substrate and forest habitat of this species.

Typus. China, Shaanxi Province, Baoji City, Meixian County, isolated from farmland soil, 2005, *T.Y. Zhang* (holotype HGUP 18622, culture ex-type GUCC 18622).

Mycelium consisting of subhyaline to brown, septate, branched, smooth, thin-walled, 1.5–2 µm diam hyphae. *Synnemata* scattered or gregarious, up to (1073.5–)1351–4411(–5028.5) µm tall, with a compact cylindrical stipe, dark brown to black, unbranched or infrequently branched, somewhat interwoven and rough-walled towards the base, (351.5–)421.5–1942.5(–2006) × (24–)29.5–91.5(–95.5) µm, fertile at the upper portion forming a clavate or cylindrical conidial head, brown to olive grey, (415–)440–2938.5(–3041) × (107–)151–398.5(–399) µm. *Setae* absent. *Conidiophores* infrequently branched, irregularly mono- or bi- to terverticillate, pale brown to brown, septate, smooth, occasionally reduced to conidiogenous cells, usually aggre-

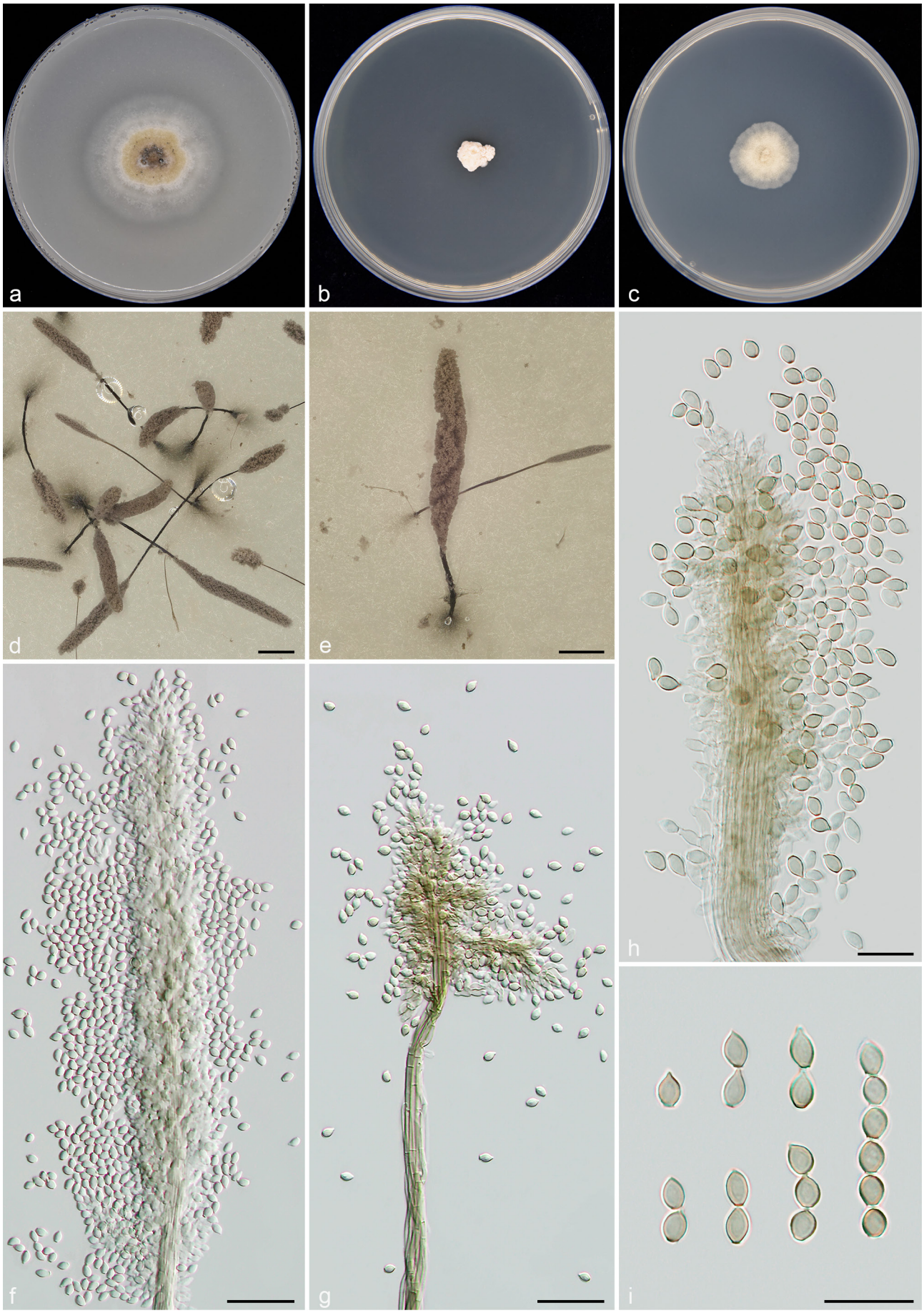

Fig. 14 *Cephalotrichum silvanum* (culture ex-type GUCC 18622). a–c. Colony on OA, PDA and SNA; d, e. synnemata; f, h. detail of the apical portion of synnema; g. top of synnema showing divergent conidiophores; i. obovoid to broadly fusoid conidia in chains. — Scale bars: d, e = 500 µm, f, g = 20 µm, all others = 10 µm.

gated in dense synnemata, (9–)14–44.5(–71.5) × 2–3 µm. *Conidiogenous cells* terminal, solitary or caespitose at the ends of the stipe hyphae, subhyaline to pale brown, ampulliform to cylindrical, smooth and thin-walled, (3.5–)4–6(–6.5) × 2.5–3 µm, with a distinct shoulder tapering gradually to a cylindrical annellated zone 1.5–2.5 µm wide. *Conidia* obovoid to broadly fusoid, apex subobtuse to bluntly pointed, base broadly truncated with thickened and darkened secession scars, smooth to finely roughened, brown to olive brown, single or in short chains, 4–5 × 2.5–3 µm (av. ± SD = 4.4 ± 0.3 × 3 ± 0.1 µm, n = 30). Sexual morph not observed.

Culture characteristics — Colonies on OA reaching up to 32–35 mm diam after 21 d at 25 °C, moderately expanding, olive brown or buff brown centre with white to hyaline outer ring, conspicuous synnemata in centre region, margin entire. On PDA reaching 9–11 mm diam, compact, white or cream-coloured, raised in the centre, folded, cerebriform, lobate margin, with sparse aerial mycelium, synnemata not produced. On SNA attaining 17–29 mm diam, floccose to loosely cottony, cream to grey brown, spreading and lacking synnemata, slightly raised to umbonate at centre, with a regular margin.

Additional material examined. China, Guangxi Province, Guilin City, isolated from forest soil, 2005, *Y.L. Jiang* (HGUP 18623), living culture GUCC 18623.

Notes — In the phylogenetic analysis based on the four-gene concatenated dataset, *C. silvanum* was nested among *C. lignatile* and *C. microsporum*, but formed a separate lineage with high statistical support (Fig. 2). Furthermore, this new species has lower nucleotide homology with the latter two species in ITS (2 and 6 bp), LSU (0 and 0 bp), *tef1* (16 and 21 bp) and *tub2* (32 and 27 bp). Our phylogenetic results showed that the three are not conspecific and can be easily differentiated based on the morphology of their synnemata and conidia. *Cephalotrichum silvanum* is clearly distinct from *C. lignatile*, which has obovoid to irregularly fusiform, smooth-walled, pale brown to brown and larger conidia (4.5–6.5 × 2.5–4 µm), as well as shorter synnemata (280–465 µm) (Woudenberg et al. 2017b); *C. microsporum* differs by its ovoid to ellipsoidal, 3.5–5 × 2–3 µm, green brown, and smooth conidia, and shorter synnemata (500–1000 µm) (Sandoval-Denis et al. 2016b; Fig. 10).

Cephalotrichum stemonitis (Pers.) Nees, Mag. Ges. Naturf. Freunde Berlin 3: 20. 1809 — Fig. 15

Basionym. *Isaria stemonitis* Pers., Comm. Fung. Clav. (Lipsiae): 234. 1797.
Synonyms. *Periconia stemonitis* (Pers.) Pers., Syn. Meth. Fung. (Göttingen) 2: 687. 1801.
Stysanus stemonitis (Pers.) Corda, Icon. Fungorum (Prague) 1: 22. 1837.
Doratomyces stemonitis (Pers.) F.J. Morton & G. Sm., Mycol. Pap. 86: 70. 1963.
Periconia subulata Nees, Nova Acta Phys.-Med. Acad. Caes. Leop.-Carol. Nat. Cur. 9: 238. 1818.
Stilbum subulatum (Nees) Spreng., Syst. Veg., 16th ed. 4: 547. 1827.
Pachnocybe subulata (Nees) Berk., Engl. Fl., Fungi, 2nd ed., 5: 333. 1836.
Graphium subulatum (Nees) Sacc., Syll. Fung. 4: 612. 1886.
Ceratopodium subulatum (Nees) Kuntze, Rev. Gen. Pl. 2: 847. 1891.
Doratomyces neesii Corda, Deutschl. Fl., Abt. 3, Pilze Deutschl. 2: 65. 1829.
Echinobotryum atrum Corda, Deutschl. Fl., Abt. 3, Pilze Deutschl. 3: 51. 1831.
Stilbum setosum Wallr., Fl. Crypt. Germ. (Norimbergae) 2: 329. 1833.
Periconia setosa (Wallr.) Rabenh., Deutschl. Krypt.-Fl. (Leipzig) 1: 118. 1884.
Sporocybe setosa (Wallr.) Sacc., Syll. Fung. (Abellini) 4: 607. 1886.
Cephalotrichum setosum (Wallr.) Kuntze, Rev. Gen. Pl. (Leipzig) 3: 453. 1898.
Stilbum typhinum Wallr., Fl. Crypt. Germ. (Norimbergae) 2: 330. 1833.
Graphium typhinum (Wallr.) Sacc., Syll. Fung. (Abellini) 4: 617. 1886.
Ceratopodium typhinum (Wallr.) Kuntze, Revis. Gen. Pl. (Leipzig) 2: 847. 1891.
Echinobotryum parasitans Corda, Pracht-Flora. 17: 1839.
Stysanus capitatus Reinke & Berthold, Zerselg. d. Kartoff. 1: 51. 1879.
Stysanus ramifer Rolland, Bull. Soc. Mycol. France 6. 106: 1890.
Stysanus tubericola Ellis & Dearn., Proc. Canad. Inst. 1. 90: 1897.

Descriptions — Morton & Smith (1963), Domsch et al. (2007).

Materials examined. China, Qinghai Province, Dulan County, isolated from grassland soil, 2007, *Y.L. Jiang* (HGUP 18624), living culture GUCC 18624; Dari County, isolated from grassland soil, 2007, *H.Q. Pan* (HGUP 18625), living culture GUCC 18625; Gansu Province, Lanzhou City, Yongdeng County, isolated from lawn soil, 2006, *Y.L. Jiang* (HGUP 18626), living culture GUCC 18626.

Notes — *Cephalotrichum stemonitis* was chosen by Hughes (1958) as the type species of *Cephalotrichum*, which is characterised by producing an echinobotryum-like synasexual morph with fusoid, 8–19 × 6–7.5 µm, coarsely warted and apically beaked conidia (Abbott 2000, Sandoval-Denis et al. 2016b; Fig. 15). According to the phylogenetic inference in the present study, our three newly collected isolates cluster in a clade closely related to *C. stemonitis* with high statistical support (Fig. 1). *Cephalotrichum stemonitis* is closely related to *C. hinnuleum*, but differs by 27 bp in the combined dataset. The morphological characters of our studied specimens fit well with *C. stemonitis* (Fig. 13). Moreover, *C. hinnuleum* can be easily distinguished from *C. stemonitis* based on its echinobotrym-like morph, and has smaller (8.5–10 × 5.5–7 µm), ovoid to navicular, warted, and slightly pointed conidia (Sandoval-Denis et al. 2016b). In contrast, *C. stemonitis* produces fusoid, coarsely warted, dark brown and larger conidia (8–19 × 6–7.5 µm) (Sandoval-Denis et al. 2016b; Fig. 15).

Cephalotrichum tenuissimum Woudenb. & Seifert, Stud. Mycol. 88: 149. 2017 — Fig. 16

Description — Woudenberg et al. (2017b).

Materials examined. China, Qinghai Province, Jainca County, isolated from forest soil, 2006, *T.Y. Zhang* (HGUP 18627), living culture GUCC 18627; Chongqing City, Beibei District, isolated from farmland soil, 2005, *Y.L. Jiang* (HGUP 18628), living culture GUCC 18628.

Notes — *Cephalotrichum tenuissimum* was previously reported as a saprophytic fungus isolated from soil, and was introduced by Woudenberg et al. (2017b). Based on the phylogenetic analyses, our newly obtained isolates clustered together with *C. tenuissimum*, and were sister to *C. brunneisporum* and *C. multisynnematum* with full statistical support (Fig. 1). Morphologically, *C. tenuissimum* can be readily distinguished from other members of *Cephalotrichum* by its ellipsoidal, pale green brown and smooth conidia with truncate base and rounded apex (Fig. 16). In this study, our isolates and *C. tenuissimum* have basically the same morphological characteristics. Furthermore, it is noteworthy that this is the second report on this taxon, representing a new record from China, and extending its distribution to China from its original location in the USA (Woudenberg et al. 2017b).

Cephalotrichum verrucisporum (Y.L. Jiang & T.Y. Zhang) Y.L. Jiang & T.Y. Zhang, Mycotaxon 117: 224. 2011 — Fig. 17

Basionym. *Doratomyces verrucisporus* Y.L. Jiang & T.Y. Zhang, Mycotaxon 104: 133. 2008.

Description — Jiang & Zhang (2008).

Materials examined. China, Tibet Autonomous Region, Changdu City, isolated from willow forest soil, 2006, *Y.L. Jiang* (HGUP 18629), living culture GUCC 18629; Guizhou Province, Guiyang City, Huaxi Wetland Park, isolated from lawn soil, 16 June 2019, *X. Zhang* (HGUP18630), living culture GUCC 18630.

Notes — *Cephalotrichum verrucisporum* is a saprophytic fungus isolated from mountain soil, sand dune soil, agricultural soil, and indoor air in China, the Netherlands, and Germany (Woudenberg et al. 2017b). This species was originally described as *Doratomyces verrucisporus* (Jiang & Zhang 2008).

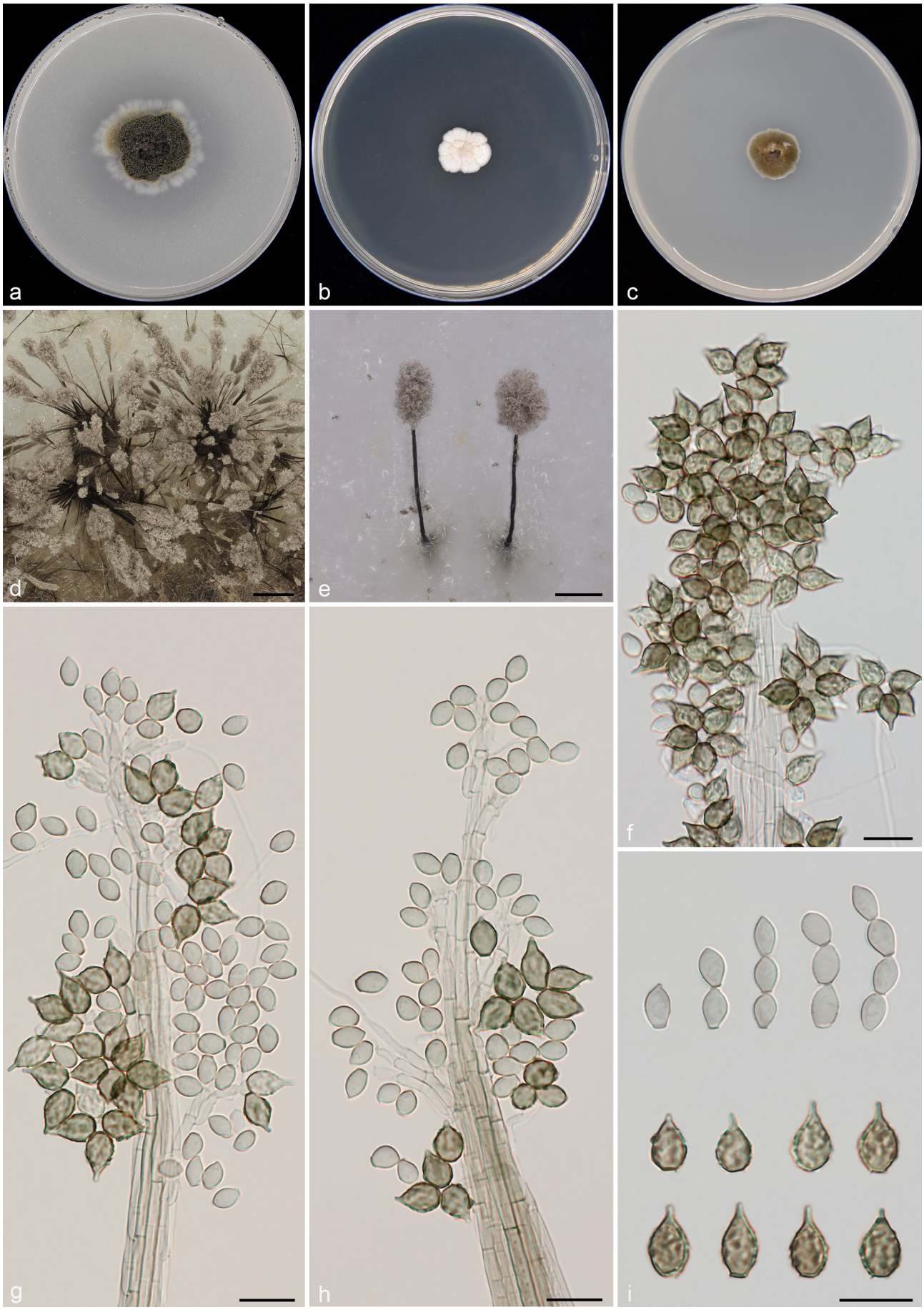

Fig. 15 *Cephalotrichum stemonitis* (GUCC 18624). a–c. Colony on OA, PDA and SNA; d, e. synnemata; f–h. tip of synnema with annellidic conidiogenous cells and conidia; i. ellipsoidal to cylindrical annelloconidia and fusoid solitary conidia. — Scale bars: d = 500 µm, e = 200 µm, all others = 10 µm.

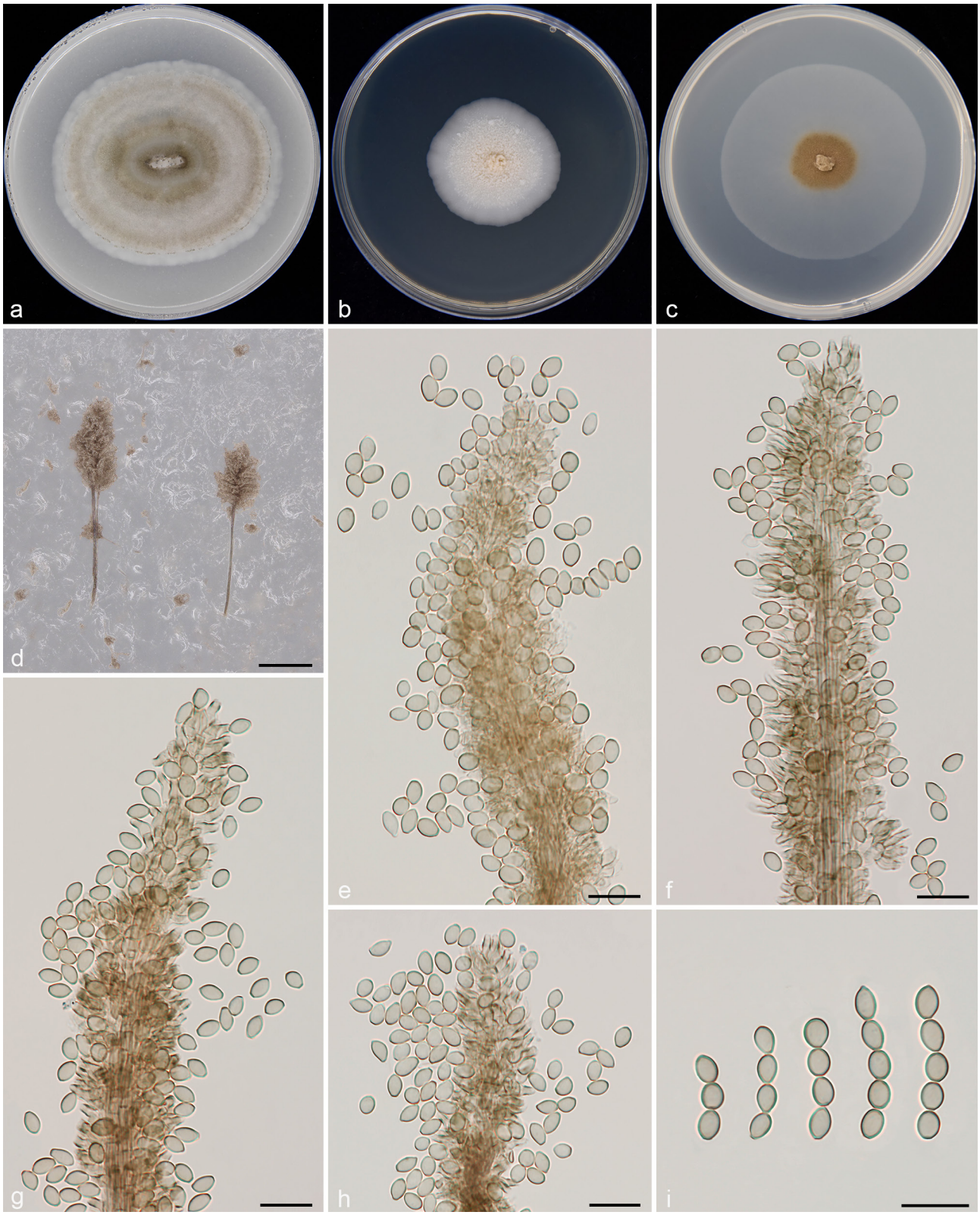

Fig. 16 *Cephalotrichum tenuissimum* (GUCC 18627). a–c. Colony on OA, PDA and SNA; d. synnemata; e–g. detail of the apical portion of a synnema; h. conidiophores, polyblastic conidiogenous cells bearing conidia; i. ellipsoidal conidia in chains. — Scale bars: d = 200 µm, all others = 10 µm.

Later, it was transferred to the genus *Cephalotrichum* as *C. verrucisporum* (Jiang et al. 2011). According to our phylogenetic inference based on the four loci dataset, our two newly collected strains clustered with *C. verrucisporum* with high statistical support (Fig. 2), and the nucleotide homology between GUCC 18629 and CBS 187.78 for ITS, LSU, *tef1* and *tub2* is high at 100 % (565/565 bp), 100 % (846/846 bp), 99 % (954/957 bp) and 100 % (538/538 bp), respectively. Morphologically, it differs from its sister species by its globose to ovoid, rough, dark brown and larger conidia (6–9 × 3–5.5 µm) (Fig. 17), while *C. oligotrophicum* has ellipsoidal to ovoid, pale brown, smooth and smaller conidia (5.5–7.5 × 3–4.5 µm) (Jiang et al. 2017).

Microascus Zukal, Verh. Zool.-Bot. Ges. Wien 35: 339. 1885

Synonyms. *Peristomium* Lechmere, Compt. Rend. Hebd. Séances Acad. Sci. 154: 178. 1912.
Masonia G. Sm., Trans. Brit. Mycol. Soc. 35: 149. 1952.
Masoniella G. Sm., Trans. Brit. Mycol. Soc. 35: 237. 1952.

Type species. *Microascus longirostris* Zukal

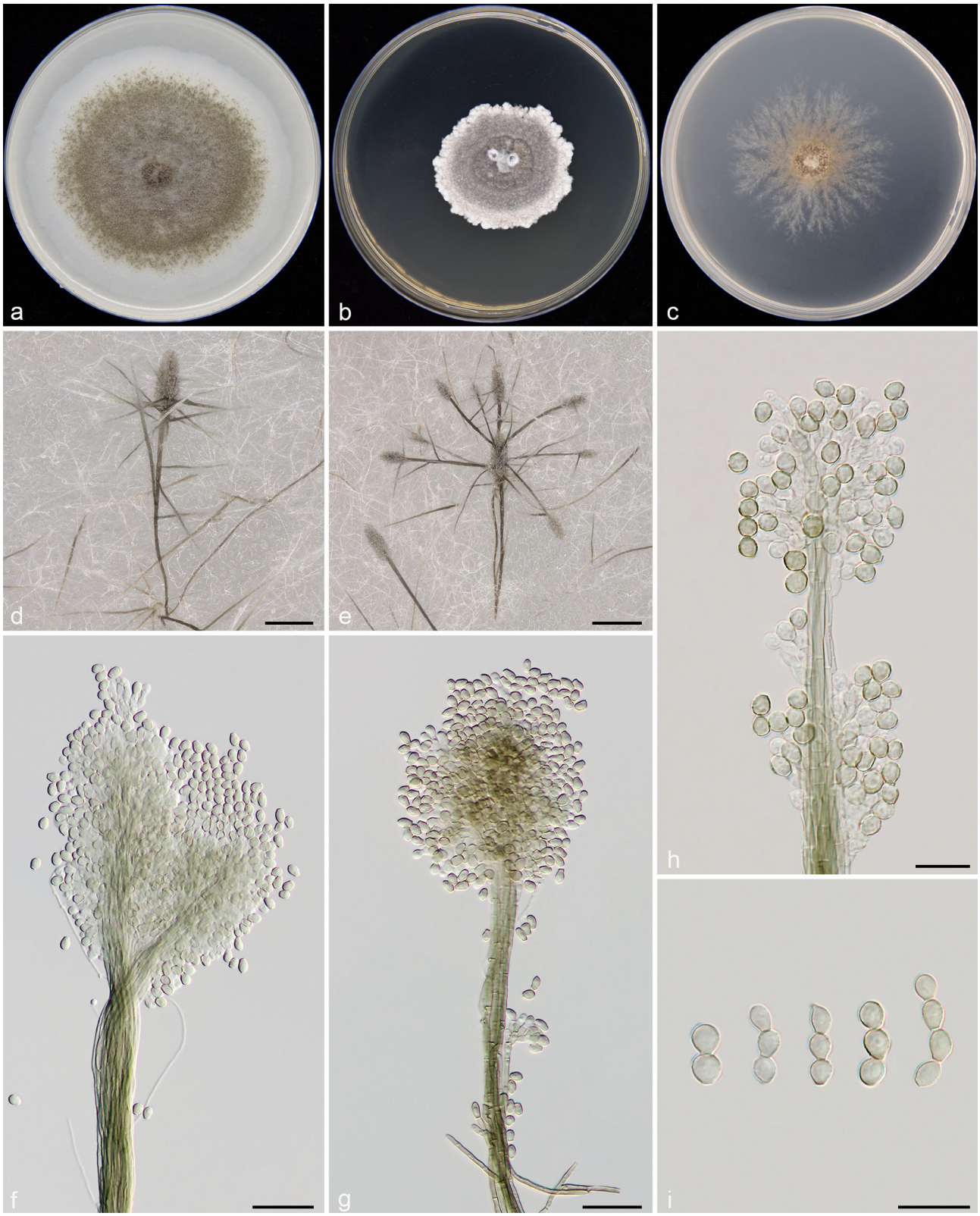

Fig. 17 *Cephalotrichum verrucisporum* (GUCC 18629). a–c. Colony on OA, PDA and SNA; d, e. divergent synnemata; f, g. detail of the apical portion of a synnema; h. tip of synnema with annellidic conidiogenous cells and conidia; i. globose to ovoid conidia in chains. — Scale bars: d = 200 µm, e = 250 µm, f, g = 20 µm, all others = 10 µm.

Notes — *Microascus* was established by Zukal (1985) with *M. longirostris* as the type species and its members are widespread, occurring in abundance in soil, indoor environments and plant debris. Furthermore, some species are also recognised as important animal or human opportunistic pathogens (Zukal 1885, Barron et al. 1961, Mohammedi et al. 2004, Brasch et al. 2019, Mhmoud et al. 2021). Recent studies revealed that *Microascus* is highly polyphyletic, and that members of *Microascus* belong to at least three distinct genera of *Microascaceae*, of which numerous species with scopulariopsis-like morphs remain undefined (Jagielski et al. 2016, Sandoval-Denis et al. 2016a, Woudenberg et al. 2017a). Based on molecular phylogenetic evidence, the genus now includes taxa with a more diverse range of morphological features. Besides the four new species (*M. ampulliformis*, *M. echinulatus*, *M. qinghaiensis* and *M. truncatus*) described in the present study, 16 species have

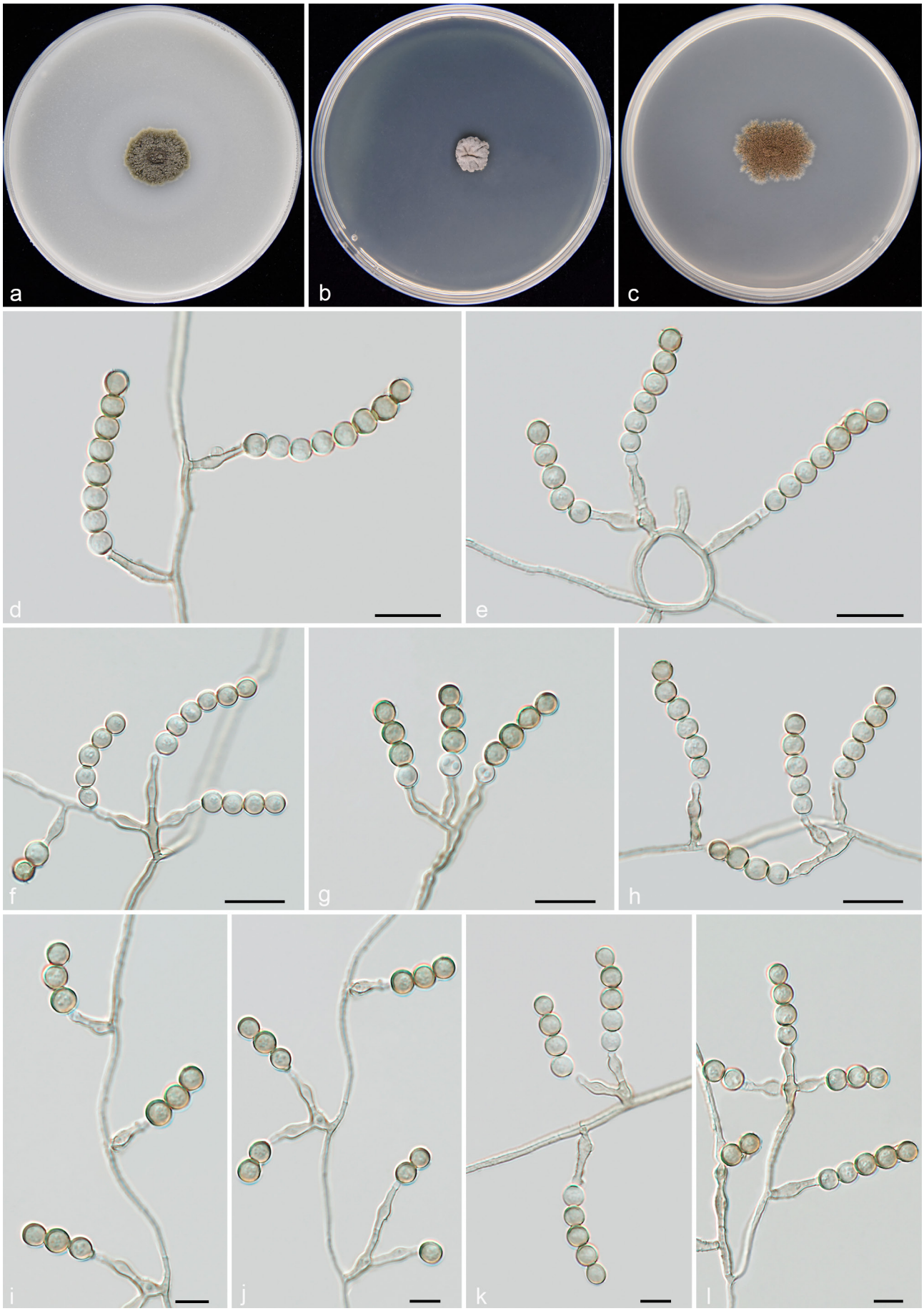

Fig. 18 *Microascus ampulliformis* (culture ex-type GUCC 18631). a–c. Colony on OA, PDA and SNA; d, f–i. conidiophores with conidiogenous cells and conidia. e. conidiophores arising from hyphal coils; j–l. branched conidiophores. — Scale bars: d–h = 10 µm, all others = 5 µm.

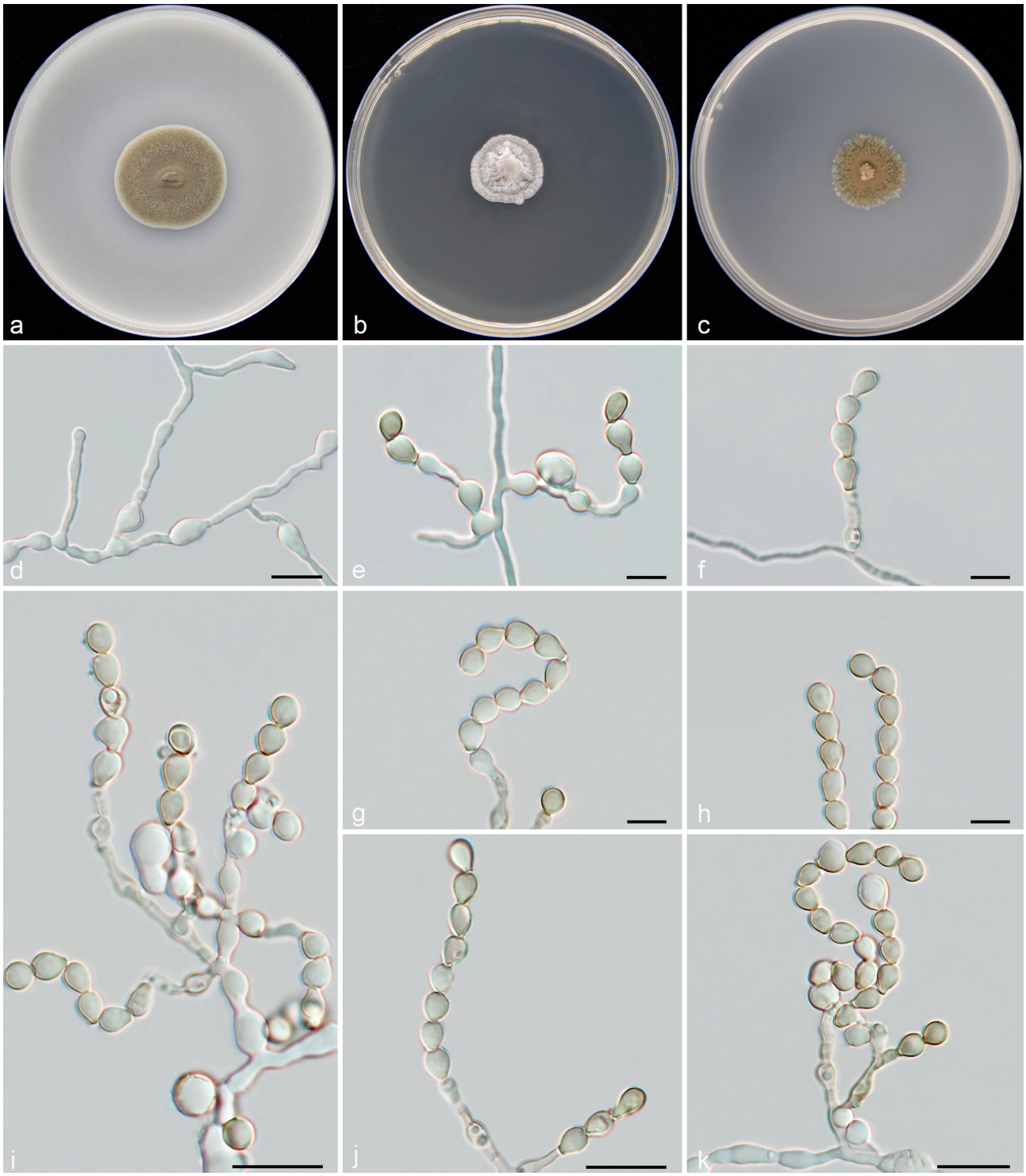

Fig. 19 *Microascus atrogriseus* (GUCC 18633). a–c. Colony on OA, PDA and SNA; d, e. swollen hyphae and conidiophores; f–h. broadly ellipsoidal conidia in chains; i–k. branched conidiophores. — Scale bars: d, i–k = 10 µm, all others = 5 µm.

been confirmed to be distributed in China (Sandoval-Denis et al. 2016a, Woudenberg et al. 2017a, Sun et al. 2020, Zhang et al. 2017, 2021).

Microascus ampulliformis T.P. Wei & Y.L. Jiang, *sp. nov*. — MycoBank MB 850574; Fig. 18

Etymology. Referring to the shape of the conidiogenous cells produced by this species.

Typus. China, Fujian Province, NanPing City, isolated from farmland soil, 2004, *Y.L. Jiang* (holotype HGUP 18631, culture ex-type GUCC 18631).

Mycelium consists of subhyaline to medium brown, septate, branched, rough-walled, 1–2.5 µm wide hyphae, occasionally forming hyphal coils. *Conidiophores* erect, pale brown, clavate or subcylindrical, straight to gently curved, sparsely septate, simple or branched, mostly reduced to conidiogenous cells, (8.5–)11–48.5(–51) × 1.5–3 µm. *Conidiogenous cells* annellidic, terminal or lateral, hyaline to pale brown, cylindrical or ampulliform, solitary on vegetative hyphae, or clustered on conidiophores, smooth or finely roughened, with inconspicuous apical collarette, 5–11(–11.5) × (1.5–)2–3 µm. *Conidia* globose, sessile or on short protrusions, smooth or finely verruculose, the colour of immature conidia changed from greyish to greenish olivaceous or dark brown, 3.5–4.5(–5) × (3.5–)4–4.5 µm (av. ± SD = 4.2 ± 0.3 × 4.2 ± 0.2 µm, n = 30), arranged in long chains, up to (7–)8–36(–37) µm long. Sexual morph, chlamydospores and solitary conidia not observed.

Culture characteristics — Colonies on OA reaching up to 19–31 mm diam after 21 d at 25 °C, floccose to loosely cottony, flat to slightly raised, olivaceous grey or buff green centre, with white to hyaline outer ring, margin entire to undulate. On PDA reaching 13–23 mm diam, compact, pale olivaceous grey to smoke grey, finely felty, with sparse aerial mycelium, raised in the centre, hemispherical, folded, cerebriform, margin slightly undulate. On SNA attaining 15–28 mm diam, moderately expanding, dark yellow to brown, with abundant aerial hyphae, slightly raised to umbonate at centre, with fimbriate margin.

Additional material examined. China, Guizhou Province, Guiyang City, Tianhetan Tourist Holiday Resort, isolated from forest litter, 16 Nov. 2018, *X. Zhang* (HGUP 18632), living culture GUCC 18632.

Notes — Morphological and phylogenetic data support our strains as a new species of *Microascus*. *Microascus ampulliformis* is phylogenetically allied to *M. restrictus* and *M. verrucosus*, but *M. ampulliformis* showed high heterogeneity, forming a monophyletic clade as the sister branch to the latter two species, which was genetically distant from other reported members of *Microascus* (Fig. 1). Nonetheless, this new species differs from the phylogenetically related species *M. verrucosus* by 32 bp in the four loci dataset. Morphologically, this species is clearly distinguished from those species by the absence of solitary conidia. Moreover, *M. restrictus* differs from *M. ampulliformis* by its globose to obovoidal, dark brown and larger conidia (4.5–6 × 4–5.5 µm vs 3.5–5 × 3.5–4.5 µm), as well as subhyaline, smooth-walled and longer annellides (7–19 × 2–4.5 µm vs 5–11.5 × 1.5–3 µm) (Sandoval-Denis et al. 2016a); *M. verrucosus* differs from our strain in having globose to subglobose, dark brown, and larger conidia (5–7 × 4.5–6 µm), as well as shorter annellides (8–10 × 1–3 µm) (Sandoval-Denis et al. 2016a).

Microascus atrogriseus Woudenb. & Samson, Stud. Mycol. 88: 14. 2017 — Fig. 19

Basionym. *Masonia grisea* G. Sm., Trans. Brit. Mycol. Soc. 35: 149. 1952.
Synonym. *Masoniella grisea* (G. Sm.) G. Sm., Trans. Brit. Mycol. Soc. 35: 237. 1952.

Description — Woudenberg et al. (2017a).

Materials examined. China, Qinghai Province, Yushu Tibetan Autonomous Prefecture, Yushu City, isolated from meadow soil, 2007, *H.Q. Pan* (HGUP 18633), living culture GUCC 18633; Sichuan Province, Leshan City, Mount Emei, isolated from shrub soil, 2005, *Y.L. Jiang* (HGUP 18634), living culture GUCC 18634.

Notes — In this study, the phylogenetic result shows that our two new collections (GUCC 18633 and GUCC 18634) cluster together with *M. atrogriseus*, sharing a sister relationship to *M. pseudopaisii* with high statistical support (Fig. 2). Morphologically, the most remarkable features of *M. atrogriseus* is the presence of broadly ellipsoidal to short clavate and hazel conidia (Woudenberg et al. 2017a). The morphological characters of our studied specimens fit well with *M. atrogriseus* (Fig. 18). *Microascus atrogriseus* was originally isolated as a culture contaminant in London, England, and subsequently from soil and the indoor environment (Woudenberg et al. 2017a). This study expands its habitat range from England, Germany and the Netherlands to China, and further confirms it to be saprophytic.

Microascus chinensis Jin Yu et al., Fungal Biology 120: 594. 2016 — Fig. 20

Description — Jagielski et al. (2016).

Materials examined. China, Qinghai Province, Xining City, isolated from vegetable soil, 2004, *H.F. Wang* (HGUP 18635), living culture GUCC 18635; Guizhou Province, Meitan County, on decaying *Camellia sinensis* leaf litter, 10 Aug. 2019, *T.P. Wei* (HGUP 18636), living culture GUCC 18636.

Notes — *Microascus chinensis* was collected from human nails and an unknown clinical specimen in Beijing, China, and was introduced by Jagielski et al. (2016). Multi-locus phylogenetic analyses indicate that this species is sister to *M. micronesiensis* and is fully supported as phylogenetically distinct (Fig. 2). Moreover, this taxon has lower nucleotide homology with the phylogenetically related species *M. micronesiensis* in ITS (556/571 bp, 97 %), LSU (860/868 bp, 99 %), *tef1* (822/833 bp, 99 %) and *tub2* (468/489 bp, 96 %). Morphologically, its distinguishing features include clavate or ellipsoidal ascospores with a single and inconspicuous germ pore, as well as ellipsoidal, 2–4 × 2–3.5 µm, smooth-walled and dark brown conidia (Jagielski et al. 2016; Fig. 19), whereas *M. micronesiensis* differs by its broadly obovoid, hyaline or subhyaline and larger conidia (3–4.5 × 2–3.5 µm), as well as the lack of a sexual morph (Woudenberg et al. 2017a).

Microascus echinulatus T.P. Wei & Y.L. Jiang, *sp. nov.* — MycoBank MB 850575; Fig. 21

Etymology. The epithet refers to the minutely echinulate hyphae.

Typus. China, Qinghai Province, Xining City, isolated from vegetable soil, 2004, *Y.L. Jiang* (holotype HGUP 18637, culture ex-type GUCC 18637).

Mycelium superficial or immersed, hyphae septate, branched, subhyaline to olivaceous brown, verruculose or minutely echinulate, thick-walled, 1.5–2.5 µm wide. *Conidiophores* solitary, lageniform or rarely subcylindrical, smooth to finely roughened, brown to olive brown, usually reduced to conidiogenous cells arising directly from vegetative hyphae, (7.5–)8–44.5(–65.5) × (1–)1.5–3 µm. *Conidiogenous cells* ampulliform or pyriform, hyaline to pale brown, smooth to verruculose, straight or slightly curved, solitary on aerial hyphae, or clustered on the apex of conidiophores, with non-flared collarette, (2.5–)3.5–10.5(–11) × 1.5–3 µm. *Conidia* formed in chains, up to 6.5–52(–55) µm long, pyriform to broadly ellipsoidal, with a truncate base, the colour of conidia changed from subhyaline to olivaceous brown to pale black, and gradually from smooth to sparsely warted, 3.5–4(–4.5) × 3–4 µm (av. ± SD = 3.8 ± 0.3 × 3.4 ± 0.2 µm, n = 30). Sexual morph not observed.

Culture characteristics — Colonies on OA attaining 30–47 mm diam after 21 d at 25 °C, spreading, immersed, cream-coloured or pale grey to olivaceous grey from edge to centre, with moderate aerial mycelium, slightly granular at the centre, margin crenated. On PDA reaching 19–29 mm diam, compact, with a pale black to yellow grey centre, yellow grey to cream-coloured at periphery, with sparse aerial mycelium, folded, raised in the centre, margin slightly undulate. On SNA attaining 33–41 mm diam, moderately expanding, with abundant aerial hyphae, velvety to finely granular, white to pale brown at the centre, with a dark yellow or pale grey and regular margin, with conspicuous radial gaps.

Additional material examined. China, Qinghai Province, Xining City, isolated from vegetable soil, 2004, *Y.L. Jiang* (HGUP 18638), living culture GUCC 18638.

Notes — The two isolates representing *M. echinulatus* were resolved as a strongly supported genealogically exclusive lineage in the phylogeny inferred from the combined dataset (Fig. 2). Despite *M. echinulatus* sharing a sister relationship with *M. sparsimycelialis*, it differs from the latter by 58 bp (ITS 16 bp, LSU 4 bp, *tef1* 27 bp and *tub2* 11 bp) in the combined dataset. Furthermore, they can also be distinguished based on their morphological characteristics, as *M. echinulatus* is characterised by pyriform to broadly ellipsoidal, subhyaline to olivaceous brown or pale black conidia, and verruculose or minutely echinulate hyphae (Fig. 21). However, *M. sparsimycelialis* produces ovoid to globose, pale brown, and larger

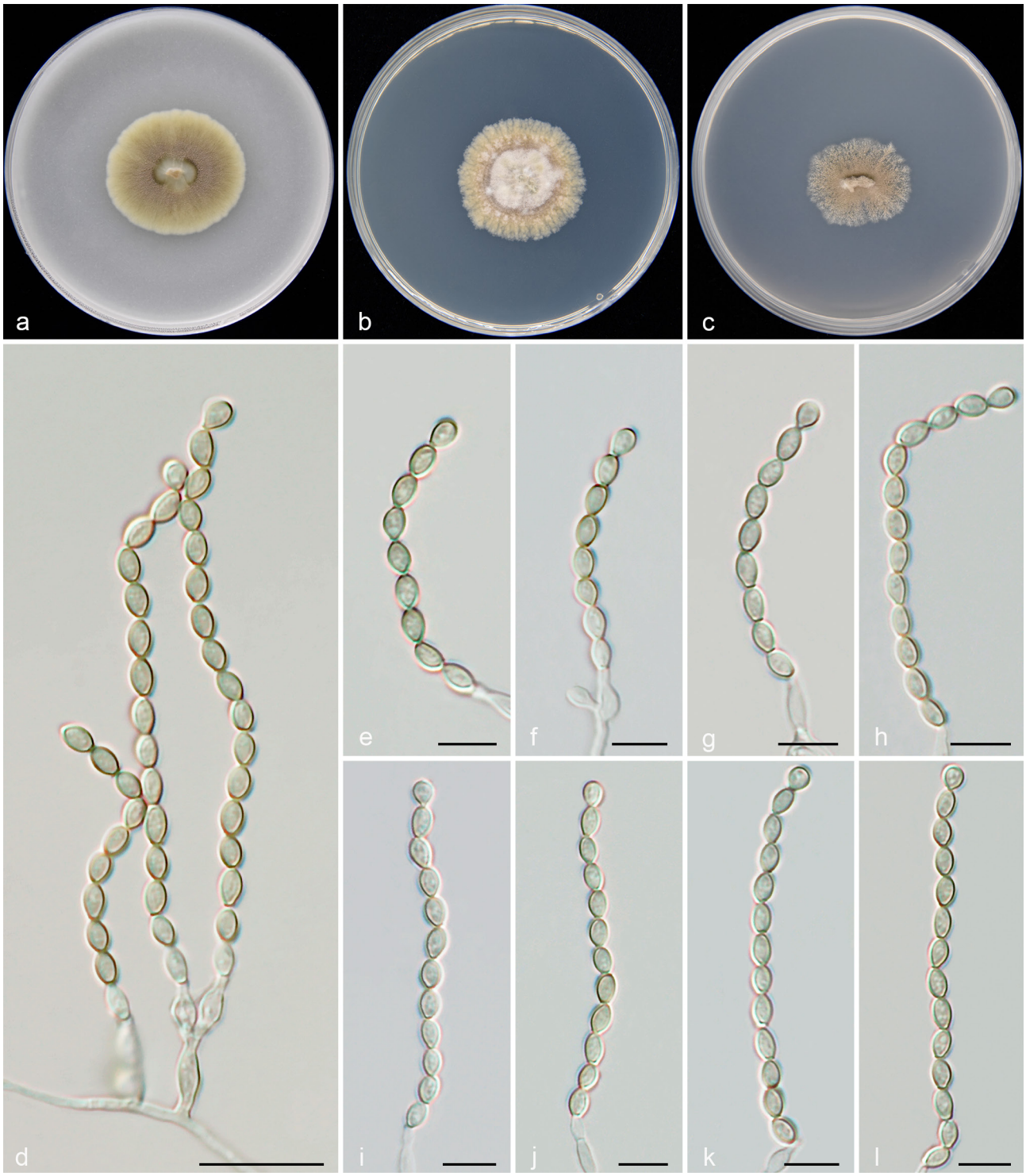

Fig. 20 *Microascus chinensis* (GUCC 18635). a–c. Colony on OA, PDA and SNA; d. branched conidiophores; e–k. flask-shape conidiogenous cells bearing conidia; l. ellipsoidal conidia in chains. — Scale bars: d = 10 µm, all others = 5 µm.

conidia (3.5–6 × 3–5.5 µm vs 3.5–4.5 × 3–4 µm), and lacks verruculose or echinulate hyphae (Zhang et al. 2021).

Microascus melanosporus (Udagawa) Woudenb. & Samson, Stud. Mycol. 88: 19. 2017 — Fig. 22

Basionym. *Scopulariopsis melanospora* Udagawa, J. Agric. Sci. (Tokyo) 5: 18. 1959.

Description — Woudenberg et al. (2017a).

Materials examined. China, Qinghai Province, Xunhua County, isolated from orchard soil, 2006, *Y.M. Wu* (HGUP 18639), living culture GUCC 18639; Xunhua County, isolated from farmland soil, 2006, *Y.M. Wu* (HGUP 18640), living culture GUCC 18640; Chindu County, isolated from flower bed soil, 2007, *H.Q. Pan* (HGUP 18641), living culture GUCC 18641; Guizhou Province, Anshun City, Puding County, isolated from farmland soil, 15 Nov. 2022, *T.P. Wei* (HGUP 18642), living culture GUCC 18642.

Notes — This species was originally described as *Scopulariopsis melanospora* (Udagawa 1959) and was later transferred to the genus *Microascus* as *M. melanosporus* (Woudenberg et al. 2017a). *Microascus melanosporus* is a saprobic species with a worldwide distribution and has been recorded on soil, plant debris, plaster, the indoor environment and dust in Germany, the Netherlands, Poland, South Africa and the USA (Woudenberg et al. 2017a). In this study, it was also distributed in Qinghai and Guizhou Provinces of China. Multi-locus phylogenetic analysis shows that our four newly collected isolates clustered together

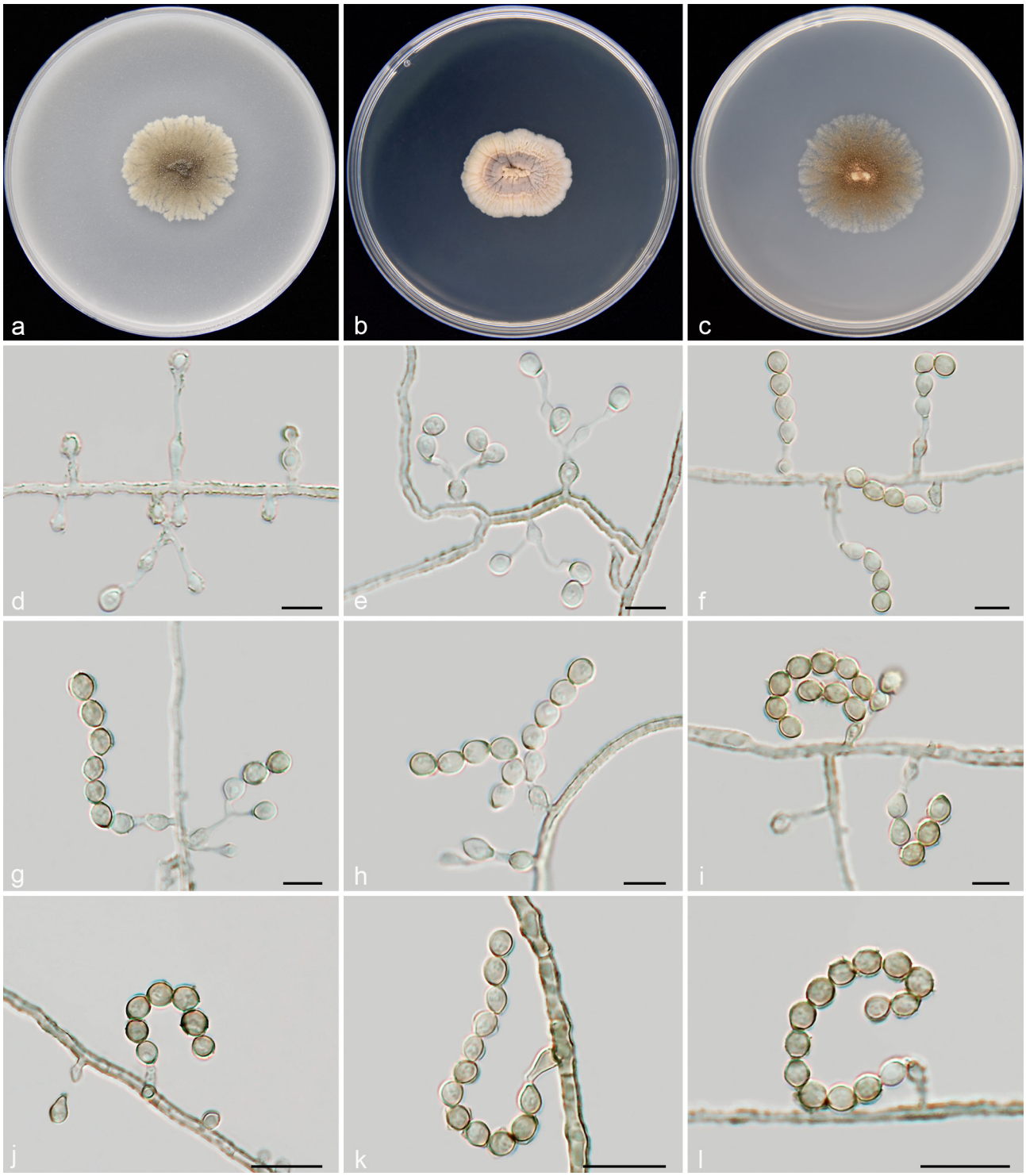

Fig. 21 *Microascus echinulatus* (culture ex-type GUCC 18637). a–c. Colony on OA, PDA and SNA; d. hyphae with minutely echinulate; e. branched conidiophores; f–i. pyriform to ellipsoidal conidia in chains; j–l. conidiophores reduced to conidiogenous cells. — Scale bars: d–i = 5 µm, all others = 10 µm.

with *M. melanosporus*, sharing a sister relationship to *M. hollandicus* and *M. paisii* with strong support (Fig. 2). These newly isolated strains and *M. melanosporus* basically have the same morphological characteristics (Fig. 22).

Microascus qinghaiensis T.P. Wei & Y.L. Jiang, *sp. nov.* — MycoBank MB 850576; Fig. 23

Etymology. Name refers to Qinghai, the location where it was collected.

Typus. China, Qinghai Province, Yushu Tibetan Autonomous Prefecture, Chindu County, isolated from flower bed soil, 2007, *Y.L. Jiang* (holotype HGUP 18643, culture ex-type GUCC 18643).

Vegetative hyphae pale brown to olive brown, septate, branched, slightly rough, thick-walled, 2–3.5 µm diam. *Conidiophores* slightly pigmented to dark brown, solitary, septate, flexuous, subcylindrical or slightly swollen, branched, slightly rough to tuberculate in older parts, sometimes reduced to conidiogenous cells, (4.5–)11–45(–50.5) × 1.5–3 µm. *Conidiogenous cells* annellides, cylindrical to ampulliform, subhyaline to pale brown, smooth to finely rough-walled, terminal and intercalary on conidiophores or lateral on vegetative hyphae, tapering to a distinct neck, (1.5–)2–12(–13.5) × 1.5–3 µm. *Conidia* globose to subglobose, olivaceous grey to dark brown, smooth, thick-walled, base truncate or with inconspicuous scars, apical ends obtusely rounded, (3–)3.5–4.5(–5) × 3.5–4.5(–5) µm (av. ±

Fig. 22 *Microascus melanosporus* (GUCC 18639). a–c. Colony on OA, PDA and SNA; d, f, g. conidiophores and conidiogenous cells bearing conidia; e. germinating conidia; h. hyphal circle; i, j. branched conidiophores. — Scale bars: g, i = 5 µm, all others = 10 µm.

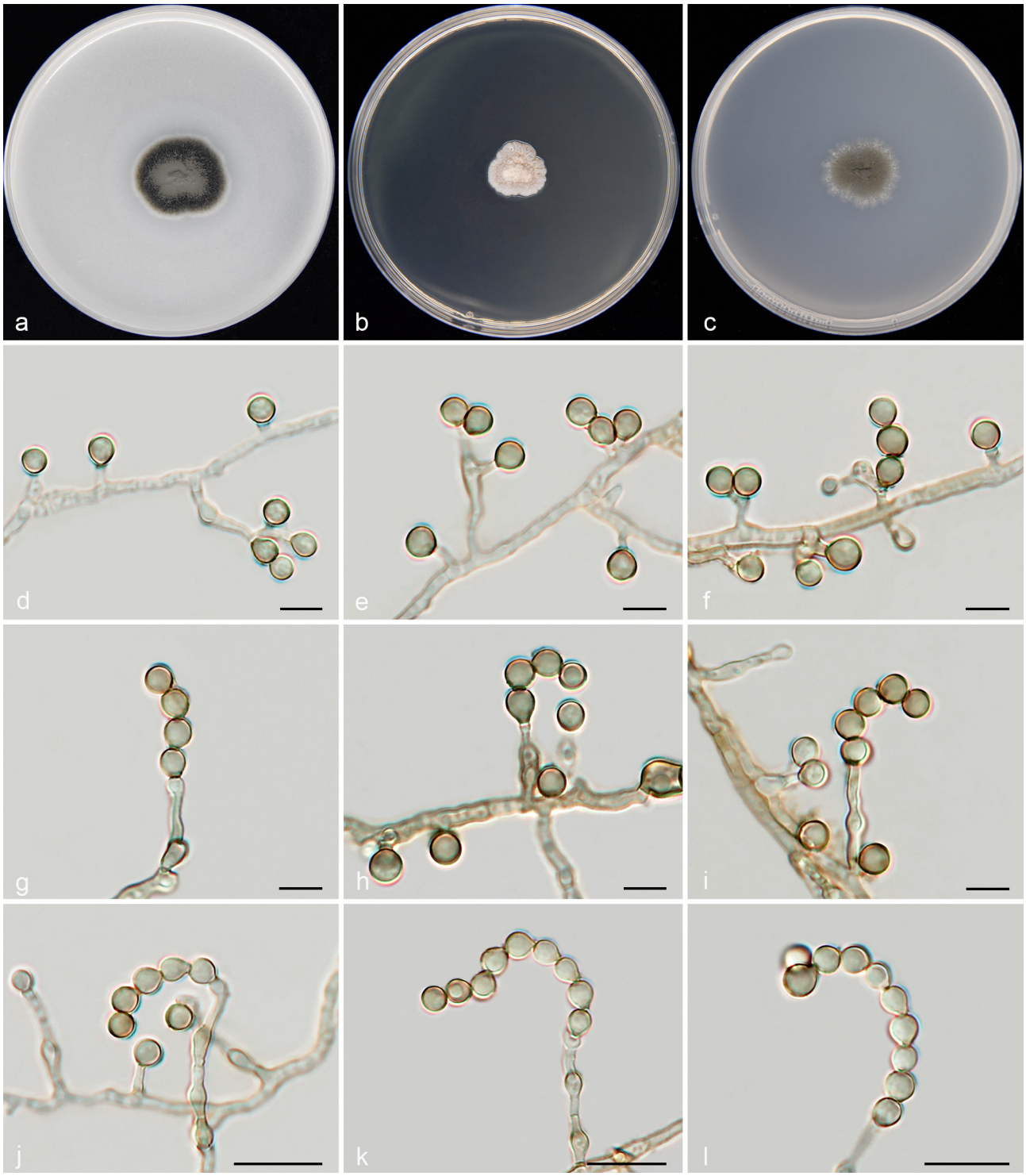

Fig. 23 *Microascus qinghaiensis* (culture ex-type GUCC 18643). a–c. Colony on OA, PDA and SNA; d–g. conidiophores, conidiogenous cells and conidia; h, i. conidiophores reduced to conidiogenous cells; j–l. globose to subglobose conidia in chains. — Scale bars: d–i = 5 µm, all others = 10 µm.

SD = 4.1 ± 0.3 × 4 ± 0.3 µm, n = 30), arranged in long chains, up to (7–)7.5–46(–57.5) µm long, sometimes producing solitary conidia. Sexual morph not observed.

Culture characteristics — Colonies on PDA attaining 21–27 mm diam after 21 d at 25 °C, moderately expanding, finely felty, slightly raised, olivaceous black centre with white outer ring, aerial mycelium moderately dense, margin regular. On PDA reaching 15–18 mm diam, finely felty, compact, cream-coloured or pale pink, with sparse aerial mycelium, raised in the centre, folded, cerebriform, margin entire to undulate. On SNA attaining 19–21 mm diam, spreading, flat, olivaceous grey at centre, white to smoke grey at the periphery, with abundant aerial hyphae, velvety to slightly granular at centre, with fimbriate margin.

Additional material examined. China, Qinghai Province, Yushu Tibetan Autonomous Prefecture, Chindu County, isolated from flower bed soil, 2007, *H.Q. Pan* (HGUP 18644), living culture GUCC 18644.

Notes — Our two strains representing *M. qinghaiensis* cluster as a separate branch in *Microascus*, and are sister to *M. cleistocarpus* and *M. hyalinus* with full statistical support (Fig. 2). *Microascus qinghaiensis* differs from the latter two species by nucleotide differences in ITS (18 and 22 bp), LSU (5 and 3 bp), *tef1* (19 and 19 bp) and *tub2* (32 and 32 bp). Furthermore, *M. qinghaiensis* can also be distinguished from *M. cleistocarpus* and *M. hyalinus* by morphological characteristics. *Microascus qinghaiensis* differs from *M. cleistocarpus* and *M. hyalinus* by the absence of a sexual morph. Conidia of *M. cleistocarpus* are larger (4.5–6.5 × 3.5–4.5 µm vs 3–5 × 3.5–5 µm), obovoid,

Fig. 24 *Microascus truncatus* (culture ex-type GUCC 18645). a–c. Colony on OA, PDA and SNA; d. conidiophores, conidiogenous cells and conidia; e, f. conidia in simple chains arising from conidiogenous cells; g, h. hyphal coil. — Scale bars: e, f = 5 µm, all others = 10 µm.

and hyaline to hazel (Woudenberg et al. 2017a); *M. hyalinus* differs by its hyaline to pale brown, ovoid and narrower conidia (3.5–5 × 2–3.5 µm vs 3–5 × 3.5–5 µm), often covered with mucilaginous material (Malloch & Cain 1971).

Microascus truncatus T.P. Wei & Y.L. Jiang, *sp. nov.* — MycoBank MB 850577; Fig. 24

Etymology. Named after the broadly truncate conidia produced by this fungus.

Typus. China, Hubei Province, Shiyan City, Fang County, isolated from farmland soil, 2006, *Y.L. Jiang* (holotype HGUP 18645, culture ex-type GUCC 18645).

Mycelium hyaline to pale brown, smooth, sparsely septate, branched, 1–3 µm diam, sometimes coiled. *Conidiophores* erect, pale brown, occasionally branched, clavate or subcylindrical, straight to gently curved, sparsely septate, mostly reduced to conidiogenous cells, (7–)8.5–20(–26) × 1.5–2.5 µm. *Conidiogenous cells* lateral or terminal on conidiophores or aerial hyphae, cylindrical or ampulliform, solitary, hyaline to pale brown, smooth-walled, erect or curved, constricted at base, with non-flared collarette, 4–12(–12.5) × 1.5–2.5(–3) µm. *Conidia* formed in chains, up to 7.5–86(–87) µm long, globose to subglobose, greenish olivaceous or dark brown, the base with a prominent truncate hilum, usually sparsely warted, 3.5–4(–4.5) × 3.5–4 µm (av. ± SD = 4.1 ± 0.2 × 3.7 ± 0.2 µm,

n = 30). Sexual morph, chlamydospores and solitary conidia were not observed.

Culture characteristics — Colonies on OA attaining 58–61 mm diam after 21 d at 25 °C, moderately expanding, finely felty, with conspicuous radial gaps, olivaceous black centre with pale brown to smoke grey outer ring, aerial hyphae abundant, with fimbriate margin. On PDA reaching 27–36 mm diam, compact, cream-coloured or pale brown to whitish from margin to centre, with sparse aerial mycelium, raised in the centre, folded, cerebriform, with a regular margin. On SNA attaining 64–67 mm diam, moderately expanding, flat, smoke grey or cream-coloured to grey brown with conspicuous concentric rings, aerial mycelium moderately dense, velvety to granular at centre, radially striated, margin entire.

Additional material examined. China, Zhejiang Province, Zhoushan City, Putuo District, isolated from forest soil, 2007, *J.J. Xu* (HGUP 18646), living culture GUCC 18646.

Notes — Based on the analysis of DNA sequences of four markers, *M. truncatus* is resolved as the closest phylogenetic relative to *M. croci*, which serves as the basal taxon of this lineage. However, there are significant genetic differences and phylogenetic distances between the two species (Fig. 2). Although *M. truncatus* is phylogenetically allied to *M. croci*, it is genetically distinct by 16 bp in the four loci dataset. Morphologically, *M. croci* resembles *M. truncatus*, and lacks a sexual morph. Nonetheless, conidia of *M. croci* are globose or ellipsoidal to short clavate, pale brown and larger (3.5–5 × 3–4 µm), as compared to the globose to subglobose, greenish olivaceous or dark brown and smaller conidia (3.5–4.5 × 3.5–4 µm) of *M. truncatus* (Sandoval-Denis et al. 2016a; Fig. 24). Therefore, our phylogenetic and morphological data confirm this taxon as a distinct species in *Microascus*.

DISCUSSION

The taxonomy of *Cephalotrichum* has been widely studied in recent years, and several long-standing questions concerning the species boundaries of this genus have been elucidated based on molecular phylogenetic analyses (Sandoval-Denis et al. 2016b, Woudenberg et al. 2017b). MycoBank currently lists 90 epithets in *Cephalotrichum* (https://www.mycobank.org, December 2023); however, some of these taxa still lack living cultures and molecular data, and their taxonomic placements have not been proven by phylogenetic studies, which complicates the revision of *Cephalotrichum* (Sandoval-Denis et al. 2016b, Jiang et al. 2017, Woudenberg et al. 2017b, Das et al. 2020). Consequently, to resolve the phylogenetic position of these species in *Cephalotrichum*, they need to be re-collected, sequenced and epitypified. As stated in the results section, the 24 species of *Cephalotrichum* were recognized in this study by combining the results of a multi-locus sequence analysis and phenotypic data, which chiefly clustered in 11 subclades (Fig. 1), including four novel species proposed here, namely *C. brunneisporum*, *C. lageniforme*, *C. multisynnematum* and *C. silvanum*. The production of abundant synnemata and dry airborne conidia under oligotrophic conditions are the key morphological characteristics that distinguishes *Cephalotrichum* from other genera of *Microascaceae*, such as *Microascus*, *Scopulariopsis* and *Wardomyces* (Sandoval-Denis et al. 2016b, Woudenberg et al. 2017b). We found that *C. brunneisporum*, *C. lageniforme*, *C. microsporum*, *C. silvanum* and *C. tenuissimum* produced fewer synnemata than most other species of *Cephalotrichum*, but their hyphae stick to the substrate surface, forming fine hyphal networks, and produce large numbers of solitary conidia, which might be a survival strategy to promote the spore dispersal in different environments.

As reported by Sandoval-Denis et al. (2016a), the scopulariopsis-like morphs are polyphyletic and include two distinct lineages (*Microascus* and *Scopulariopsis*) residing in *Microascaceae*, which are clearly different from their allied genera *Pithoascus*, *Pseudoscopulariopsis* and *Yunnania* (Fig. 1). Despite these differences, their species boundaries remain incompletely resolved due to historical confusion and limited molecular data. On the other hand, *Microascus* is currently the largest genus of *Microascaceae* with 89 accepted species names recorded in MycoBank (December 2023). Some of these *Microascus* taxa are based on lost specimens or have invalid names, which means they practically exist only as undefined taxa in scientific literature. The ambiguous identities of these species have hindered taxonomic resolution of the genus *Microascus*. In this study, to better define the species boundaries and reveal the evolutionary relationship of *Microascus*, we performed multi-gene phylogenetic analyses using sequence dataset consisting of four gene regions (ITS, LSU, *tef1* and *tub2*) with increased taxon sampling and morphological analysis. The current results resolved 49 species in the genus *Microascus* with high statistical support (Fig. 2), of which four correspond to the novel species proposed here, viz., *M. ampulliformis*, *M. echinulatus*, *M. qinghaiensis* and *M. truncatus*. In recent years, using the updated phylogenetic framework, more species are continuously discovered and accepted in *Microascus*, such as *M. aculeatus*, *M. collaris*, *M. ennothomasiorum*, *M. rothbergiorum*, *M. spinosporus* (Brasch et al. 2019, Sun et al. 2020, Zhang et al. 2021, Crous et al. 2022). Overall, all 49 phylogenetic species of *Microascus* recognised can be identified with ITS, LSU, *tef1* and *tub2* gene sequences. One anomaly is *M. alveolaris*, *M. appendiculatus*, *M. campaniformis*, *M. cinereus*, *M. cirrosus*, *M. gracilis*, *M. levis*, *M. macrosporus*, *M. pyramidus* and *M. terreus*, who do not form clearly separated and highly supported phylogenetic clades (Fig. 2). This is most likely due to the small number of isolates included for these species, or the current four gene regions alone do not provide stable and reliable resolution for their delimitation. However, a final conclusion cannot be drawn because we could not gain access to their ex-type cultures and lack additional isolates.

Cephalotrichum and *Microascus* are a heterogeneous group of fungi with a worldwide distribution that includes saprobes, plant endophytes and pathogens (Abbott 2000, Guarro et al. 2012, Sandoval-Denis et al. 2016a, b, Woudenberg et al. 2017a, b, Crous et al. 2022, Mamaghani et al. 2022). In addition, some species have been described as colonisers or pathogens of mammals, including insects, animals and humans (De Hoog et al. 2011, Lackner et al. 2014, Sandoval-Denis et al. 2013, 2016a, b, Brasch et al. 2019, Álvarez-Uría et al. 2021, Mhmoud et al. 2021). In the present study, the 47 newly collected strains and most isolates that have been reported thus far were obtained from soil and decaying vegetable material. As saprophytes, they can adapt to a plant or animal-fungal associated lifestyle, as well as play a very vital role in cellulose degradation and hydrolysis of keratinous materials such as pelage, nails and skin. Another point of attention is the exception of *C. gorgonifer*, as no other members of *Cephalotrichum* are regarded as human pathogens, and also not known as producers of mycotoxins (Álvarez-Uría et al. 2021). Although many strains of *C. gorgonifer* are isolated from soil, the indoor or built environments, this species has been repeatedly detected in clinical samples, mostly human respiratory systems, and its ability to grow at 40 °C is also a good indication of the opportunistic pathogenicity of the species. In addition, *M. chinensis* and *M. melanosporus* are described as important opportunistic pathogens of animals and humans (Baddley et al. 2000, De Hoog et al. 2011, Guarro et al. 2012, Sandoval-Denis et al. 2013, Jagielski et al. 2016), but in this paper, isolates of these two species were obtained

from soil and plant litter, respectively, indicating that they can also be saprophytic.

In recent years, with the development of molecular approaches and the availability of fossil calibration data, the estimation of divergence times using molecular-clock dating has been used as objective evidence for higher ranking of taxa. Multi-gene phylogenetic analysis resolved most genera of *Microascaceae* as monophyletic groups, but there is still no strong consensus on the divergence times within this family. In our molecular clock analyses, the crown age of *Microascaceae* was around 210.37 Mya, the divergence times of the genus range from 35.08 Mya to 162.99 Mya and those of the species range from 2.52 Mya to 91.64 Mya (Fig. 3). Deeper in the tree, *Cephalotrichum* is phylogenetically allied to *Wardomyces* and *Gamsia*, with the three lineages estimated to diverge from each other about 40 Mya and 74 Mya, respectively. Despite they share a sister relationship, the divergence time of over 34 Mya and the striking morphological differences strongly support their classification as separate genera. Notably, our inferred divergence time corroborated the results of previous molecular phylogenetic studies on *Wardomyces* (Sandoval-Denis et al. 2016a, b). The molecular dating analysis indicated that the lineage appeared to be polyphyletic, with species distributed in three closely related subclades that diverged from each other about 47 Mya and 58 Mya (Fig. 3). However, since morphological differences between these species are not constant, it is necessary to analyse more taxa to provide morphological evidence (Sandoval-Denis et al. 2016a, b). Furthermore, the divergence times also supported the delimitation of several scopulariopsis-like genera with very similar sexual morphs in previous studies (Lackner et al. 2014, Sandoval-Denis et al. 2016a, b, Woudenberg et al. 2017a, Su et al. 2021), viz., *Acaulium*, *Fairmania*, *Microascus*, *Pithoascus*, *Pseudoscopulariopsis*, *Scopulariopsis* and *Wardomycopsis*. In our study, *Acaulium* was inferred as the sister group to *Fairmania* and *Wardomycopsis*, and the molecular dating analysis results were consistent with previous phylogenetic views (Sandoval-Denis et al. 2016a, b, Zhang et al. 2021; Fig. 3). The three lineages diverged about 61 Mya and 94 Mya, earlier than the later time limit of the other accepted genera in the family, supporting their existence as generic-level taxa. *Microascus* was placed as sister to *Pithoascus*, with two subclades estimated to diverge from each other about 76 Mya; *Pseudoscopulariopsis* was inferred to be sister to *Scopulariopsis*, with both lineages estimated to diverge from each other about 66 Mya. Importantly, our divergence time estimates suggested that *Microascus* members started to diverge at 70.46 Mya, while the common ancestor of the extant *Scopulariopsis* is estimated to have lived in 36.14 Mya, with the latter being about 34 Mya younger than the former (Fig. 3). In total, the genus-level classification of *Microascaceae* should not only be well-supported by multi-gene phylogeny and phenotypic traits, but also possess a divergence time of over 35 million years ago.

Acknowledgements This study was supported by the Guizhou Provincial Basic Research Program (Natural Science) (No. (2023) Key 005) and the National Natural Science Foundation of China (No. 32060009).

Declaration on conflict of interest The authors declare that there is no conflict of interest.

REFERENCES

Abbott SP. 2000. Holomorph studies of the Microascaceae. Ph.D. dissertation. Department of Biological Sciences, University of Alberta, Canada.

Abbott SP, Lumley TC, Sigler L. 2002. Use of holomorph characters to delimit Microascus nidicola and M. soppii sp. nov., with notes on the genus Pithoascus. Mycologia 94: 362–369.

Abbott SP, Sigler L. 2001. Heterothallism in the Microascaceae demonstrated by three species in the Scopulariopsis brevicaulis series. Mycologia 93: 1211–1220.

Abbott SP, Sigler L, Currah RS. 1998. Microascus brevicaulis sp. nov., the teleomorph of Scopulariopsis brevicaulis, supports placement of Scopulariopsis with the Microascaceae. Mycologia 90: 297–302.

Álvarez-Uría A, Escribano P, Parra-Blanco V, et al. 2021. First report of an invasive infection by Cephalotrichum gorgonifer in a neutropenic patient with hematological malignancy under chemotherapy. Journal of Fungi 7: 1089.

Baddley JW, Moser SA, Sutton DA, et al. 2000. Microascus cinereus (anamorph Scopulariopsis) brain abscess in a bone marrow transplant recipient. Journal of Clinical Microbiology 38: 395–397.

Bainier G. 1907. Mycothèque de l'École de Pharmacie, XIV. Scopulariopsis (Penicillium pro parte) genre nouveau de mucédinées. Bulletin Trimestriel de la Société Mycologique de France 23: 98–105.

Barron GL, Cain RF, Gilman JC. 1961. The genus Microascus. Canadian Journal of Botany 39: 1609–1631.

Beimforde C, Feldberg K, Nylinder S, et al. 2014. Estimating the Phanerozoic history of the Ascomycota lineages: combining fossil and molecular data. Molecular Phylogenetics and Evolution 78: 386–398.

Benton MJ, Donoghue PCJ, Asher RJ. 2009. Calibrating and constraining molecular clocks. The Timetree of Life: 35–86. England (Oxford), Oxford University Press.

Berbee ML, Taylor JW. 2010. Dating the molecular clock in fungi – how close are we? Fungal Biology Reviews 24: 1–16.

Bouckaert R, Vaughan TG, Barido-Sottani J, et al. 2019. BEAST 2.5: an advanced software platform for Bayesian evolutionary analysis. PLOS Computational Biology 15: e1006650.

Brasch J, Beck-Jendroschek V, Iturrieta-González I, et al. 2019. A human subcutaneous infection by Microascus ennothomasiorum sp. nov. Mycoses 62: 157–164.

Chuaseeharonnachai C, Suetrong S, Nuankaew S, et al. 2020. Synnematotriadelphia gen. nov. (S. stilboidea comb. nov. and S. synnematofera comb. nov.) and Triadelphia hexaformispora sp. nov. in the family Triadelphiaceae. Mycological Progress 19: 127–137.

Clements FE, Pound R. 1896. New species of fungi. Botanical Survey of Nebraska 4: 5–23.

Corda ACJ. 1829. In: Sturm J (ed.), Deutschlands Flora, III (Die Pilze Deutschlands) 2, heft 7.

Corda ACJ. 1837. Icones fungorum huscusque cognitorum 1. Czech Republic, Prague.

Crous PW, Boers J, Holdom D, et al. 2022. Fungal Planet description sheets: 1383–1435. Persoonia 48: 261–371.

Crous PW, Verkley GJM, Groenewald JZ, et al. 2019. Fungal Biodiversity. [Westerdijk Laboratory Manual Series no.1.] Utrecht, Westerdijk Fungal Biodiversity Institute, Utrecht, The Netherlands.

Darriba D, Taboada GL, Doallo R, et al. 2012. jModelTest 2: more models, new heuristics and parallel computing. Nature Methods 9: 772–772.

Das K, You YH, Lee SY, et al. 2020. A new species of Thelonectria and a new record of Cephalotrichum hinnuleum from Gunwi and Ulleungdo in Korea. Mycobiology 48: 341–350.

Dayarathne MC, Maharachchikumbura SS, Jones EG, et al. 2019. Phylogenetic revision of Savoryellaceae and evidence for its ranking as a subclass. Frontiers in Microbiology 10: 840.

De Beer ZW, Seifert KA, Wingfield MJ. 2013. The ophiostomatoid fungi: their dual position in the Sordariomycetes. In: Seifert KA, De Beer ZW, Wingfield MJ (eds), The ophiostomatoid fungi: expanding frontiers. CBS biodiversity series 12: 1–19. CBS-KNAW Fungal Biodiversity Centre, The Netherlands.

De Hoog GS, Guarro J, Gené J, et al. 2011. Atlas of clinical fungi. CD-ROM version 3.1. CBS-KNAW Fungal Biodiversity Centre, Utrecht, The Netherlands.

Domsch KH, Gams W, Anderson TH. 2007. Compendium of soil fungi, 2nd edn. IHW Verlag, Eching, Germany.

Dos Reis M, Donoghue PCJ, Yang ZH. 2015. Bayesian molecular clock dating of species divergences in the genomics era. Nature Reviews Genetics 17: 71–80.

Ehrenberg CG. 1818. Sylvae mycologicae berolinenses. Formis Theophili Bruschcke.

Ellis MB. 1971. Dematiaceous Hyphomycetes. Commonwealth Mycological Institute, Kew, England.

Garnica S, Riess K, Schön ME, et al. 2016. Divergence times and phylogenetic patterns of Sebacinales, a highly diverse and widespread fungal lineage. PLoS ONE 11: e0149531.

Glass NL, Donaldson GC. 1995. Development of primer sets designed for use with the PCR to amplify conserved genes from filamentous ascomycetes. Applied and Environmental Microbiology 61: 1323–1330.

Guarro J, Gené J, Stchigel AM, et al. 2012. Atlas of soil ascomycetes. CBS Biodiversity Series. CBS-KNAW Fungal Biodiversity Centre, Utrecht, The Netherlands.
Hall TA. 1999. BioEdit: a user-friendly biological sequence alignment editor and analysis program for Windows 95/98/NT. Nucleic Acids Symposium Series 41: 95–98.
Hammill TM. 1977. Transmission electron microscopy of annellides and conidiogenesis in the synnematal hyphomycete Trichurus spiralis. Canadian Journal of Botany 55: 233–244.
Hasselbring H. 1896. Comparative study of the development of Trichurus spiralis and Stysanus stemonitis. Botanical Gazette Crawfordsville 29: 312–322.
Hedman MH. 2010. Constraints on clade ages from fossil outgroups. Paleobiology 36: 16–31.
Ho SYW. 2020. The molecular evolutionary clock: theory and practice. Springer, Cham, Switzerland.
Hughes SJ. 1958. Revisiones hyphomycetum aliquot cum appendice de nominibus rejiciendis. Canadian Journal of Botany 36: 727–836.
Issakainen J, Jalava J, Hyvönen J, et al. 2003. Relationships of Scopulariopsis based on LSU rDNA sequences. Medical Mycology 41: 31–42.
Jagielski T, Kosim K, Skóra M, et al. 2013. Identification of Scopulariopsis species by partial 28S rRNA gene sequence analysis. Polish Journal of Microbiology 62: 303–306.
Jagielski T, Sandoval-Denis M, Yu J, et al. 2016. Molecular taxonomy of scopulariopsis-like fungi with description of new clinical and environmental species. Fungal Biology 120: 586–602.
Jiang JR, Cai L, Liu F. 2017. Oligotrophic fungi from a carbonate cave, with three new species of Cephalotrichum. Mycology 8: 164–177.
Jiang YL, Xu JJ, Wu YM, et al. 2011. Studies on Cephalotrichum from soils in China – twelve new species and two new combinations. Mycotaxon 117: 207–225.
Jiang YL, Zhang TY. 2008. Two new species of Doratomyces from soil. Mycotaxon 104: 131–134.
Kirk PM, Spooner BM. 1984. An account of the fungi of Arran, Gigha and Kintyre. Kew Bulletin 38: 503–597.
Lackner M, De Hoog GS, Yang L, et al. 2014. Proposed nomenclature for Pseudallescheria, Scedosporium and related genera. Fungal Diversity 67: 1–10.
Letunic I, Bork P. 2021. Interactive Tree Of Life (iTOL) v5: an online tool for phylogenetic tree display and annotation. Nucleic Acids Research 49: 293–296.
Li XL, Ojaghian MR, Zhang JZ, et al. 2017. A new species of Scopulariopsis and its synergistic effect on pathogenicity of Verticillium dahliae on cotton plants. Microbiological Research 201: 12–20.
Link HF. 1809. Observationes in ordines plantarum naturales. Berlinische Magazin 3: 3–42.
Liu JK, Hyde KD, Jeewon R, et al. 2017. Ranking higher taxa using divergence times: a case study in Dothideomycetes. Fungal Diversity 84: 75–99.
Lu GQ, Moriyama EN. 2004. Vector NTI, a balanced all-in-one sequence analysis suite. Briefings in Bioinformatics 5: 378–388.
Lukoschek V, Scott Keogh J, Avise JC. 2012. Evaluating fossil calibrations for dating phylogenies in light of rates of molecular evolution: a comparison of three approaches. Systematic Biology 61: 22–43.
Lumbsch HT, Huhndorf SM. 2007. Outline of Ascomycota – 2007. Myconet 13: 1–58.
Malloch D. 1970. New concepts in the Microascaceae illustrated by two new species. Mycologia 62: 727–740.
Malloch D, Cain RF. 1971. The genus Kernia. Canadian Journal of Botany 49: 855–867.
Mamaghani NA, Saremi H, Javan-Nikkhah M, et al. 2022. Endophytic Cephalotrichum spp. from Solanum tuberosum (potato) in Iran – a polyphasic analysis. Sydowia 74: 287–301.
Mhmoud NA, Siddig EE, Nyuykonge B, et al. 2021. Mycetoma caused by Microascus gracilis: a novel agent of human eumycetoma in Sudan. Transactions of The Royal Society of Tropical Medicine and Hygiene 115: 426–430.
Miossec C, Morio F, Lepoivre T, et al. 2011. Fatal invasive infection with fungemia due to Microascus cirrosus after heart and lung transplantation in a patient with cystic fibrosis. Journal of Clinical Microbiology 49: 2743–2747.
Mohammedi I, Piens MA, Audigier-Valette C, et al. 2004. Fatal Microascus trigonosporus (anamorph Scopulariopsis) pneumonia in a bone marrow transplant recipient. European Journal of Clinical Microbiology and Infectious Diseases 23: 215–217.
Morton FJ, Smith G. 1963. The genera Scopulariopsis Bainier, Microascus Zukal, and Doratomyces Corda. Mycological Papers 86: 1–96.
Nylander JAA. 2004. MrModeltest v2.2. Program distributed by the author: 2. Evolutionary Biology Centre, Uppsala University.
Peterson R, Grinyer J, Nevalainen H. 2011. Secretome of the Coprophilous Fungus Doratomyces stemonitis C8, Isolated from Koala Feces. Applied and Environmental Microbiology 77: 3793–3801.
Píchová K, Pažoutová S, Kostovčík M, et al. 2018. Evolutionary history of ergot with a new infrageneric classification (Hypocreales: Clavicipitaceae: Claviceps). Molecular Phylogenetics and Evolution 123: 73–87.
Prieto M, Wedin M. 2013. Dating the diversification of the major lineages of Ascomycota (Fungi). PLoS ONE 8: e65576.
Rambaut A. 2018. FigTree, version 1.4.4. Computer program and documentation distributed by the author at http://tree.bio.ed.ac.uk/software/figtree/.
Rambaut A, Drummond AJ, Xie D, et al. 2018. Posterior summarization in Bayesian phylogenetics using Tracer 1.7. Systematic Biology 67: 901–904.
Rehner SA, Buckley E. 2005. A Beauveria phylogeny inferred from nuclear ITS and EF1-α sequences: evidence for cryptic diversification and links to Cordyceps teleomorphs. Mycologia 97: 84–98.
Ronquist F, Teslenko M, Van der Mark P, et al. 2012. MrBayes 3.2: efficient Bayesian phylogenetic inference and model choice across a large model space. Systematic Biology 61: 539–542.
Ropars J, Cruaud C, Lacoste S, et al. 2012. A taxonomic and ecological overview of cheese fungi. International Journal of Food Microbiology 155: 199–210.
Rozewicki J, Li S, Amada KM, et al. 2019. MAFFT-DASH: integrated protein sequence and structural alignment. Nucleic Acids Research 47: 5–10.
Saccardo PA. 1878. Fungi Veneti novi vel critici vel mycologiae Venetae addendi. Series VIII. Michelia 1: 239–275.
Saccardo PA. 1886. Sylloge Hyphomycetum. Sylloge Fungorum 4: 1–807.
Samson RA, Houbraken J, Thrane U, et al. 2010. Food and indoor fungi. CBS Laboratory Manual Series 2. CBS-Fungal Biodiversity Centre, Utrecht.
Sandoval-Denis M, Gené J, Sutton DA, et al. 2016a. Redefining Microascus, Scopulariopsis and allied genera. Persoonia 36: 1–36.
Sandoval-Denis M, Guarro J, Cano-Lira JF, et al. 2016b. Phylogeny and taxonomic revision of Microascaceae with emphasis on synnematous fungi. Studies in Mycology 83: 193–233.
Sandoval-Denis M, Sutton DA, Fothergill AW, et al. 2013. Scopulariopsis, a poorly known opportunistic fungus: spectrum of species in clinical samples and in vitro responses to antifungal drugs. Journal of Clinical Microbiology 51: 3937–3943.
Seifert KA, Morgan-Jones G, Gams W, et al. 2011. In: The genera of Hyphomycetes. CBS biodiversity series 9. CBS-KNAW Fungal Biodiversity Centre, Utrecht, The Netherlands.
Shao CL, Xu RF, Wang CY, et al. 2015. Potent antifouling marine dihydroquinolin-2(1H)-one-containing alkaloids from the gorgonian coral-derived fungus Scopulariopsis sp. Marine Biotechnology 17: 408–415.
Skóra M, Bulanda M, Jagielski T. 2015. In vitro activities of a wide panel of antifungal drugs against various Scopulariopsis and Microascus species. Antimicrobial Agents and Chemotherapy 59: 5827–5829.
Sprengel K. 1827. Systema Vegetabilium. Ed. 16. 4: 1–592.
Stamatakis A. 2014. RAxML version 8: a tool for phylogenetic analysis and post-analysis of large phylogenies. Bioinformatics 30: 1312–1313.
Steenwyk JL, Shen XX, Lind AL, et al. 2019. A robust phylogenomic time tree for biotechnologically and medically important fungi in the genera Aspergillus and Penicillium. mBio 10: e00925.
Su L, Zhu H, Sun P, et al. 2021. Species diversity in Penicillium and Acaulium from herbivore dung in China, and description of Acaulium stercorarius sp. nov. Mycological Progress 20: 1539–1551.
Sun B, Zhou Y, Chen AJ. 2020. Two new Microascus species with spinous conidia isolated from pig farm soils in China. Mycoscience: 61: 190–196.
Sung GH, Poinar Jr GO, Spatafora JW. 2008. The oldest fossil evidence of animal parasitism by fungi supports a Cretaceous diversification of fungal-arthropod symbioses. Molecular Phylogenetics and Evolution 49: 495–502.
Swart HJ. 1964. A study of the production of coremia in three species of the genus Trichurus. Antonie van Leeuwenhoek 30: 257–260.
Swift ME. 1929. Contributions to a mycological flora of local soils. Mycologia 21: 204–221.
Tamura K, Stecher G, Kumar S. 2021. MEGA11: Molecular Evolutionary Genetics Analysis version 11. Molecular Biology and Evolution 38: 3022–3027.
Taylor TN, Krings M, Taylor EL. 2014. Fossil fungi. Academic Press, New York.
Taylor TN, Krings M, Taylor EL. 2015. 10 Fungal diversity in the fossil record. In: McLaughlin D, Spatafora J (eds), Systematics and Evolution. The Mycota, vol 7B: 259–278. Springer, Berlin, Heidelberg.
Tedersoo L, Sánchez-Ramírez S, Koljalg U, et al. 2018. High-level classification of the Fungi and a tool for evolutionary ecological analyses. Fungal Diversity 90: 135–159.
Tischer M, Gorczak M, Bojarski B, et al. 2019. New fossils of ascomycetous anamorphic fungi from Baltic amber. Fungal Biology 123: 804–810.

Udagawa S. 1959. Taxonomic studies of fungi on stored rice grains. III. Penicillium group (penicillia and related genera) 2. Journal of Agricultural Science Tokyo Nogyo Daigaku 5: 5–21.

Vaidya G, Lohman DJ, Meier R. 2011. SequenceMatrix: concatenation software for the fast assembly of multi-gene datasets with character set and codon information. Cladistics 27: 171–180.

Van de Sande WW, Fahal A, Verbrugh H, et al. 2007. Polymorphisms in genes involved in innate immunity predispose toward mycetoma susceptibility. The Journal of Immunology 179: 3065–3074.

Vilgalys R, Hester M. 1990. Rapid genetic identification and mapping of enzymatically amplified ribosomal DNA from several Cryptococcus species. Journal of Bacteriology 172: 4238–4246.

Vilgalys R, Sun BL. 1994. Ancient and recent patterns of geographic speciation in the oyster mushroom Pleurotus revealed by phylogenetic analysis of ribosomal DNA sequences. Proceedings of the National Academy of Sciences of the United States of America 91: 4599–4603.

Von Arx JA, 1975. Revision of Microascus with the description of a new species. Persoonia 8: 191–197.

Wang XH, Halling RE, Hofstetter V, et al. 2018. Phylogeny, biogeography and taxonomic reassessment of Multifurca (Russulaceae, Russulales) using three-locus data. PLoS ONE 13: e0205840.

Wang XW, Han PJ, Bai FY, et al. 2022. Taxonomy, phylogeny and identification of Chaetomiaceae with emphasis on thermophilic species. Studies in Mycology 101: 121–243.

White TJ, Bruns T, Lee S, et al. 1990. Amplification and direct sequencing of fungal ribosomal RNA genes for phylogenetics. In: Innis MA, Gelfand DH, Sninsky JJ, et al. (eds), PCR Protocols: a guide to methods and applications: 315–322. Academic Press, San Diego, California, USA.

Woudenberg JHC, Meijer M, Houbraken J, et al. 2017a. Scopulariopsis and scopulariopsis-like species from indoor environments. Studies in Mycology 88: 1–35.

Woudenberg JHC, Sandoval-Denis M, Houbraken J, et al. 2017b. Cephalotrichum and related synnematous fungi with notes on species from the built environment. Studies in Mycology 88: 137–159.

Wright JE, Marchand S. 1972. Micoflora del suelo de la Argentina. III. Dos interesantes géneros sinemáticos: Trichurus y Doratomyces. Boletín de la Sociedad Argentina de Botánica 14: 305–310.

Zhang YL, Wu YM, Zhang TY. 2014. Notes on soil dematiaceous hyphomycetes from Hainan Province China I. Mycosystema 33: 945–953.

Zhang ZF, Liu F, Zhou X, et al. 2017. Culturable mycobiota from Karst caves in China, with descriptions of 20 new species. Persoonia 39: 1–31.

Zhang ZF, Zhou SY, Eurwilaichitr L, et al. 2021. Culturable mycobiota from Karst caves in China II, with descriptions of 33 new species. Fungal Diversity 106: 29–136.

Zhao RL, Li GJ, Sánchez-Ramírez S, et al. 2017. A six-gene phylogenetic overview of Basidiomycota and allied phyla with estimated divergence times of higher taxa and a phyloproteomics perspective. Fungal Diversity 84: 43–74.

Zhu H, Li D, Yan Q, et al. 2018. α-Pyrones, secondary metabolites from fungus Cephalotrichum microsporum and their bioactivities. Bioorganic Chemistry 83: 129–134.

Zhu L, Song J, Zhou JL, et al. 2019. Species diversity, phylogeny, divergence time, and biogeography of the genus Sanghuangporus (Basidiomycota). Frontiers in Microbiology 10: 812.

Zukal H. 1885. Ueber einige neue Pilze, Myxomyceten und Bakterien. Verhandlungen der Zoologisch-Botanischen Gesellschaft Wien 35: 333–342.

Zutz C, Bacher M, Parich A, et al. 2016. Valproic acid induces antimicrobial compound production in Doratomyces microspores. Frontiers in Microbiology 7: 510.